



UNIVERSITÀ DI PISA
Department of Computer Science

REASONING ALGORITHMICALLY IN GRAPH NEURAL
NETWORKS

DOCTORAL DISSERTATION

CANDIDATE

Danilo Numeroso

SUPERVISOR

Davide Bacciu

February 16, 2024

Danilo Numeroso: *Reasoning Algorithmically in Graph Neural Networks*,
Doctoral Dissertation
© February 16, 2024

ABSTRACT

The development of artificial intelligence systems with advanced reasoning capabilities represents a persistent and long-standing research question. Traditionally, the primary strategy to address this challenge involved the adoption of *symbolic* approaches, where knowledge was explicitly represented by means of symbols and explicitly programmed rules. However, with the advent of machine learning, there has been a paradigm shift towards systems that can autonomously learn from data, requiring minimal human guidance. In light of this shift, in latest years, there has been increasing interest and efforts at endowing neural networks with the ability to reason, bridging the gap between data-driven learning and logical reasoning. Within this context, Neural Algorithmic Reasoning (NAR) stands out as a promising research field, aiming to integrate the structured and rule-based reasoning of algorithms with the adaptive learning capabilities of neural networks, typically by tasking neural models to mimic classical algorithms. In this dissertation, we provide theoretical and practical contributions to this area of research. We begin with a review of foundational principles necessary for the understanding of the notions presented in this thesis, followed by a comprehensive overview of the most important NAR principles. Proceeding forward, we explore the connections between neural networks and tropical algebra, deriving powerful architectures that are *aligned* with algorithm execution. These architectures are thus proven to be able to approximate some *min*-aggregated dynamic programming algorithms up to arbitrary precision. Furthermore, we discuss and show the ability of such neural *reasoners* to learn and manipulate complex algorithmic and combinatorial optimization concepts, such as the principle of strong duality. Here, we rigorously evaluate this capacity through extensive quantitative and qualitative studies. Finally, in our empirical efforts, we validate the real-world utility of NAR networks across different practical scenarios. This includes tasks as diverse as planning problems, large-scale edge classification tasks and the learning of polynomial-time approximate algorithms for NP-hard combinatorial optimisation problems. Through this comprehensive exploration, we aim to showcase the potential and versatility of integrating algorithmic reasoning in machine learning models.

ACKNOWLEDGEMENTS

I owe the inception of these acknowledgements to a truly exceptional human being, **Davide Bacciu**. Since the time of my master's thesis, I have consistently felt an unwavering trust from him – perhaps more than I ever had in myself. Throughout these three years, you have been a supervisor, a psychologist, and, most importantly, a friend. Your continuous support has been invaluable, and I can never express my gratitude enough.

I wish to thank the international reviewers of this thesis, **Christopher Morris** and **Nils Morten Kriege**, for giving me the opportunity to revise some of the concepts I (thought I) grasped, through their comments and constructive criticisms. I also wish to thank my PhD coordinator: **Antonio Brogi**, and my internal committee: **Alessio Conte**; **Alina Sirbu**; and **Antonio Frangioni**, for guiding and providing me with valuable feedback during these years.

Many thanks to **Alessio Gravina** and **Valerio De Caro**, with whom I had the pleasure to share the office throughout the entire duration of this PhD. Thanks for all the discussions, the occasional battles for GPU resources, and the laughs we had. This journey would have been only half as enjoyable without your presence.

I would also like to thank each and every one of the UniPi people I had the opportunity to know during these years, especially **Francesco Landolfi** who always had the time to listen to my ramblings (and vice versa!).

Sincere thanks are due to **Petar Veličković**. Since our first meeting, he always took my ideas seriously, sharing with me his honest and valuable thoughts and giving me the opportunity to grow professionally.

Immense gratitude belongs to **Yingqian Zhang**, for warmly welcoming me at the *Technische Universiteit Eindhoven* and for giving me the opportunity to collaborate with amazing people. In this regard, I sincerely thank **Wouter Kool**, with whom I had the pleasure (and the duty!) to organise parts of the *EURO Meets NeurIPS 2022* competition.

Special thanks are due to **Luca Begnardi**, **Riccardo Lo Bianco**, **Fabio Mercurio** and **Ya Song**. The memories of the time we spent together, during coffee breaks/tea breaks is something I will never forget about.

Heartfelt thanks go to two of the most genuinely good-hearted people I have ever known, “**Pit**” and **Marcin**. You'll probably never read these words but... *dzięki*.

I couldn't conclude this paragraph without first thanking **Edwin van Weert**. You truly made me feel home and really added that extra to the overall dutch experience. Say *hi* to *Coco*. I nearly forgot... thank you **Ziva**! As strange as it may sound, thanks to you, I don't think I will ever forget

how to count in dutch: *één, twee, drie, vier, vijf, zes, zeven, acht, negen, tien!* This is some memory I will jealously guard with me. *Dank je wel!*

I had the luck to visit the *University of Cambridge*, where I had *the* most intense and fun period of my entire PhD. A huge thank you goes to **Pietro Liò**, to whom I will always be grateful for giving me such opportunity and for his kindness. Throughout my stay in Cambridge, I always had the impression that he genuinely cared I was, first of all, enjoying myself. I would also like to thank **Dobrik Georgiev**, for all our inspiring discussions and exchange of ideas, and of course for his relentless dedication and commitment. This paragraph could never be complete without a word of acknowledgements to the amazing folks I met there: **Donato Crisostomi; Federico Siciliano; Francesco Ceccarelli; Francesco Prinzi; Gianluca Carlini; Lorenzo Giusti; Maria Sofia Bucarelli; and Pietro Barbiero** (thanks for the bike!). I will always remember the *intense* night before NeurIPS submission(s), as well as our barbecues at the Jesus Green.

I suspect the cardinality of the set of people I met during these years and influenced me positively is uncountable, so a general thanks goes to all of the folks I didn't have the opportunity to mention here.

PERSONAL ACKNOWLEDGEMENTS – *in italian*

Un grazie speciale va a **Anna Orfanò**, per avermi aiutato a superare alcuni dei momenti più difficili che ho affrontato nella mia vita. Porterò sempre con me le nostre chiacchierate.

Il più sentito dei grazie va alla mia famiglia:

- **Mamma e Babbo**, a nulla sarebbe valso tutto il mio impegno se voi non foste stati sempre al mio fianco, a sorreggermi. Grazie.

- **Matti**, avere la possibilità di essere tuo fratello e di poterti aiutare nelle tue scelte future è uno dei miei più grandi orgogli. Averti nella mia vita è una fortuna.

- **Mara**, perchè ormai sei famiglia. Affrontare questo cammino con te al mio fianco è stato, ed è, un privilegio. Qualsiasi cosa affronterò in futuro, bella o brutta, so che la affronterò insieme a te. Grazie per esserci sempre.

Grazie a tutta la *Varano crew*: **Ciro Leonardi; Francesco Bondi; Gaia Volpi; Lorenzo Cassi; Marcello Ceresini e Riccardo Verbeni**. Grazie per aver aggiunto spensieratezza e leggerezza in questi tre anni.

Un ultimo saluto, e un doveroso grazie, va ad una persona che queste parole non potrà mai leggerle. Credo tu non le possa neanche ascoltare, ma spero di sbagliarmi. *Cia', 'a no'!*

CONTENTS

1	Introduction	1
1.1	Objectives	3
1.2	Thesis outline	3
I Background		
2	Preliminaries	7
2.1	Graphs	7
2.1.1	Graph Theory	8
2.1.2	Instances of graphs	12
2.1.3	Computational problems on graphs	13
2.2	Combinatorial Optimisation	15
2.2.1	The P vs NP dilemma	16
2.2.2	Linear Programming	17
2.2.3	Duality	18
2.3	Algorithms	19
2.3.1	A simple notation for representing algorithms	20
2.3.2	Algorithmic guarantees	20
2.3.3	Algorithms as discrete functions	21
2.3.4	Graph algorithms	22
2.3.5	Dynamic programming	28
2.4	Graph Networks	30
2.4.1	A brief historical tour of GNs	31
2.4.2	Desiderata of Graph Networks	32
2.4.3	Iterative vs Feedforward Message Passing	35
3	Neural Algorithmic Reasoning	41
3.1	Why learn algorithms?	41
3.2	Principles of Algorithmic Reasoning	44
3.2.1	Algorithmic alignment	45
3.2.2	The Encode-Process-Decode architecture	46
3.2.3	Step-wise supervision	50
3.3	Learnt algorithms as inductive priors	51
II Contribution		
4	Learning Dynamic Programming	57
4.1	Approximate min-DP algorithms	57
4.1.1	Alignment of encoders and decoders	58
4.1.2	Processor alignment and DP approximation	61
4.1.3	Effects on network design	64
4.2	Planning via learnt heuristics	66
4.2.1	Learning consistent heuristics	68
4.2.2	Experimental evaluation	71
5	Learning Combinatorial Algorithms	77
5.1	Leveraging Strong Duality	77
5.1.1	Model architecture	79

5.1.2	Experimental evaluation	82
5.1.2.1	Executing Ford-Fulkerson	82
5.1.2.2	Brain Vessel Graph benchmark	88
5.2	Learning CO-approximation via algorithmic primitives	93
5.2.1	Selecting relevant primitives	93
5.2.2	Model architecture.	95
5.2.3	Experimental evaluation	95
III Conclusion		
6	Closing Remarks	105
IV Appendix		
A	List of publications	125
B	List of talks	127

1

INTRODUCTION

From the earliest forms of calculation conducted with the Sumerian abacus to the intricate mechanisms of the Antikythera mechanism, the essence of computation has always lingered in the shadows of human advancement. Throughout history, our innate desire to understand, quantify, and predict the world around us has driven the development of instruments and methods that aid our cognitive capabilities. With the dawn of the 20th century, computer science emerged, not merely as an academic discipline, but as the backbone of the modern society. Today, computer science stands at the intersection of mathematics, logic and engineering, driving innovation, reshaping industries, and revolutionising how we devise solutions to everyday challenges.

In this regard, in the vast landscape of computer science, two distinct paradigms of problem-solving have arisen over the years – algorithms and machine learning.

Algorithms, in particular, have been at the heart of computer science since its inception and represent the keystone upon which every computer scientist builds their knowledge and expertise. Algorithms are sequences of instructions that are meticulously juxtaposed to devise solutions to computational problems, often bolstered by rigorous theoretical guarantees – typically in the form of pre- and post-conditions. When executed with inputs that adhere to their specified preconditions, algorithms can solve complex problems with precision, delivering results that consistently meet the expected postconditions. However, their deterministic nature is both their strength and limitation. Most algorithmic inputs originate from problems observed in the vast complexity of the real world. These problems, rich in detail and context, are then translated and abstracted to accommodate the strict preconditions that algorithms demand. This translation, unfortunately, comes at the price of possible loss of information, making it hard to find exact solutions with classical algorithms.

In such a noisy and ever-evolving world, machine learning has emerged as a flexible paradigm, adept at navigating the uncertainties and intricacies inherent in *natural*¹ data. Machine learning, especially its most notable subset, Neural Networks, represents the modern computational approach to solve tasks and problems. At its core, machine learning is about enabling computers to learn and discover patterns from data, using this knowledge to make decisions or predictions. Unlike algorithms, then, neural networks are not explicitly programmed to perform a task in a certain way, but they rather learn to adapt themselves as they are exposed to more and more examples. Their strength, therefore, lies in their adaptability. Neural networks can process and generalise across diverse inputs, making them

¹ As opposed to “abstract” data typical of algorithms, we use the term “natural” to refer to the unprocessed, raw data that can be observed in the real world.

particularly well-suited for natural data. Often, neural networks that are trained on a particular data distribution can be used as-is or as a starting point to tackle computational tasks that are different from the original one (Reyes et al., 2015). Algorithms, in comparison, do not show this degree of adaptability. They are designed to tackle a specific problem and typically need manual interventions to adapt to a new one. Machine learning flexibility, however, also comes at a cost. Indeed, neural networks, *deep* neural models, often lack the robust theoretical guarantees that accompany classical algorithms. As a general rule of thumb, the more complex the neural architecture is, the less we can say about the learnt function, even though great efforts are being made in order to make deep learning *interpretable* (Burkart & Huber, 2021; Numeroso & Bacciu, 2021; Bacciu & Numeroso, 2022). Furthermore, neural networks usually struggle to generalise their knowledge in out-of-distribution² scenarios (Neyshabur et al., 2017). Algorithms, on the other hand, have the inherent ability to generalise to any input meeting its pre-conditions.

At first glance, thus, the algorithmic and neural paradigms may be perceived as diametrically opposed. However, by careful assessment of their properties, they can actually be envisioned as complementary approaches, each addressing the shortcomings of the other. Where algorithms fall short in the face of task flexibility and data adaptability, neural networks excel; and where neural networks operate in absence of theoretical guarantees, algorithms excel. This synergy suggests a potential convergence of the two paradigms – a unified approach that harnesses the deterministic strength of algorithms and the adaptive flexibility of neural networks.

Stimulated by this fascinating perspective, researchers began exploring towards incorporating the principled and structured knowledge of algorithms into learning models, laying the foundation for what is now recognised as Neural Algorithmic Reasoning (NAR) (Veličković & Blundell, 2021). Broadly speaking, neural algorithmic reasoning strives to enable neural networks to demonstrate reasoning abilities, specifically mirroring the reasoning inherent in classical algorithms (i.e., the ability of slowly processing input data in a principled manner in order to return a desired outcome). In particular, the integration of *algorithmic knowledge* in machine learning models is typically performed by instructing neural networks to *execute* classical algorithms.

The key motivations for such integration are multiple. First, enabling reasoning in neural networks could mitigate the limitations of traditional neural networks, particularly in their susceptibility to overfitting, not to mention that it is a long-standing research goal (Khardon & Roth, 1997). Moreover, *neural algorithmic reasoners*³ are, by their very nature, knowledge of classical algorithms encoded in their parameters. This unlocks various possibilities to leverage such algorithmic expertise as *prior knowledge* and utilise it for problems that might benefit from the application of

² Out-of-distribution scenarios refer to situations where neural networks face data that differs noticeably from their training distribution.

³ Throughout this dissertation, we will be using this term to refer to neural networks that can execute classical algorithms.

said algorithmic knowledge (i.e., effectively using algorithms as *inductive bias*).

1.1 OBJECTIVES

Inspired by the above premises, this dissertation aims to explore the potential of neural algorithmic reasoners, particularly regarding their abilities to *learn to execute classical algorithms* and *validate* the effectiveness of employing trained algorithmic reasoners as inductive priors for related downstream tasks.

The main contributions of this thesis are aimed at addressing these two research questions, particularly in the context of graphs, given that many classical algorithms of interest are developed and designed for structured data (Cormen et al., 2009). Additionally, we will be seeking to provide evidence for the previously mentioned questions from both theoretical and empirical viewpoints.

To address the concern regarding *learnability* of classical algorithms, we propose a theoretical framework drawing connections between graphs, neural networks and tropical algebra (Landolfi et al., 2023). In this setting, equivalence between algorithms, particularly dynamic programming algorithms, and neural networks will be established. We will also demonstrate how to derive a powerful neural network architecture suitable for learning algorithms based on such connections.

Moving outside the context of dynamic programming algorithms, we propose to learn algorithms through duality (Numeroso et al., 2023), effectively showing how we can borrow concepts from various areas related to algorithms, such as combinatorial optimisation, to enhance the extent to which algorithmic reasoning can be encoded into neural networks. This contribution also serves as a first practical example of how algorithms, used as inductive priors, can aid to solve standard machine learning tasks more accurately.

On this line, we present two more contributions: an algorithmic reasoner that learns *consistent* heuristic functions for planning problems (Numeroso et al., 2022); and an extensive study on the effectiveness of *transferring* algorithmic knowledge to NP-hard combinatorial optimisation problems (Georgiev et al., 2023).

Moreover, as a side objective, this thesis also endeavors to serve as an introductory guide to the world of Neural Algorithmic Reasoning, particularly through its [chapter 3](#), tailored to be comprehensible for those unfamiliar with NAR.

1.2 THESIS OUTLINE

In the following, we provide a brief outline regarding the content of this thesis:

In [chapter 2](#), we review foundational and theoretical concepts pivotal to this research. This chapter introduces the fundamental principles of graph theory, combinatorial optimisation, algorithms, and finally, an exploration into the machine learning paradigm that utilizes graph structures, known as Graph Networks.

In [chapter 3](#), we present an introduction to Neural Algorithmic Reasoning (NAR). This chapter will explore and discuss practical scenarios in which the straightforward application of algorithms fail, and actionable interventions to mitigate said issues.

In [chapter 4](#), we focus on the primary contributions of this thesis related to the learning of *min*-aggregated dynamic programming algorithms. The chapter delves into both the theoretical and practical facets of these algorithms, drawing connections with tropical algebra and introducing strategies to enhance path planning in dynamic programming contexts using learnt heuristics.

In [chapter 5](#), our exploration revolves around the learning of algorithms specifically aimed at combinatorial optimisation problems. This chapter presents empirical validations on the utility of various algorithmic biases, including leveraging strong duality the application of algorithmic priors for solving combinatorial problems.

In [chapter 6](#), we summarise the content of this dissertation, as well as adding some concluding remarks and discuss future research avenues.

Finally, the appendix contains the full list of publications and talks given during my PhD.

Part I

BACKGROUND

2

PRELIMINARIES

In this chapter, we delve into the foundational and theoretical concepts essential to the understanding and development of the research presented in this PhD thesis. This chapter is structured as follows.

The first section, *Graphs*, serves as a basis for comprehending the subsequent topics. Here, we explore the fundamental principles and definitions of graph theory, a branch of mathematics and computer science that deals with the study of graphs and their properties.

The second section, *Combinatorial Optimisation*, delves into the area of combinatorial problems. We define what combinatorial optimisation problems are and discuss their connections to decision problems, as well as introduce a categorisation into different classes of complexity.

Moving forward, the third section, *Algorithms*, delves into the area of computational problem-solving techniques. It discusses the deep interconnection between algorithms and combinatorial optimisation problems, and how the former have historically been applied for solving the latter. We also examine algorithms as discrete functions, discussing the consequential challenges of learning them through gradient-based methods.

The final section, *Graph Networks*, introduces a machine learning paradigm that leverages and processes graph structures. This section provides the necessary background for understanding how graph networks work and their similarities and applications for learning and behaving like algorithms.

2.1 GRAPHS

Graphs are mathematical structures that offer a flexible and powerful framework to model a vast array of real-world systems and phenomena. Their inherent strength lies in the capability to represent pair-wise¹ relationships and dependencies between entities in a simple and visually comprehensible manner. This characteristic positions graphs as the primary choice for modelling complex notions across numerous scientific fields.

In the realm of social sciences, for instance, graphs are instrumental in modeling social networks where nodes represent individuals and edges depict social connections (Nettleton, 2013). This modeling enables deep insights into social dynamics and community structures (Liben-Nowell & Kleinberg, 2003; Kumar et al., 2006, 2022). Similarly, in biological sciences,

¹ For the sake of completeness, in the context of hypergraphs, relationships can extend beyond pair-wise connections to involve multiple entities simultaneously. However, within the context of this thesis we will always consider standard graphs and pair-wise relationships among objects.

graphs have proven useful for enhancing our understanding of genetic networks and protein-to-protein interaction networks, thanks to their inherent ability to represent molecular structures where nodes represent atoms of elements and edges symbolise chemical bonds (Rietman et al., 2011; Winterbach et al., 2013).

The domain of combinatorial optimisation, a branch of mathematics and computer science that seeks optimal solutions in discrete and combinatorial structures, is another key area where graphs are of invaluable importance. A more detailed exploration of combinatorial optimisation problems will be carried out in section 2.2. For the purpose of this section, it is sufficient to mention that numerous combinatorial problems, such as the *Maximum Flow Problem* (Fulkerson et al., 1955) and the *Travelling Salesman Problem* (Robinson, 1949) can be efficiently encoded within the domain of graphs. Not only does this simplify the visualisation of these problems, but also aids in finding solutions, through the use of (graph) algorithms. For instance, transportation is a prime example of the practical usage of graphs in the field of combinatorial optimisation. Here, nodes can represent waypoints like airports or train stations, and edges embody the connections between these points, enabling optimization of route planning (Dantzig & Ramser, 1959), congestion management (Kumar et al., 2005), and infrastructure development (Hakimi, 1964).

In essence, graphs are of fundamental importance in the field of computer science, and the continuing evolution of graph-based methodologies (including in the sphere of deep learning) motivates the necessity for a comprehensive discussion of graphs in the subsequent sections.

2.1.1 Graph Theory

In the field of graph theory, a graph g is defined as a tuple $g = \langle \mathcal{V}, \mathcal{E}, \mathcal{X}_{\mathcal{V}}, \mathcal{X}_{\mathcal{E}} \rangle$. In particular, \mathcal{V} represents a collection of entities known as *nodes*, and \mathcal{E} denotes a set of *edges* (or *links*), expressing relations between elements of \mathcal{V} . $\mathcal{X}_{\mathcal{V}}$ and $\mathcal{X}_{\mathcal{E}}$ indicate the potential set of node and edge features, respectively, providing the possibility to attach useful information to them. Such pieces of information are highly valuable when conducting operations on graphs, such as computing statistics, executing algorithms and extracting potentially useful patterns from them.

Typically, graphs can be classified into different types, mainly depending on the structure of the edge set \mathcal{E} . In the following, we furnish formal definitions of general graph structures and their properties. Unless specified otherwise, most of the definitions hereafter refer to graphs devoid of node and edge features, denoted as $g = \langle \mathcal{V}, \mathcal{E} \rangle$.

Definition 1 (Undirected Graph). *Let g be a graph. Then, g is an undirected graph if and only if the elements in \mathcal{E} are unordered pair of vertices, hence $\mathcal{E} \subseteq \{\{u, v\} \mid u, v \in \mathcal{V}\}$.*

Definition 2 (Directed Graph). *Let g be a graph. Then, g is a directed graph if and only if the elements in \mathcal{E} are ordered pair of vertices, hence $\mathcal{E} \subseteq \{(u, v) \mid u, v \in \mathcal{V}\}$. In such case, u is called head (or source) and v is called tail (or target).*

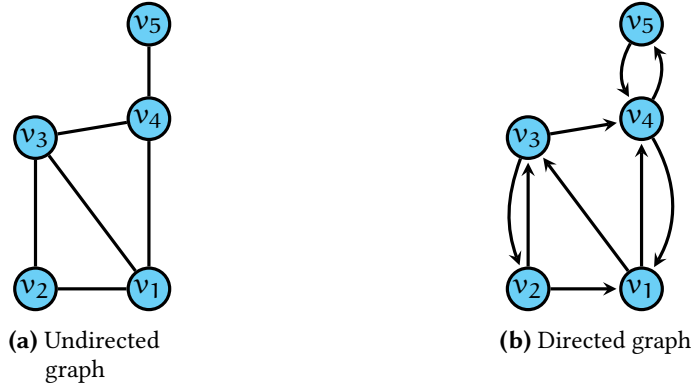


Figure 2.1: Visual representation of undirected and directed graphs. In (b), node adjacencies $\{(v_1, v_4), \{v_2, v_3\}, \{v_4, v_5\}\}$ are bi-directional connections and may be expressed as undirected edges. Equivalently, all edges in (a) may be replaced by two directed edges.

The two above definitions outline the difference between undirected and directed graphs (see illustration in Figure 2.1). In other words, a directed edge (u, v) expresses a unidirectional relation from u to v . It is important to point out that an undirected edge can be thought of as the union of two contrarily oriented edges, i.e. $\{u, v\} = \{(u, v), (v, u)\}$. Therefore, w.l.o.g, we consider undirected graphs as their directed versions, by substituting each non-oriented edge $\{u, v\}$ for two oriented edges (u, v) and (v, u) . For the rest of this thesis, whenever needed, we always refer to undirected edges with curly brackets notation, i.e. $\{u, v\}$ and to directed edges with round brackets, i.e. (u, v) .

Definition 3 (Outgoing/Ingoing Edges). *Let g be a directed graph. The set of outgoing edges of an arbitrary node $v \in \mathcal{V}$ is defined as $\mathcal{E}_v^{\text{out}} = \{(v, x) \mid \forall x \in \mathcal{V} : (v, x) \in \mathcal{E}\}$. The set of ingoing edges of v is then defined as $\mathcal{E}_v^{\text{in}} = \{(x, v) \mid \forall x \in \mathcal{V} : (x, v) \in \mathcal{E}\}$.*

Definition 4 (Adjacency). *Let g be an undirected graph and $u, v \in \mathcal{V}$. Then, u and v are adjacent if $\{u, v\} \in \mathcal{E}$.*

Definition 5 (Adjacency Matrix). *Let g be a graph. The adjacency matrix $\mathbf{A} = [a_{uv}] \in \{0, 1\}^{|\mathcal{V}| \times |\mathcal{V}|}$ is a square matrix where $a_{uv} = \{u, v\} \in \mathcal{E}$.*

The adjacency property of two nodes can be defined for directed graphs as well. The only difference is that the adjacency between two nodes u and v depends on the direction of the edge joining the nodes. More precisely, in a directed graph if $(u, v) \in \mathcal{E}_u^{\text{out}}$, u can be said adjacent to v , but this does not necessarily hold from v to u , unless $(v, u) \in \mathcal{E}_v^{\text{in}}$ too (see nodes u and w in Figure 2.1b).

This entails a subtle difference for an adjacency matrix of an undirected graph and that of a directed one. In particular, in case of undirected graphs, if there is an edge from u to v , there is also an edge for v to u . That means that the adjacency matrix \mathbf{A} is symmetric, i.e. $\mathbf{A} = \mathbf{A}^T$, whereas for a directed graph it may occur that $\mathbf{A} \neq \mathbf{A}^T$.

Definition 6 (Neighbourhood). *Let g be an undirected graph. Let $v \in \mathcal{V}$ be a node of g . Thus, the neighbourhood of v is defined as:*

$$\mathcal{N}(v) = \{x \in \mathcal{V} \mid \{x, v\} \in \mathcal{E}\}.$$

Definition 7 (Node degree). *Let g be an undirected graph. Let $v \in \mathcal{V}$ be a node of g . The node degree $d(v) : \mathcal{V} \rightarrow \mathbb{N}$ is defined as the cardinality of its neighbourhood, i.e. $d(v) = |\mathcal{N}(v)|$.*

Also for neighbourhood and node degree, there is distinction for nodes in undirected graphs and directed graphs. As relations in undirected graphs are symmetric, if $u \in \mathcal{N}(v)$, then $v \in \mathcal{N}_u$ as well. However, in directed graphs there is clear distinction between the set of in-neighbours $\mathcal{N}_v^{\text{in}} = \{x \in \mathcal{V} \mid (x, v) \in \mathcal{E}_v^{\text{in}}\}$ and out-neighbours $\mathcal{N}_v^{\text{out}} = \{x \in \mathcal{V} \mid (v, x) \in \mathcal{E}_v^{\text{out}}\}$, similarly to the concepts of in-going and out-going edges. As a consequence, we derive in-degree and out-degree from in and out neighbours.

Definition 8 (Finite Path). *Let g be a graph. A finite path in g is a sequence of nodes $\pi = v_1 v_2 \dots v_n$ for which it holds that $\forall v_i, v_{i+1} \in \pi : (v_i, v_{i+1}) \in \mathcal{E}$.*

Definition 9 (Finite Cycle). *Let g be a graph. π is a finite cycle if and only if π is a finite path and $\pi = v_1 v_2 \dots v_n v_1$.*

Definition 10 (Reachability). *Let g be a graph and $u, v \in \mathcal{V}$ two arbitrary nodes. We say that u is reachable from v if there exist a path π from u to v , i.e. $\pi = u x_1 x_2 \dots x_n v$, where $x_i \in \mathcal{V}$.*

Definition 11 (Connectivity). *Let g be a graph. g is said to be connected if and only if $\forall u, v \in \mathcal{V}$, v is reachable from u . A graph which is not connected is called disconnected.*

These seemingly simple concepts are of crucial importance for many problems in the real-world. For example, via connectivity and reachability one can verify that a computer network is connected, hence all end-points can communicate with one another. Furthermore, concepts of cycles and paths are at the basis of the class of vehicle routing problems, which are widely used to model real problems such as route-delivery optimisation.

Definition 12 (Hamiltonian Path). *Let g be a graph. π is a hamiltonian path if and only if π is a path such that $|\pi| = |\mathcal{V}|$ and $\forall 1 \leq i < j \leq |\pi| : \pi_i \neq \pi_j$.*

A hamiltonian path can be thought of as a path that passes through every single node exactly once. This concept is of high importance as it is closely related to the more familiar Travelling Salesman Problem (TSP). Consequently, hamiltonian paths are relevant for all families of route optimisation problems as well as task scheduling (Simonin et al., 2011).

Definition 13 (Isomorphism). *Let g and g' be graphs. If there is a bijective function $f : \mathcal{V}_g \rightarrow \mathcal{V}_{g'}$ such that $(u, v) \in \mathcal{E}_g \iff (f(u), f(v)) \in \mathcal{E}_{g'}$, then g and g' are called isomorphic.*

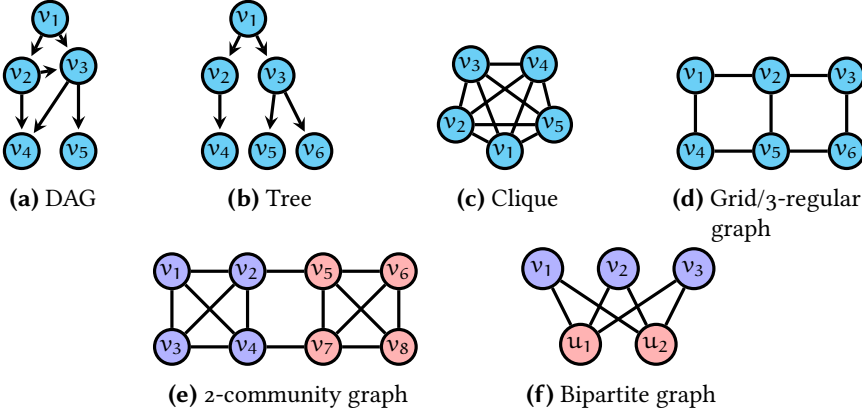


Figure 2.2: Illustration of various graph types. For better clarity, self-loops are not shown. In the grid illustration, v_1, v_3, v_4 and v_6 possess self-loops, ensuring the graph’s 3-regularity.

In simpler terms, two graphs are isomorphic if there is a bijection between their nodes that preserves adjacency. This means that the two graphs are essentially the same graph with a different labelling of nodes. From a machine learning perspective, graph isomorphism are deeply intertwined with the expressive capacity of learning models for graphs. As we will see in [section 2.4](#), graph networks, the central deep learning architectures for learning on graphs, are essentially *structural transductions* and deeply connected to the notion of graph isomorphism. Transductions can be intended as mathematical functions $\mathcal{T} : \mathbb{A} \rightarrow \mathbb{B}$. In the context of deep learning for graphs, any element in \mathbb{A} and \mathbb{B} is assumed to be a graph $g = \langle \mathcal{V}, \mathcal{E}, \mathcal{X}_{\mathcal{V}}, \mathcal{X}_{\mathcal{E}} \rangle$. Now, we conclude this section by discussing IO-isomorphic transductions.

Definition 14 (Skeleton). Let $g = \langle \mathcal{V}, \mathcal{E}, \mathcal{X}_{\mathcal{V}}, \mathcal{X}_{\mathcal{E}} \rangle$ be a graph. The skeleton of g , denoted by $skel(g)$, is the graph obtained by ignoring the set of node and edge features (i.e., $skel(g) = \langle \mathcal{V}, \mathcal{E} \rangle$).

Definition 15 (IO-isomorphism). Let $g = \langle \mathcal{V}, \mathcal{E}, \mathcal{X}_{\mathcal{V}}, \mathcal{X}_{\mathcal{E}} \rangle$ be a graph and let $\mathcal{T} : \mathcal{X} \rightarrow \mathcal{Y}$ be a structural transduction. Then if $\forall g \in \mathcal{X} : skel(g) = skel(\mathcal{T}(g))$, then \mathcal{T} is said to be an IO-isomorphism.

Fundamentally, an IO-isomorphism is a structural transduction that preserves the topology of g , while possibly altering its set of node and edge features. Hence, such transductions can be framed as **graph relabelling** methods, which refer to the process of assigning new labels to the set of nodes (and possibly edges), preserving the underlying structure. Some popular applications of graph relabelling methods involve *graph isomorphism* tests as well as graph processing with deep learning architectures. Both applications will be discussed more thoroughly in the next sections.

2.1.2 Instances of graphs

Above, we introduced the general concept of graph. We can, however, categorise graphs into different families that exhibit a very specific (and similar within the corresponding family) topology. In the following, we discuss some of the most well-known families of graphs that will ease understanding of the research contributions presented in this thesis. [Figure 2.2](#) illustrates a visual example for each type of graphs defined herein.

Definition 16 (Directed Acyclic Graph (DAG)). *A directed graph g is a Directed Acyclic Graph (DAG) if there are no directed cycles. Formally, if $g = (\mathcal{V}, \mathcal{E})$ where $\mathcal{E} \subset \mathcal{V} \times \mathcal{V}$, then g is a DAG if and only if $\nexists v_1, v_2, \dots, v_k \in \mathcal{V}$ such that $(v_i, v_{i+1}) \in \mathcal{E}$ for $1 \leq i < k$ and $(v_k, v_1) \in \mathcal{E}$.*

DAGs are used in many fields including computer science and physics. They are notably used to represent dependencies among tasks, as in a project management tool or in a build system, where each vertex is a task and there is an edge from v to w if task v must be completed before task w can start.

Definition 17 (Tree). *Let g be a DAG. Thus, g is a tree if and only if $\exists! r \in \mathcal{V} . |\mathcal{E}_v^{\text{in}}| = 0$ and $\forall v \in \mathcal{V} \setminus \{r\} : (v, v) \notin \mathcal{E} \wedge |\mathcal{E}_v^{\text{in}}| = 1$.*

Intuitively, each node in a tree can be connected to multiple “successors” (but not itself), and is required to only have one parent (i.e., in-degree must be 1). The only exception is represented by the root node r , which has in-degree equal to 0. A tree can then be categorised as a special case of a DAG. Trees are frequently used as a data structure in computer science to represent hierarchical relations. In fact, as opposed to DAGs, we can always partition the set of nodes in different “sets”, called levels. To easily understand this concept, consider the function $\text{succ}(v) = \{u \mid u \in \mathcal{N}^{\text{out}}(v)\}$ that, given a node v , returns the set of “out neighbours”, called *successors*. Intuitively, we can define the root node r as being at level 0 and its direct successors (i.e., $\text{succ}(r)$) as being at level 1. Consequently, $\text{succ}(\text{succ}(r))$ are at level 2, and so on. This tree-structure underpins, for instance, filesystems in modern operative system ([Mathur et al., 2007](#)) as well as programming languages ([Slonneger & Kurtz, 1995](#)).

Definition 18 (Clique). *Let g be a graph. g is a clique if and only if $\forall u \neq v \in \mathcal{V} : (u, v) \in \mathcal{E}$.*

In other words, each node is connected to every other node. Cliques represent completely interconnected groups of entity. This topology can often be used to represent problems of computational geometry in the form of graphs, such as the convex hull or the aforementioned TSP.

Definition 19 (k-regular graph). *Let g be a graph. g is k-regular if and only if $\forall v \in \mathcal{V} : |\mathcal{N}(v)| = k$.*

Definition 20 (2D grid). *Let g be a graph. g is a 2D grid its nodes and edges can be placed on a regular lattice in two dimensions, such that adjacent nodes are only connected (possibly) to themselves and horizontally and vertically with each other.*

For a visual representation of 2D grids, refer to [Figure 2.2](#). Grid graphs are often used to represent spatial relationships. For instance, in computer vision or image processing, pixels in an image may be treated as nodes of a grid graph, with edges connecting each pixel to its neighbours.

Definition 21 (*k*-community graph). *Let g be a graph. g is a k -community graph if $\exists C_1, C_2, \dots, C_k \subset \mathcal{V} : \mathcal{V} = C_1 \cup C_2 \cup \dots \cup C_k$ and $\forall i \neq j C_i \cap C_j = \emptyset$, and such that $\forall u, v \in C_i, w \in C_j : i \neq j$, the probability that there is an edge (u, v) is higher than the probability that there is an edge (v, w) .*

Hence, a k -community graph is partitioned into k communities C , where a community $C \subset \mathcal{V}$ is a subset of nodes such that the nodes within the community are more densely connected to each other than to the nodes outside the community.

Definition 22 (Bipartite graph). *Let $g = \langle \mathcal{V}, \mathcal{E}, \dots \rangle$ be a graph. g is a bipartite graph if $\exists \mathcal{V}_1, \mathcal{V}_2 \subset \mathcal{V} : \mathcal{V}_1 \cap \mathcal{V}_2 = \emptyset \wedge \mathcal{V} = \mathcal{V}_1 \cup \mathcal{V}_2$ such that $\forall (u, v) \in \mathcal{E} : u \in \mathcal{V}_1 \wedge v \in \mathcal{V}_2$.*

Bipartite graphs can be thought of as two sets of nodes representing different entities which depend on each other. For example, bipartite graphs are exploited to represent the state of mixed integer programs (MIPs), where we aim to find the minimising assignment to a set of variables (\mathcal{V}_1) subjected to a set of constraints (\mathcal{V}_2).

2.1.3 Computational problems on graphs

In this section, we explore some popular computational problems associated with graphs. As we will analyse in [section 2.3](#), these problems are often targeted by algorithms for their resolution and their inherent difficulty can vary widely.

Problem 1 (Reachability). *Let g be a graph and $u, v \in \mathcal{V}$. Then, the reachability problem asks to determine whether there is a path π from node u to node v in the graph.*

Similarly to [Definition 10](#), reachability is the problem of determining whether a certain destination can be reached from a given starting point. This problem forms the basis of many other graph problems, typically in the form of a “subproblem” (i.e., it must be solved prior to resolution of the main problem).

Problem 2 (Shortest path). *Let $g = \langle \mathcal{V}, \mathcal{E}, \mathcal{W} \rangle$ be a graph and $u, v \in \mathcal{V}$, where $w_{uv} \in \mathcal{W}$ is a “weight” assigned to each edge (u, v) in the graph. The shortest path problem asks to find a path $\pi = u \dots v$ such that $c(\pi) = \sum_i w_{\pi_i, \pi_{i+1}}$ is minimum.*

The shortest path problem is common in applications like navigation, where the nodes represent locations and the edge weights represent the cost of traversing that edge (typically in terms of time or distance).

Problem 3 (Minimum Spanning Tree (MST)). *Let $g = \langle \mathcal{V}, \mathcal{E}, \mathcal{W} \rangle$ be an undirected, connected graph. A minimum spanning tree $t \subseteq g$ is a subgraph of g such that t is a tree spanning all the nodes in g and the total weight of the selected edges in t is minimised.*

The MST problem is related to shortest path, and constitutes an important subproblem for a rich collection of more complex graph problems. Indeed, it is used as a subgoal in the popular *Christofides* heuristic (Christofides, 1976), an algorithm that is used to retrieve suboptimal solutions for the TSP.

Problem 4 (Maximum Flow (Max-Flow)). *Let $g = \langle \mathcal{V}, \mathcal{E}, \mathcal{C} \rangle$ be a graph, with $c_{uv} \in \mathcal{C}$ being a “capacity” assigned to each edge (u, v) in the graph. Let $s \in \mathcal{V}$ be the “source” node and $t \in \mathcal{V}$ be the “target” node. The maximum flow problem is concerned with finding a flow $f : \mathcal{E} \rightarrow \mathbb{R}$ such that the total amount of flow from s to t is maximised, and flow assignments f_{uv} do not exceed capacities c_{uv} .*

The Maximum Flow problem models scenarios such as traffic flow or data transfer in a network, where the goal is to maximise the throughput from source to sink. Differently from the presented problems so far, MaxFlow poses additional challenges. In fact, an *optimal* solution for this problem has to satisfy two major constraints. The first one is presented in the above problem definition (i.e., edge capacity constraint), while the second is called *flow conservations*. Respectively, the edge capacity constraint can be described as follows:

$$\forall (u, v) \in \mathcal{E} . f_{uv} \leq c_{uv}, \quad (2.1)$$

whereas flow conservation is formally stated as:

$$\forall u \in \mathcal{V} \setminus \{s, t\} : \left(\sum_{(u,v) \in \mathcal{E}} f_{uv} + \sum_{(v,u) \in \mathcal{E}} f_{vu} \right) = 0 \quad (2.2)$$

$$\wedge \left(\sum_{(s,v) \in \mathcal{E}} f_{sv} = - \sum_{(v,t) \in \mathcal{E}} f_{vt} \right).$$

Equation (2.2) states precisely that all the flow coming out from the source must reach the target node (i.e., their algebraic sum is 0), or, equivalently, that no intermediate node is allowed to retain flow. Typically, MF seeks the maximum solution to (2.1) and (2.2). The entire MF problem can then be mathematically described as:

$$\max \sum_{(s,v) \in \mathcal{E}} f_{sv} \quad \text{subject to } (2.1) \wedge (2.2). \quad (2.3)$$

Problem 5 (Minimum (s, t) Cut (Min-Cut)). *Let $g = \langle \mathcal{V}, \mathcal{E}, \mathcal{W} \rangle$ be a graph, with $w_{ij} \in \mathcal{W}$ being a “weight” assigned to each edge (i, j) in the graph. Let $s, t \in \mathcal{V}$. The minimum (s, t) cut problem seeks to find a partition of nodes $(\mathcal{V}_s, \mathcal{V}_t)$ such that $s \in \mathcal{V}_s$ and $t \in \mathcal{V}_t$ and the sum of the weights w_{ij} associated with edges (i, j) crossing the partition (i.e., $i \in \mathcal{V}_s$ and $j \in \mathcal{V}_t$) is minimised.*

Intuitively, the minimum (s, t) cut problem seeks to identify the set of *bottleneck* edges, such that the sum of their weights is minimal, whose removal *disconnects* s from t . This problem is closely related to maximum flow. Actually, the two problems are linked by the Max-Flow Min-Cut theorem (Dantzig & Fulkerson, 2003), which states that the value of the maximum flow is equal to the value of the minimum cut in a flow network. Furthermore, this theorem establishes a *dual* relation between min-cut and max-flow. Duality is a property of, especially, linear programs, which will be discussed more thoroughly in section 2.2. Both min-cut and max-flow fit in the linear programming framework.

Problem 6 (Travelling Salesman Problem). *Let $g = \langle \mathcal{V}, \mathcal{E}, \mathcal{W} \rangle$ be a clique. Given a starting node v , The Travelling Salesman Problem (TSP) asks for the shortest possible hamiltonian path π that visits each node exactly once and returns to v .*

Problem 7 (Vehicle Routing Problem). *Let $g = \langle \mathcal{V}, \mathcal{E}, \mathcal{W} \rangle$ be a clique. The Vehicle Routing Problem (VRP) is a generalisation of the TSP which asks for n paths π_1, \dots, π_n such that $\pi_1 \cap \dots \cap \pi_n = \emptyset$ and $\pi_1 \cup \dots \cup \pi_n = \mathcal{V}$. Furthermore, each π_i is a hamiltonian path on the subgraph formed by the nodes traversed by π_i .*

TSP and VRP are classic problems in computer science and operations research. They have several practical applications, such as route optimisation for delivery services.

Problem 8 (Vertex K Center Problem). *Let g be a graph. Given $k \in \mathbb{N}$, the Vertex K Center Problem asks for a set of k nodes $C \subseteq \mathcal{V}$ such that the maximum distance from any node to the nearest center in C is minimised.*

The Vertex K Center Problem (Hakimi, 1964) is extremely important to optimise emergency facility locations. For example, in a network representing a city, the vertices could represent potential locations for hospitals, and the goal is to place k hospitals in a way that minimises the maximum distance anyone has to travel to reach the nearest hospital.

2.2 COMBINATORIAL OPTIMISATION

Combinatorial Optimisation (CO) is a branch of computer science which is concerned with finding the best configuration of elements within a discrete and finite set of objects, subject to a (possibly empty) set of constraints. Issues related to CO problems hold substantial practical relevance, especially concerning modern industrial applications. Actually, the Travelling Salesman Problem, described in Problem 6, can be categorised as a combinatorial optimisation problem, with wide-ranging applications spanning from genome arrangement (Sankoff & Blanchette, 1998) and system biology (Johnson & Liu, 2006) to route optimisation (Xu & Che, 2019) and logistics (Baniasadi et al., 2020). Furthermore, the Vertex K Center Problem (Problem 8) may also be considered under the framework of combinatorial optimisation

Formally, a combinatorial optimisation problem is a tuple $\mathcal{P} = \langle \mathcal{J}, \mathcal{F}, m \rangle$, where \mathcal{J} is a set of possible instances for \mathcal{P} , given an instance $p \in \mathcal{J}$, \mathcal{F} is the set of *feasible* solutions (i.e., the ones satisfying all the constraints) and m is the *objective function* which given a feasible solution $y \in \mathcal{F}$, assigns a measure of *quality* to it. Solving p requires finding the optimal solution y^* , which is typically defined as:

$$y^* = \arg \max\{m(y) \mid y \in \mathcal{F}\}. \quad (2.4)$$

W.l.o.g, any combinatorial optimisation problem can be expressed either as a minimisation or a maximisation problem. As in combinatorial problems the optimisation is conducted on (usually large) discrete spaces, graphs serve as a natural framework for encoding such problems, given their inherent ability to represent discrete objects and relations that exist between them. Indeed, all the problems presented in [subsection 2.1.3](#) are combinatorial optimisation problems.

Furthermore, CO problems can vary in complexity, in the sense that given two combinatorial optimisation problems (e.g., TSP and Shortest Path), one may be more difficult than the other. In particular, for each combinatorial problem \mathcal{P} , we can derive its corresponding *decision* problem. The decision version seeks to determine whether there exists a feasible solution y , satisfying a particular measure m_0 . Hence, the main difference between combinatorial and decision problems lies in the output space of solutions. In particular, the latter asks a question that requires a binary solution (i.e., *yes* or *no*), whereas a solution to the former is an assignment of the problem variables. Notwithstanding this distinction, the close relation between combinatorial and decision problems enables to (informally) “categorise” combinatorial problems in the well-known classes of complexity which are originally defined for their decision versions: P, NP, NP-Complete and NP-Hard. A more comprehensive exploration of the differences between these classes will be provided in [subsection 2.2.1](#).

2.2.1 The P vs NP dilemma

Leveraging their connection to decision problems, combinatorial optimisation problems can be classified into a well-defined stratification of complexity classes. Although there exist a variety of different complexity classes and different categorisations, here we focus on a small fraction (but arguably the most crucial): P and NP.

P is defined as the class of problems that can be solved efficiently in *polynomial time*. In other words, the time required to find an optimal solution to these problems is proportional to a polynomial function of the problem’s size. Precisely, given a problem \mathcal{P} , there exists an algorithm A that can solve optimally all of its instances $p \sim \mathcal{P}$ in at most $O(n^k)$ operations, where n is p ’s size and k is some constant.

NP, instead, is the class of problems that can be *verified* in polynomial time. This means that if we had a *certificate* of a solution, we could use it to verify that the given solution is correct in polynomial time.

A straightforward consequence of these definitions is that $P \subseteq NP$, namely any problem *solvable* in polynomial time is also trivially *verifiable*

in polynomial time. The converse implication (i.e., $\text{NP} \subseteq \text{P}$), which asks whether a problem that is verifiable in polynomial time can also be solved efficiently is, however, still unverified. This constitutes the popular P vs NP question (Cook, 2000) and is arguably the most fundamental question within the field of computer science.

Furthermore, broader categories such as NP-completeness (NP-C) and NP-hardness (NP-H) are usually defined to account for the most challenging computational problems within NP and beyond. Informally, NP-C consists of problems that are both in NP and are “at least as hard” as any other problem in NP. NP-H, instead, includes problems for which verifiability is not even possible in polynomial time (thus, they may not even be in NP itself), making them the hardest problems to deal with.

The consequence of the P vs NP dilemma is that, at the time of writing, for some challenging NP-C and NP-H problems there exists no polynomial-time exact algorithm for solving them. This implies that for many practical problems of interests, we have to rely on polynomial-time approximation algorithms, also referred to as *heuristics*. When employing such strategies, the focus becomes to find “good” solutions in a reasonable amount of time, even though they are not optimal. Certainly, *exact* algorithms still exist but they require exponential time (i.e., $O(k^n)$), often making their use infeasible for practical large-scale problems.

Historically, development of specialised heuristics for NP-C/NP-H combinatorial problems has been a central topic in combinatorial optimisation and computer science for a very long time (Robinson, 1949; Fulkerson et al., 1955; Dantzig & Ramser, 1959; Hakimi, 1964). Such heuristics typically require significant expertise and effort in their development and engineering.

2.2.2 Linear Programming

Linear Programming (or *linear programs*) (LP), is a mathematical framework used to model a variety of combinatorial optimisation problems where dependencies between the problem variables and between the problem constraints can be expressed using linear relationships. Mathematically, a LP can be phrased as:

$$\min \left\{ \mathbf{c}^\top \mathbf{x} \mid \mathbf{x} \in \mathbb{R}^n \wedge \mathbf{A}\mathbf{x} \leq \mathbf{b} \wedge \mathbf{x} \geq 0 \right\}. \quad (2.5)$$

Here, \mathbf{c} is the vector of coefficients for the objective function, \mathbf{x} is the vector of variables, \mathbf{A} is the matrix of coefficients for the constraints, and \mathbf{b} is the vector of constants in the constraints.

In many practical situations, however, the variables of a problem must take on integer values. This leads to the concept of Integer Linear Programming (ILP), where the constraints are linear, as in LP, but some constraints may enforce integrality of some problem variables:

$$\min \left\{ \mathbf{c}^\top \begin{bmatrix} \mathbf{x} \\ \mathbf{y} \end{bmatrix} \mid \mathbf{x} \in \mathbb{R}^{n-k} \wedge \mathbf{y} \in \mathbb{Z}^k \wedge \mathbf{A}\mathbf{x} \leq \mathbf{b} \wedge \mathbf{x} \geq 0 \right\}. \quad (2.6)$$

Despite their apparent simplicity, LP and ILP accounts for a multitude of problems of practical relevance. By extension, ILP broadens the applicability of LP to problems requiring discrete solutions. For instance, equation (2.3) is actually a LP. More in general, all problems presented in subsection 2.1.3 find their representations within either the LP (e.g., max-flow/min-cut) or the ILP framework (e.g., TSP and Shortest Path).

2.2.3 Duality

The concept of duality is of fundamental importance in the theory of linear programming. Specifically, duality establishes a relationship between a given LP problem, known as the *primal problem*, and another LP problem called the *dual problem*. In the duality theory, these two problems are tightly connected and interesting properties arise from their relation. Notably, the dual problem is derived from the primal problem and possesses the characteristic that the optimal value of the dual problem provides a bound (either upper or lower) on the optimal value of the primal problem. In order to see such upper/lower bound relationship, first consider the primal LP problem in explicit form as follows:

$$\begin{aligned} & \underset{\mathbf{x}}{\text{maximise}} && \mathbf{c}^\top \mathbf{x} \\ \text{(P)} & \text{subject to} && \mathbf{A}\mathbf{x} \leq \mathbf{b} \\ & && \mathbf{x} \geq 0, \end{aligned} \tag{2.7}$$

which is equivalent to (2.5). From (P), the dual problem (D) is constructed by introducing a vector of dual variables \mathbf{y} corresponding to the constraints of the primal problem. The dual problem can thus be formulated as follows:

$$\begin{aligned} & \underset{\mathbf{y}}{\text{minimise}} && \mathbf{b}^\top \mathbf{y} \\ \text{(D)} & \text{subject to} && \mathbf{A}^\top \mathbf{y} \geq \mathbf{c} \\ & && \mathbf{y} \geq 0. \end{aligned} \tag{2.8}$$

By analysing (2.7) and (2.8), we note that the dual problem is a maximisation problem if the primal problem is a minimisation problem (and viceversa). The *Weak Duality Theorem* formally establishes the bound relationship between (P) and (D). W.l.o.g, assuming a maximisation (P) and a minimisation (D), then the Weak Duality Theorem is stated as follows:

Theorem 1 (Weak Duality Theorem). *Let \mathbf{x}_0 be a feasible solution of the primal problem (P). Let \mathbf{y}_0 be a feasible solution of the dual problem (D). Then:*

$$\mathbf{b}^\top \mathbf{y}_0 \geq \mathbf{c}^\top \mathbf{x}_0.$$

In essence, this theorem guarantees that the objective value of the dual solution will always be greater than or equal to the objective value of the primal solution. Conversely, if (P) is a minimization problem and (D)

is a maximization problem, the theorem's conclusion would be $\mathbf{c}^\top \mathbf{x}_0 \geq \mathbf{b}^\top \mathbf{y}_0$.

Furthermore, relationship between a (P) and a (D) can be even stronger. Specifically, solving one of the two problems might yield an objective function value that exactly matches that of its counterpart. This concept is formally captured in the *Strong Duality Theorem*:

Theorem 2 (Strong Duality Theorem). *If the primal problem (P) has an optimal solution \mathbf{x}^* , then the dual problem (D) also has an optimal solution \mathbf{y}^* , and the optimal values of the primal and dual problems are equal, that is,*

$$\mathbf{b}^\top \mathbf{y}^* = \mathbf{c}^\top \mathbf{x}^*.$$

Both strong and weak duality have practical implications of significant value. In particular, the aforementioned bound relations underpin various algorithms and optimization techniques in combinatorial optimisation. Notable examples in this regards are the *simplex method* (Dantzig, 1990) and the family of *branch-and-bound* methods, effectively showing practical relevance of duality even in the context of ILP. Another notable implication is that duality provides a framework for establishing relationships between seemingly different optimisation problems. Indeed, the dual of one problem may correspond to another combinatorial problem of practical relevance. Max-flow and min-cut, as discussed earlier in [subsection 2.1.3](#), are a well-known example of such a connection.

To conclude this section, duality is then a significant concept in combinatorial optimisation. As we will see in the next chapters of this thesis, duality is at the basis of one of the developed approaches for learning algorithms during this thesis work.

2.3 ALGORITHMS

Algorithms lie at the heart of computer science and discrete mathematics, encompassing principles, methodologies, and techniques that form the building blocks of computational problem-solving. The study and development of algorithms influence multiple areas, ranging from mathematics to biology and (combinatorial) optimisation. Recently, algorithms have made their way into artificial intelligence models, aiming at empowering learning models by leveraging the inherent *reasoning* capabilities of these paradigms. The task of teaching algorithms, however, presents substantial challenges, particularly for gradient-based methods. In this section, we establish the notation used to represent algorithms, essential for comprehending the precise ways in which algorithms can be processed and learnt (which will be analysed in the following chapters). Additionally, we discuss the main difficulties algorithms present to machine learning models and discuss several graph algorithms within the context of the previously introduced notation.

2.3.1 A simple notation for representing algorithms

An algorithm is typically defined as a computational procedure that, taken an input, performs a *sequence* of well-defined instructions on that input to eventually produce an output (Cormen et al., 2009). At a high level, algorithms operate similarly to mathematical functions $f : \mathbb{A} \rightarrow \mathbb{B}$, in the sense that they accept an input and produce an output (both possibly multidimensional). The subtle difference lies in the fact that, while functions simply establish a relation between an input and a output (i.e., $f(\mathbf{a}) = \mathbf{b}$), algorithms lay out the exact procedure needed to convert input \mathbf{a} to output \mathbf{b} . This procedure can be considered as a *reasoning* process, where we apply the sequence of algorithm steps, denoted as A_t , to slowly transform \mathbf{a} to \mathbf{b} :

$$\mathbf{a} \xrightarrow{A_0} \mathbf{a}^{(1)} \xrightarrow{A_1} \dots \xrightarrow{A_{T-2}} \mathbf{a}^{(T-1)} \xrightarrow{A_{T-1}} \mathbf{b}.$$

As outlined above, then, an algorithm A is composed of a set of inputs, a set of *intermediate* transformations of the inputs (i.e., *hints*), and the set of final outputs. For the rest of this thesis we will always refer to and consider an algorithm A as the set of its input, hints and output. The whole set of hints plus the final output is referred to as *algorithm trajectory*. Furthermore, as we will explore in the next sections, algorithms usually store and use (some of) the intermediate hints $\{\mathbf{a}^{(1)}, \dots, \mathbf{a}^{(T-1)}\}$ for subsequent steps. This is why these types of algorithms are often referred to as *iterative algorithms*, emphasising that the solution is constructed through a series of iterations where the output of an iteration may become (part of) the input for the subsequent step. It is not unusual that at time t , $\mathbf{a}^{(t)}$ represents the complete *state* of algorithm A , meaning that no additional information beyond $\mathbf{a}^{(t)}$ is required to compute the value at step $t + 1$. In this scenario, the hint $\mathbf{a}^{(t)}$ becomes the new input for the computation of $\mathbf{a}^{(t+1)} = A_t(\mathbf{a}^{(t)})$. As we will explore in [subsection 2.3.4](#), this concept holds true for a considerable number of important algorithms.

2.3.2 Algorithmic guarantees

In the preceding section, we explored the notion that algorithms are fundamentally a series of *extremely specific* instructions. When executed in the correct sequence, these instructions invariably produce a predictable outcome. Indeed, the main criterion for labeling a sequence of instructions as an algorithm is that they must be unambiguous, leaving no possibility for misinterpretation. Specifically, any given instruction I , when applied to a well-defined state S_t , will result in a well-defined subsequent state S_{t+1} . In simpler terms, given our knowledge of the characteristic of a state S_t and the *effect* that a specific instruction will have when applied to it, we can invariably *predict* the subsequent state S_{t+1} , for any possible instantiation of the state S_t .

This intuition is at the core of algorithms, and it is referred to as *correctness* of algorithms. In essence, an algorithm is provably correct when,

for any input that meets a set of specified *preconditions*, it invariably produces an output that meets a set of specified *postconditions* (i.e., “correct” output). This implies that, when analysing the correctness of a specific algorithm A , it is crucial to define precisely which states S_t can be processed by the instructions of A . This reasoning applies all the way back to S_0 , effectively imposing constraints on the inputs and thus establishing the acceptable inputs values of A (i.e. preconditions).

Given these two “ingredients” (i.e., well-definess of the states and specificity of the instructions), an algorithm is ensured to operate within a clearly defined space, and its dynamics can be analysed and proven correct. This is, perhaps, the most important feature of algorithmics in general, as it enables us to confirm with certainty that an algorithm will consistently produce the correct output for a given set of inputs.

2.3.3 Algorithms as discrete functions

In the domain of deep learning and neural networks, the predominant use case is approximating continuous functions. Indeed, the *Universal Approximation Theorem* (Hornik et al., 1989) for neural networks essentially states that feedforward networks with (at least) a single hidden layer containing a finite number of neurons can approximate *any* continuous functions on compact subsets of \mathbb{R}^n , under mild assumptions on the activation functions. This theorem however, does not extend to the learnability of discrete functions. Previously, we mentioned that algorithms can be thought of as being similar to mathematical functions. If analysed under this lens, however, the *modus operandi* of algorithms makes them resemble discrete functions rather than continuous functions, since algorithms involve discrete operations and decisions.

Take, for instance, the algorithm of searching an element within a list of integers. This algorithm can be represented as a function $A : \mathbb{L} \times \mathbb{N} \rightarrow \{0, 1\}$ (with \mathbb{L} being the space of all possible lists) such that:

$$A(L, x) = \begin{cases} 1 & \text{if } x \in L \\ 0 & \text{otherwise} \end{cases} . \quad (2.9)$$

Similarly, consider the operation of pushing an element e onto a stack or queue Q :

$$\text{push}(Q, e) = Q' = Q \cup \{e\}. \quad (2.10)$$

It is evident from the aforementioned examples that these algorithms can indeed be framed as discrete functions and, as such, do not admit differentiability across their entire domain. This poses a challenge when we wish to integrate such functions into neural network architectures, which inherently rely on the notion of gradients and differentiability to learn and adapt. This is a problem not only when considering end-to-end learnability of algorithms, but also when we plan to integrate neural networks with external memory modules, such as queues. Push and pop operations to and from these types of memories do not provide

the necessary gradients to enable gradient-based optimisation of neural networks.

2.3.4 Graph algorithms

Here, we present and discuss a selection of relevant *graph algorithms* (i.e., algorithms designed to operate on graphs). We explore in detail how these algorithms play an important role in solving common combinatorial problems, such as shortest path, max-flow and the TSP. We anticipate that many of the algorithms discussed herein form the backbone of many of the research investigations undertaken and presented in this dissertation.

BELLMAN-FORD ALGORITHM. The Bellman-Ford algorithm (Bellman, 1958) is a computational procedure designed to solve the shortest path problem (see Problem 2) in weighted graphs $g = \langle \mathcal{V}, \mathcal{E}, \mathbf{W} \rangle$. A pseudocode for Bellman-Ford is provided in Algorithm 1.

Algorithm 1 Bellman-Ford algorithm

```

1: procedure BELLMANFORD( $g, s$ )
2:   for all node  $v$  in  $\mathcal{V}_g$  do
3:      $d[v] \leftarrow \infty$ 
4:      $\text{pred}[v] \leftarrow \text{NULL}$ 
5:    $d[s] \leftarrow 0$ 
6:   for  $i = 1$  to  $|\mathcal{V}_g| - 1$  do
7:     for all edge  $(u, v)$  in  $\mathcal{E}_g$  do
8:       if  $d[v] > d[u] + w_{uv}$  then
9:          $d[v] \leftarrow d[u] + w_{uv}$ 
10:         $\text{pred}[v] \leftarrow u$ 
11:  return  $\langle d, \text{pred} \rangle$ 

```

If analysed under the notation presented in subsection 2.3.1, Bellman-Ford can be decomposed in input, hints and output. Precisely, $\text{input} = \{\mathbf{A}, \mathbf{W}, s, \mathbf{d}^{(0)}\}$, where \mathbf{A} and \mathbf{W} are, respectively, the adjacency matrix and weight matrix of the graph, s is the source node and $\mathbf{d}^{(0)}$ is the initial estimates of the shortest paths from s to all other nodes in the graph. The algorithm begins by initialising distances to the source node as 0 and to all other nodes as $+\infty$. It then performs a sequence of intermediate transformations of the inputs, called *relaxation* steps, in order to transform the initial distance vector $\mathbf{d}^{(0)}$ to the final distance vector \mathbf{d} :

$$\mathbf{d}^{(0)} \xrightarrow{A_0} \mathbf{d}^{(1)} \xrightarrow{A_1} \dots \xrightarrow{A_{|\mathcal{V}|-2}} \mathbf{d}^{(|\mathcal{V}|-1)} \xrightarrow{A_{|\mathcal{V}|-1}} \mathbf{d}.$$

Here, the set of intermediate distance vectors $\mathbf{d}^{(t)}$ represents the set of hints of the algorithm (i.e., $\text{hints} = \{\mathbf{d}^{(1)}, \dots, \mathbf{d}^{(|\mathcal{V}|-1)}\}$). Furthermore, at each step t , the algorithm iteratively relaxes all the edges, comparing the current distance estimate $d[u]^{(t)}$ with the sum of the distance estimate of a neighbouring node $d[v]^{(t)}$ and the weight of the edge connecting

them, w_{uv} , and updating it if a shorter path is found. Mathematically, the relaxation step for node u can be formulated as:

$$d^{(t+1)}[u] = \min\{d^{(t)}[u], \min\{d^{(t)}[v] + w_{uv} \mid v \in \mathcal{N}(u)\}\}. \quad (2.11)$$

The final output is thus the final vector of distances $\mathbf{d}^{|\mathcal{V}|} = \mathbf{d}$, alongside the vector pred , where $\text{pred}[u]$ accounts for the *predecessor* of node u in the final shortest path $s \rightsquigarrow u$.

DIJKSTRA'S ALGORITHM. The Dijkstra's algorithm (Dijkstra et al., 1959) is perhaps the most popular shortest path algorithm. Essentially, it solves the exact same problem as Bellman-Ford. As such, the sets of input, hints and output are unchanged compared to those of Bellman-Ford. Pseudo-code is provided in Algorithm 2.

Algorithm 2 Dijkstra's algorithm

```

1: procedure DIJKSTRA( $g, s$ )
2:   for all vertex  $v$  in  $\mathcal{V}_g$  do
3:      $d[v] \leftarrow \infty$ 
4:      $\text{pred}[v] \leftarrow \text{NULL}$ 
5:    $d[s] \leftarrow 0$ 
6:    $Q \leftarrow \mathcal{V}_g$ 
7:   while  $Q \neq \emptyset$  do
8:      $u \leftarrow \text{extract-min}(Q, d[u])$ 
9:     remove  $u$  from  $Q$ 
10:    for all neighbor  $v$  of  $u$  in  $Q$  do
11:      if  $d[v] > d[u] + w_{uv}$  then
12:         $d[v] \leftarrow d[u] + w_{uv}$ 
13:         $\text{pred}[v] \leftarrow u$ 
14:  return  $\langle d, \text{pred} \rangle$ 

```

Notably, Dijkstra improves on Bellman-Ford by utilising a priority queue (line 8) for selecting the next node to evaluate during shortest path computation.

BREADTH FIRST SEARCH. The Breadth First Search (BFS) (Cormen et al., 2009) is an algorithm for solving the reachability problem (Problem 1) in graphs $g = \langle \mathcal{V}, \mathcal{E}, \dots \rangle$. We can break down BFS in input, hints and output, similarly to Bellman-Ford. In this case, $\text{input} = \{\mathbf{A}, s\}$, where \mathbf{A} and s are analogous to Bellman-Ford (i.e., adjacency matrix and source node). The $\text{hints} = \{\mathbf{r}^{(1)}, \dots, \mathbf{r}^{(|\mathcal{V}|-1)}\}$ represent all intermediate steps, where $r_v^{(t)} \in \{0, 1\}$ indicates whether node v is reachable from s using at most t edges. Final output can be considered to be the vector $\mathbf{r}^{(|\mathcal{V}|)}$. A pseudocode for the BFS procedure is provided in Algorithm 3.

PRIM'S ALGORITHM. The Prim's algorithm (Cormen et al., 2009) computes the MST (see Problem 3) of weighted graphs. Its pseudocode is reported in Algorithm 4.

Algorithm 3 Breadth-First Search algorithm

```

1: procedure BFS( $g, s$ )
2:   for all node  $v$  in  $\mathcal{V}_g$  do
3:      $r[v] \leftarrow 0$ 
4:    $r[s] \leftarrow 1$ 
5:   initialise an empty queue  $Q$ 
6:   push( $Q, s$ )
7:   while  $Q$  is not empty do
8:      $v \leftarrow \text{pop}(Q)$ 
9:     for all  $u$  in  $\mathcal{N}(v)$  do
10:      if  $r[u] = 0$  then
11:         $r[u] \leftarrow 1$ 
12:        push( $Q, u$ )
13:   return  $r$ 

```

Algorithm 4 Prim's algorithm

```

1: procedure PRIM( $g$ )
2:   for all node  $v$  in  $\mathcal{V}_g$  do
3:      $\text{key}[v] \leftarrow \infty$ 
4:      $\text{pred}[v] \leftarrow \text{NULL}$ 
5:   Pick any node  $s$ 
6:    $\text{key}[s] \leftarrow 0$ 
7:    $Q \leftarrow \mathcal{V}_g$ 
8:   while  $Q \neq \emptyset$  do
9:      $u \leftarrow \text{extract-min}(Q, \text{key}[s])$ 
10:    for all node  $v$  adjacent to  $u$  do
11:      if  $v \in Q$  and  $w_{uv} < \text{key}[v]$  then
12:         $\text{pred}[v] \leftarrow u$ 
13:         $\text{key}[v] \leftarrow w_{uv}$ 
14:   return  $\langle \text{key}, \text{pred} \rangle$ 

```

As can be seen by comparison with [Algorithm 2](#), the Prim's algorithm and Dijkstra bear a noticeable resemblance, as they both employ the use a greedy strategy for updating the paths and a priority queue. Decomposition to input , hints , output is then derived similarly to Dijkstra. Specifically, $\text{input} = \{\mathbf{A}\}$, $\text{hints} = \{\text{key}^{(1)}, \text{pred}^{(1)}, \dots, \text{key}^{(n)}, \text{pred}^{(n)}\}$ and $\text{output} = \{\text{key}, \text{pred}\}$.

FORD-FULKERSON. The Ford-Fulkerson algorithm ([Ford & Fulkerson, 1956](#)) is used to compute the maximum flow in a capacitated graph (see [Problem 4](#)). We provide the pseudocode for Ford-Fulkerson in [Algorithm 5](#).

Algorithm 5 Ford-Fulkerson algorithm

```

1: procedure FORDFULKERSON( $g, s, t$ )
2:   for all edge  $(u, v)$  in  $\mathcal{E}_g$  do
3:      $f_{uv} \leftarrow 0$ 
4:   while  $\exists$  augmenting path  $\pi = s, \dots, t$  in  $g_f$  do
5:      $df = \min\{c_{uv} : (u, v) \in \pi\}$ 
6:     for all edge  $(u, v)$  in  $\pi$  do
7:        $f_{uv} \leftarrow f_{uv} + df$ 
8:        $f_{vu} \leftarrow f_{vu} - df$ 
9:   return  $f$ 

```

Differently from the previous algorithms, Ford-Fulkerson is composed of two distinct sub-routines: (i) finding an *augmenting path* from s to t (i.e., a path within a residual graph² that allows for increased flow through the network); (ii) update the flow assignment $f^{(t)}$. In [Algorithm 5](#), sub-routine (i) is encoded at line 4, whereas (ii) spans line 5–8. Furthermore, sub-routine (i) can be implemented as the Bellman-Ford algorithm.

At high level, the algorithm looks for an augmenting path from the source s to the target t in the residual graph g_f , through, say, the Bellman-Ford algorithm. The flow is then augmented along this path by the bottleneck capacity, the minimum remaining capacity of the edges in the path. The iterative process continues until no augmenting paths can be found in the residual graph. The final f represents the maximum flow from source to target.

By following our notation, thus, $\text{input} = \{\mathbf{A}, \mathbf{C}, s, t, f^{(0)}\}$ plus all the inputs that are inherited from the Bellman-Ford procedure. Similarly, hints also contains all the previously defined Bellman-Ford hints, with the addition of the sequence of flow transformations $\{f^{(1)}, \dots, f^{(T-1)}\}$. Finally, $\text{output} = \{f\}$.

CHRISTOFIDES' ALGORITHM. The Christofides algorithm, whose pseudo-code is presented in [Algorithm 6](#), is the first example of a polynomial-time algorithm for finding approximate solution to a NP-H problem, namely the TSP ([Problem 6](#)).

² A residual graph is a representation of the remaining capacity of edges in a flow network after some flow has been pushed through.

Algorithm 6 Christofides' algorithm

```

1: procedure CHRISTOFIDES( $g$ )
2:    $T \leftarrow \text{COMPUTEMST}(g)$ 
3:    $O \leftarrow \text{GETODDDEGREEENODES}(T)$ 
4:    $M \leftarrow \text{COMPUTEMINWEIGHTPERFECTMATCHING}(O)$ 
5:    $H \leftarrow T \cup M$ 
6:    $E' \leftarrow \text{COMPUTE EULERIANPATH}(H)$ 
7:    $C \leftarrow \text{Hamiltonian cycle from } E'$ 
8:   return  $C$ 

```

It operates by employing a series of algorithmic primitives, combining them in a unique way to construct a feasible tour:

1. **Minimum Spanning Tree:** first, the algorithm finds a minimum spanning tree of the given graph.
2. **Minimum Weight Perfect Matching:** ensures that all nodes in the MST have an even degree by executing a minimum weight perfect matching on all nodes with an odd degree. This is a crucial step for forming Eulerian cycles.
3. **Eulerian Circuit:** forms an Eulerian cycle by combining the previous two steps.
4. **Hamiltonian Circuit:** an Hamiltonian cycle is derived from the Eulerian path by skipping visited nodes.

An interesting property of the Christofides algorithm lies in its guarantee – it assures a solution within a $\frac{3}{2}$ factor from the optimal TSP tour. Notably, the Christofides algorithm is not the only example of approximation heuristics that leverage strong algorithmic primitives. In fact, the Clarke-Wright savings algorithm (Doyuran & Çatay, 2011) computes solution for VRP instances by leveraging lists and sorting algorithms.

GON ALGORITHM. Similarly to the Christofides' algorithm, the Gon algorithm (Gonzalez, 1985; Dyer & Frieze, 1985) is a 2-approximation strategy for the VKC problem (Problem 8). The algorithm proceeds to find 2-approximate solutions by arbitrarily choosing a “center” node v_1 to add to the center set C , and then iteratively selecting the additional centers v_i . The new v_i are chosen such that v_i is the farthest away from the already selected centers in C . For consistency with other algorithms, we report Gon's pseudocode in Algorithm 7.

GRAPH ISOMORPHISM. In subsection 2.1.1, we introduced the notion of *graph isomorphism*. When observed in the context of decision problems, this concept holds immense theoretical significance. Indeed, determining whether two graphs are isomorphic is recognized as an NP problem, but its classification as either a P problem or an NP-complete problem remains an open question (Garey & Johnson, 1979). Interestingly, it is also

Algorithm 7 Gon algorithm

```

1: procedure GON( $G, k$ )
2:   Choose an arbitrary node  $v_1$  from  $G$  and add it to center set  $C$ 
3:   for  $i = 2$  to  $k$  do
4:     Choose a vertex  $v_i$  that is farthest from the centers already in
      $C$ 
5:     Add  $v_i$  to  $C$ 
6:   return  $C$ 

```

a potential candidate for the class of NP-intermediate problems (NPI), a class that would only exist if $P \neq NP$. Consequently, finding a solution to the graph isomorphism problem would be a crucial step in answering the long-debated $P \stackrel{?}{=} NP$ question.

Algorithm 8 Weisfeiler-Lehman graph isomorphism test

```

1: procedure WLTEST( $g_1, g_2$ )
2:    $c_1^0 \leftarrow$  INITIALCOLORING( $g_1$ )
3:    $c_2^0 \leftarrow$  INITIALCOLORING( $g_2$ )
4:   while colors have not converged do
5:      $c_1^{t+1} \leftarrow$  UPDATECOLORING( $g_1, c_1^t$ )
6:      $c_2^{t+1} \leftarrow$  UPDATECOLORING( $g_2, c_2^t$ )
7:   return HAVESAMEDISTRIBUTION( $C_1, C_2$ )
8: procedure UPDATECOLORING( $g, c$ )
9:   Update coloring  $c$  based on equation (2.12)
10: procedure HAVESAMEDISTRIBUTION( $c_1, c_2$ )
11:   Check if the color distributions in  $c_1$  and  $c_2$  are the same

```

Since, as discussed in subsection 2.2.1, the debate is still unresolved, we have to rely to approximation strategies for the graph isomorphism problem. In this regard, the most popular algorithm is the *Weisfeiler-Lehman test* (Lehman & Weisfeiler, 1968). A pseudo-code for the WL test algorithm is given in Algorithm 8. In essence, the WL test is a graph coloring algorithm, which assigns an initial color c to each node of the graph and iteratively updates this coloring based on the distribution of colors in the neighbouring nodes, for each node. The iterative update can be formulated as:

$$c^{t+1}(v) = h(c^t(v), \oplus(\{c^t(u) \mid u \in \mathcal{N}(v)\})), \quad (2.12)$$

where, \oplus is a function that transforms a multiset of colors into a sequence of colors and h is a hash function that generates a new color based on the current color of a vertex and the colors of its neighbouring nodes. The choice of h and \oplus depends on practical implementation. Usually, \oplus is a function that sorts the colors in a multiset in a consistent way (typically by imposing a total order on the colors), and h is chosen to meet the typical requirements of hash functions (i.e., avoiding hash collisions). Such node-coloring scheme, however, has some limitations. In fact, the

Weisfeiler-Lehman test may erroneously classify two non-isomorphic graphs as isomorphic. However, the converse is accurate. In other words, if the WL test determines that two graphs are not isomorphic, then it is certain that the two graphs are not isomorphic.

In order to distinguish non-isomorphic graphs more effectively, we can create a hierarchy of higher-order WL tests, which are commonly referred to as k -WL, with k being the dimensionality of the coloring node vector. As equation (2.12) only uses a single color for each node, it is also known as 1-WL. Finally, we anticipate that the WL-test is tightly connected to machine learning models and neural networks that operate on graphs. We will explore this connection more deeply in section 2.4.

2.3.5 Dynamic programming

Dynamic Programming (DP) is a powerful computational paradigm (Bellman, 1966) that targets complex problems by breaking them down into simpler, overlapping subproblems, solving each subproblem just once, and building up the solution to the original problem from these solutions. DP finds applications in many areas of computer science, such as operations research (Bellman & Dreyfus, 2015), bioinformatics (Giegerich, 2000), and artificial intelligence (Bertsekas & Tsitsiklis, 1995; Lewis & Vrabie, 2009). Formally, a DP algorithm can be framed as:

$$S_i^{(k+1)} = U(\{S_j^{(k)} \mid j = 1, \dots, n\}), \quad (2.13)$$

where $S_i^{(k)}$ represents the solution of the i -th subproblem at iteration k , and U updates the solution at step $k + 1$ based on all solutions at the previous step k . Usually, practical applications assume the existence of some metric m that is set to be either minimised or maximised, in which case U is chosen to be either \min or \max .

In general, DP assumes that the optimal solution to a problem can be constructed from optimal solutions of its subproblems. This assumption is usually referred to as *principle of optimality* (Henig, 1985). A popular example of a DP algorithm is the Bellman-Ford algorithm (presented in the previous section) in the sense that it solves the shortest path problem by following the principle of optimality. Precisely, the shortest path problem $u \rightsquigarrow v$ through exactly k edges depends on the shortest path problem $u \rightsquigarrow v$ through exactly $k - 1$ edges. In simpler terms, an optimal solution to $d^{(k)}[v]$ (i.e., vector of distances in Bellman-Ford) requires an optimal solution to $d^{(k-1)}[v]$. Additionally, this property can be derived from equation (2.11). Indeed, one can note that (2.11) is a special case of (2.13), where we replace U with \min and the solutions $S_j^{(k)}$ with $d^{(k)}[j] + w_{ij}$ (i.e., w_{ii} is assumed zero).

TROPICAL ALGEBRA. In the context of dynamic programming, it is often noteworthy to discuss a closely related field, which is that of Tropical Algebra (Brugalle et al., 2000). Tropical algebra provides a mathematical framework that performs arithmetic operations on alternative semirings (usually referred to as *tropical semiring*) rather than the “conventional”

one defined on the real numbers (i.e., $\langle \mathbb{R}, +, \cdot, 0, 1 \rangle$). Formally, a semiring is an algebraic structure of the form $\langle \mathbb{A}, \oplus, \odot, \text{id}_\oplus, \text{id}_\odot \rangle$ where:

1. \mathbb{A} is a set, such as the set of real numbers \mathbb{R} or natural numbers \mathbb{N} .
2. \oplus is a commutative *binary* operation, called *addition*.
3. \odot is *binary* operation, called *multiplication*.
4. id_\oplus is the *identity* element of addition, such that $\forall a \in \mathbb{A} : (a \oplus \text{id}_\oplus) = (\text{id}_\oplus \oplus a) = a$. Additionally, id_\oplus acts as an *absorbing* element with respect to multiplication (i.e., $\forall a \in \mathbb{A} : (a \odot \text{id}_\oplus) = \text{id}_\oplus$).
5. id_\odot is the *identity* element of multiplication, such that $\forall a \in \mathbb{A} : (a \odot \text{id}_\odot) = a$.

Thus, tropical semirings are actually a *collections* of semirings (see (Litvinov & Maslov, 1998) for a comprehensive overview), where we “swap” the usual arithmetic operations of addition $\oplus = +$ and multiplication $\odot = \cdot$ with different operators, typically chosen to reflect operations common to DP algorithms. Specifically, one instance of a tropical semiring is the *min-plus* semiring, defined as $\langle \mathbb{T} = \mathbb{R} \cup \{+\infty\}, \oplus, \odot, +\infty, 0 \rangle$, where \oplus and \odot are defined as follows:

$$\begin{aligned} a \oplus b &= \min(a, b) \\ a \odot b &= a + b, \end{aligned}$$

for each a and b in \mathbb{T} , where $+\infty$ and 0 are the identity elements of $\oplus = \min$ and $\odot = +$, respectively. Such formalism provides a compact way to express many DP algorithms. To conclude the section, let us provide practical examples of the above claim. Consider two popular algorithms: (i) the Breadth First Search (BFS) algorithm; (ii) and the Bellman-Ford algorithm. These algorithms can be easily formulated within the min-plus semiring. First, note that the generalised matrix-matrix multiplication in the min-plus semiring can be expressed as:

$$[\mathbf{A} \odot \mathbf{B}]_{ij} = \bigoplus_k \mathbf{A}_{ik} \odot \mathbf{B}_{kj} = \min_k \mathbf{A}_{ik} + \mathbf{B}_{kj}. \quad (2.14)$$

Similarly, we can also define the power of matrix as:

$$\mathbf{A}^{\odot k} = \overbrace{\mathbf{W} \odot \mathbf{W} \odot \dots \odot \mathbf{W}}^{k \text{ times}}. \quad (2.15)$$

Consequently, to approximate BFS, assume we are given a graph $g = \langle \mathcal{V}, \mathcal{E} \rangle$. Now, consider the matrix $\mathbf{A}_{\mathbb{T}}$ as its adjacency matrix, where all zeros are replaced with $+\infty$ and all ones are replaced with 0 . Consider also the vector χ_s having 0 on the s -th coordinate and $+\infty$ elsewhere. Thus, BFS can be seamlessly represented in the tropical semiring as:

$$\mathbf{r}^{(|\mathcal{V}|)} = \chi_s \odot \mathbf{A}_{\mathbb{T}}^{\odot |\mathcal{V}|}. \quad (2.16)$$

Here, $\mathbf{r}^{(|\mathcal{V}|)}$ is a vector such that $\mathbf{r}^{(|\mathcal{V}|)} = 0$ if v is reachable from s and $\mathbf{r}^{(|\mathcal{V}|)} = +\infty$ otherwise. Furthermore, earlier steps $\mathbf{r}^{(t)}$ with $t < |\mathcal{V}|$ will correctly represent intermediate steps of the BFS algorithm.

Similarly, we can also compute shortest paths from a given source s to any other nodes in the graph. Suppose we are given a weighted graph $g = \langle \mathcal{V}, \mathcal{E}, \mathcal{W} \rangle$, we can define the matrix $\mathbf{W}_{\mathbb{T}}$ to be the weighted “tropical” adjacency matrix of g , where all zeros in \mathcal{W} are replaced with $+\infty$, similarly to what we have done for BFS. Precisely, \mathbf{W} is described as follows:

$$\mathbf{W}_{uv} = \begin{cases} d_{uv} \in \mathbb{T} & (u, v) \in \mathcal{E}, \\ 0 & u = v, \\ \infty & \text{otherwise.} \end{cases} \quad (2.17)$$

Equivalently to (2.16), then, the following equation will compute the shortest paths starting from a node s :

$$\mathbf{d}^{(|\mathcal{V}|)} = \chi_s \odot \mathbf{W}_{\mathbb{T}}^{\odot |\mathcal{V}|}. \quad (2.18)$$

It is easy to verify that (2.14) applied to the tropical weight matrix is equivalent to the relaxation step as in (2.11).

2.4 GRAPH NETWORKS

Graph Networks (GNs) (Bacciu et al., 2020) are a particular class of deep learning models that are specialised in handling, processing and learning from structured data in the form of graphs. Unlike traditional neural networks that operate on n -dimensional euclidean spaces, i.e. \mathbb{R}^n , or on structured data like images and sequences, GNs can be intended to work in geometrical spaces where each data point is a graph $g = \langle \mathcal{V}, \mathcal{E}, \dots \rangle$, defined as in subsection 2.1.1. The central idea behind GNs is to effectively build vectorial representations of each node by aggregating information from neighbours, allowing the model to capture global context and dependencies in the graph through multiple iterations of this mechanism, i.e. *context propagation*. These node representations need to contain sufficient information to infer desired properties on the input graphs and generalise to unseen instances. Analogous to neural networks operating on euclidean data, then, the objective is to learn *representations* that are meaningful for regression and classification tasks. Moreover, as we will explore in the following sections, node representations can be combined to obtain a single vector that serves as a representation of the entire graph. The way we combine such pieces of information is extremely important in order to achieve specific desiderata of GNs, such as the ability to process *any* graph, regardless of its size (i.e., number of nodes) and topology. In this regard, these attributes have played a pivotal role in the dissemination of GNs across numerous graph-based learning tasks, supported by a significant body of literature attesting to the efficacy of these models.

Their applications span diverse domains, including computational chemistry (Bacciu et al., 2023), social networks (Min et al., 2021), and more recently, algorithms and combinatorial optimisation (Bello et al., 2017; Veličković et al., 2019; Kool et al., 2019).

Below, we discuss the foundational concepts underpinning the development and popularisation of graph networks, highlighting key factors that helped surpass early stage limitations, and providing initial hints into how their computation is effectively suited for learning algorithms.

2.4.1 A brief historical tour of GNs

Despite becoming popular only in the last decade, the origins of graph networks, and more generally of learning for graphs, can be traced back to the 1990s. The first efforts attempted to learn representations mainly for acyclic structures, such as trees and DAGs. Notably, Sperduti & Starita (1997), briefly followed by Frasconi et al. (1998) introduced the very first learnable IO-isomorph transductions \tilde{T} (see Definition 15). These learnt transductions were heavily inspired by recursive neurons, essentially generalising on them to incorporate recursion through structure and trained via back-propagation through time (Werbos, 1990). Although these primal versions of “graph networks” look different to their contemporary counterparts, they demonstrated a groundbreaking capability of neural networks to process and learn to infer properties in structured data for the first time. Since then, these classes of models have been continuously studied and are still relevant nowadays (Bianchini et al., 2001; Bianchini et al.; Bacciu et al., 2013).

However, the aforementioned works typically presented a few, yet strong, limitations. Firstly, the architectural decisions made in the design of such models directly influence on the graph topology accepted by these types of networks. In essence, the functions executed by these models rely on *a priori* knowledge, such as the maximum number of “children” that any node in the graph may have or the existence of a *supersource* node, from which all the other nodes can be reached. Secondly, and more importantly, these models had difficulties in handling possibly cyclic graphs, due to their *recursive* nature. To elaborate, when dealing with an arbitrary *cyclic* graph g and a specific node v , computing the representation of v recursively becomes unfeasible due to its dependence on itself within the cycle.

However, a promising alternative lies in tracking the evolution of v 's representation, enabling the computation of its updated representation based on its past representation at a specific point in time. This is the breakthrough that was presented, concurrently, by Scarselli et al. (2009) and Micheli (2009) in the late 2000s. This idea essentially “breaks” cycles in the graph structure via a simple iterative **message-passing** scheme, enabling the computation of node representations within cycles and consequently the processing of cyclic graphs. Although the two algorithms share the same view, the authors implemented it in two different “flavours”. Scarselli et al. (2009) relied on a recurrent paradigm,

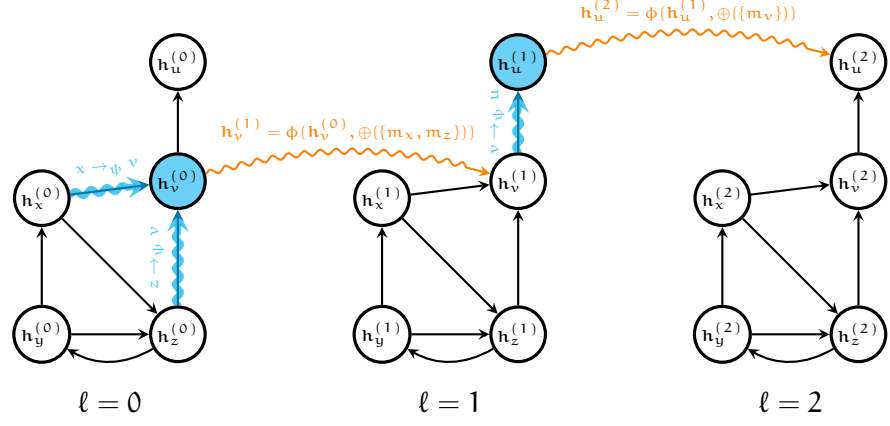


Figure 2.3: This graphic showcases how messages are computed and passed in graph networks. At step $\ell = 0$, we focus on node v . To update its representation $\mathbf{h}_v^{(0)}$, we compute messages $m_x = \psi(\mathbf{h}_v^{(0)}, \mathbf{h}_x^{(0)}, \mathbf{h}_{xv}^{(0)})$ and $m_z = \psi(\mathbf{h}_v^{(0)}, \mathbf{h}_z^{(0)}, \mathbf{h}_{zv}^{(0)})$ from its neighbours x and z . $\mathbf{h}_v^{(1)}$ is then obtained through application of (2.19). At step $\ell = 1$, u is updated based on its only neighbour v , whose has already gathered information from x and z at $\ell = 0$. As a result, at a subsequent step $\ell = 2$, $\mathbf{h}_u^{(2)}$ will be conditioned not only on $\mathbf{h}_v^{(1)}$ but also on $\mathbf{h}_x^{(0)}$ and $\mathbf{h}_z^{(0)}$, essentially expanding the range of information u has access to.

constructing the graph network as a contraction mapping and iteratively computing node representations until a fixed point was attained. [Micheli \(2009\)](#), instead, proposed a feedforward architecture which implements the message-passing scheme via multiple layers, akin to the standard modern GNs.

Building upon these pioneering works, numerous subsequent studies emerged, progressively integrating a wealth of concepts from both graph theory and neural networks into the realm of graph networks. A few noteworthy citations will be discussed more in depth in [subsection 2.4.3](#). For a comprehensive overview of graph networks, refer to ([Veličković, 2023](#)).

2.4.2 Desiderata of Graph Networks

Above, we hinted at the fact that graph networks should provide a versatile framework for processing graph-structured information. In this section, we articulate the key desiderata of graph networks, outlining the precise equations and algorithms they adopt to fulfill these requirements:

- **Topological invariance:** graph networks need to process graphs $g = \langle \mathcal{V}, \mathcal{E}, \mathcal{X}_{\mathcal{V}}, \mathcal{X}_{\mathcal{E}} \rangle$ without imposing constraints on: (i) the cardinality of \mathcal{V} and \mathcal{E} ; (ii) the graph cyclic or acyclic nature.
- **Stationarity:** the representation of a node v is independent on v 's specific identity or its position within the graph. In simpler terms,

the learnt representation of a node should depend solely on its input features $\mathbf{x}_v \in \mathcal{X}_v$ and its local neighbourhood $\mathcal{N}(v)$.

- **Effective discrimination of graphs:** graph networks should exhibit enough expressiveness to differentiate between distinct graphs and to identify isomorphic graphs as effectively as possible.

In order to embody these properties, graph networks apply a “learnt” transformation to the input features of the nodes within the graph, augmented with a message-passing algorithm to leverage the topological structure of the given graph effectively. Formally, in their most general configuration, the equation encapsulating these concepts can be distilled as (see also [Figure 2.3](#)):

$$\mathbf{h}_v^{(\ell+1)} = \phi \left(\mathbf{h}_v^{(\ell)}, \oplus \left(\left\{ \psi(\mathbf{h}_v^{(\ell)}, \mathbf{h}_u^{(\ell)}, \mathbf{h}_{uv}^{(\ell)}) \mid u \in \mathcal{N}(v) \right\} \right) \right). \quad (2.19)$$

Specifically, the above equation describes the iterative evolution of a node representation, denoted by \mathbf{h}_v , over “timesteps” denoted by ℓ (with \mathbf{h}_v^0 representing the initial vector of features $\mathbf{x}_v \in \mathcal{X}_v$). Note that by \mathbf{h}_{uv} we denote the representation of the edge (u, v) . This representation may be either a specific value (i.e., edge attribute), in which case it remains fixed for all “steps” (i.e., $\mathbf{h}_{uv}^{(\ell)} = \mathbf{x}_{uv} \in \mathcal{X}_E$, for all ℓ), or updated in a similar fashion to (2.19). To simplify the upcoming explanation, we assume the former for the remainder of this section. Typically, the above equation is characterised as a **message-passing** algorithm, composed of two distinct operations:

1. **Message computation:** a message is computed for each node in the graph and is disseminated to all neighbouring nodes. In (2.19), $\psi(\cdot)$ represents a learnable transformation and its output is the message $u \rightarrow_\psi v$ for every pair of neighbouring nodes (u, v) .
2. **State update:** incoming messages are gathered via an *aggregation function*, symbolised by \oplus . Consequently, the aggregated output is leveraged to calculate the *new* representation for node v at the subsequent “time” $\ell + 1$ using a second learnable transformation, denoted by ϕ .

The whole procedure is run in parallel for all nodes in the graph. We now discuss how the above equation satisfies all the desiderata for graph networks.

LOCAL PROCESSING OF NODE INFORMATION. Looking at (2.19) carefully, we note that the learning of a node representation is defined from the perspective of a **single** node v . This is commonly referred to as **local processing** of a graph, meaning that the computation is centered on information that are directly connected to each node, rather than considering all nodes and edges simultaneously (essentially attempting to extract features of the graph as-a-whole, e.g. spectral processing). Local processing guarantees flexibility, as equations for graph networks do not assume knowledge of the number of nodes and edges of the graph, thereby

enabling processing of graphs with any number of nodes and edges (i.e., **size invariance**). It is important to note that, through multiple iterations of the message-passing scheme presented in (2.19), this “local scope” can gradually extend and gather information from more distant parts of the graph, effectively capturing more *global* information while maintaining the primary focus on each node’s local context (refer to Figure 2.3).

PROCESSING CYCLIC GRAPHS. Above, we successfully showed how (2.19) makes a graph network size-invariant. However, to fully adhere to the topological invariance prerequisite, it is necessary to discuss how the said equation adeptly processes cyclic graphs. Figure 2.3 shows that (2.19) is in fact an iterative procedure. By unrolling the computation of (2.19), we observe that each update of the node representations at step ℓ is determined in terms of the node representations at step $\ell - 1$. As a result, mutual dependencies among node representations involved in a cycle can not exist at the same step ℓ . In other words, we “break” the cycles with an iterative approximation scheme. We anticipate that there are different ways of practically implement the “step” ℓ , which will be examined more thoroughly in subsection 2.4.3. However, the iterative message passing described herein effectively enables the processing of cyclic graphs, consequently accomplishing the **topological invariance** property.

STATIONARITY OF NODE ENCODINGS. The second desiderata of graph networks precisely states that node representations must not be dependent on the nodes’ specific identities. This is critical for capturing the underlying structural relation of nodes within the graph, regardless of their specific identities. The **stationarity** property of GNs is derived primarily from two aspects. First, the aggregation function \oplus used in (2.19) need to be independent on the considered ordering of neighbouring nodes. If this is not the case (i.e., the output of \oplus changes upon reordering of its inputs), stationarity would be violated. In fact, nodes in a graph do not usually come with a known order as in *sequences* or *trees*. Hence, if different permutations of neighbours yield different evolutions of a node representation \mathbf{h}_v , the computation of \mathbf{h}_v is non-stationary (i.e., the representation depends on the specific labeling and ordering of the nodes). To mitigate this issue, \oplus is usually selected to be a **permutation-invariant** functions, where the output remains the same for any possible permutations of the inputs. Common permutation-invariant functions employed in GNs include **sum**, **mean** and element-wise **maximum** of neighbouring nodes’ representations. Second, the use of shared parameters across all nodes in GNs contributes to stationarity. In (2.19), the same transformation (i.e., the same weights in a neural network layer) is applied equally to all nodes. This process ensures that the same learnt encoding mechanism on every node within the graph. Permutation-invariant aggregators and weight sharing together ensure that the representation of a node is dependent solely on its features and its local neighbourhood, regardless of its location within the graph and its ordering and labeling, thus achieving the stationarity property.

RELATION TO THE 1-WL TEST. Here, the attentive reader may have noticed the similarities between equation (2.12) and (2.19). In fact, the node updating function in GNs is analogous to the color updating function in the 1-WL test. Both (2.12) and (2.19) perform node-wise updates based on local neighbourhood information, although there are important divergences on the *nature* of functions being used. While the 1-WL test relies on hash functions and a *discrete* coloring algorithm (i.e., the set of possible “node features” is countable), GNs extend the procedure to utilise *continuous* functions. Despite these differences, the analogy between the 1-WL test and GNs has proven extremely useful in the design of graph networks. It is formally proven that, indeed, graph networks can only distinguish non-isomorphic graphs that can also be distinguished by the 1-WL test (Xu et al., 2019). This theoretical result is, however, conditioned on the type of permutation-invariant aggregator used in (2.19). Xu et al. (2019) show that it is possible to achieve the same expressivity as the 1-WL test if we choose \oplus to be a sum operation, whereas we achieve *strictly* less expressivity with mean and maximum. Hence, in general, the expressive capacity of graph networks is bounded by the expressivity of the 1-WL test. From a machine learning perspectives, this means that two non-isomorphic, but indistinguishable for the 1-WL test, graphs can not have two different “learnt” representations. Hence, the neural model can not generate different predictions. That is why classical GNs are often referred to as 1-WL graph networks. These limitations have inspired the research of increasingly complex k-WL graph networks, inspired by the hierarchy of k-WL tests (Morris et al., 2019). These models, however, are rarely used in practice, as the increased capacity does not always reflect an increase in model’s performance.

2.4.3 Iterative vs Feedforward Message Passing

In the context of graph networks and deep learning for graphs, there is no one single way of how information is spread across the graph. Earlier, we identified at least two different ways of how GNs exchange messages and perform aggregations among neighbours: *iterative* and *feedforward*. Although different in style, both paradigms can be studied under the unifying notation of equation (2.19). For completeness, Bacciu et al. (2020) also identify a third different category, which is that of *constructive* architectures. Although much work fall into this category (Micheli, 2009; Bacciu et al., 2018), these models are essentially feedforward architectures where training is performed layer-wise. Notwithstanding their importance in, for instance, effectively countering common vanishing/exploding gradient issues, we will focus on the difference between iterative and feedforward architectures for the remainder of this section.

The major differences between *iterative* and *feedforward* architectures lies in how equation (2.19) is instantiated and evaluated to obtain the evolutions of the node representations. As showcased in Figure 2.4, within the iterative paradigm, there is, usually, one single parametrised layer of message-passing which is called iteratively “as many times as needed” to

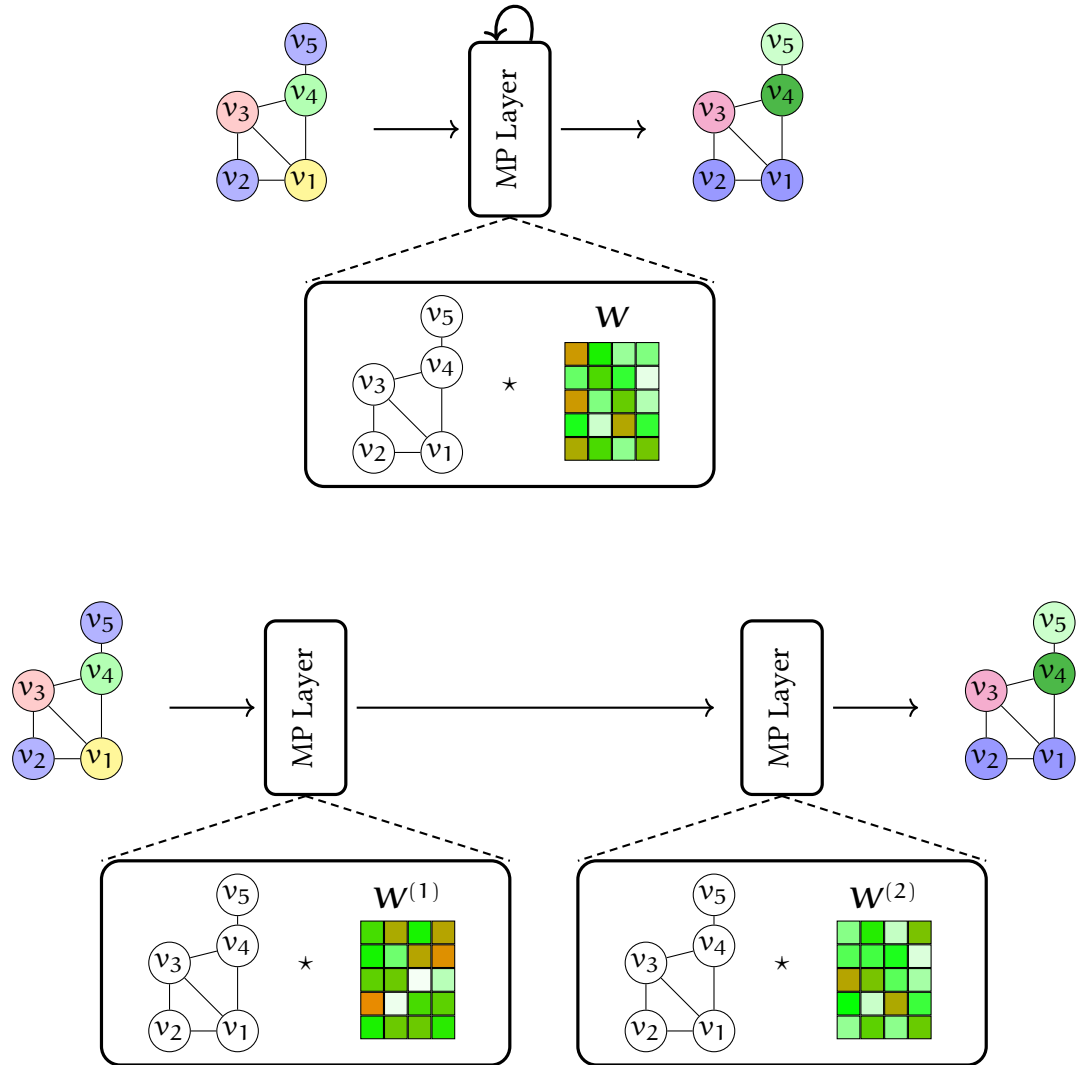


Figure 2.4: An **iterative** graph network (above) is compared to a two-layer **feedforward** graph network (below). Above, node representations are refined via iterative application of the same \mathbf{W} , as symbolised by the recurrent connection in the message-passing layer (MP layer). Below, instead, node representations are updated first by application of $\mathbf{W}^{(1)}$ in the first MP block and then updated again by the second MP block symbolised by $\mathbf{W}^{(2)}$. In the picture, \star represents application of (2.19).

spread and acquire information across an increasingly larger portion of the graph. Contrastingly, *feedforward architectures* address graph processing by means of several feedforward layers. Precisely, (2.19) formalises the learnt transformation employed by one single layer of a feedforward architecture, which may contain multiple. To understand precisely how message-passing is implemented differently in iterative and feedforward architectures, consider a simpler formulation of (2.19), described in terms of matrix multiplications:

$$\mathbf{H}^{(\ell+1)} = \sigma((\mathbf{A} + \mathbf{I})\mathbf{H}^{(\ell)}\mathbf{W}^{(\ell)}). \quad (2.20)$$

Here, we isolate the parameters \mathbf{W} from the previous equation (2.19), which were implicitly included in ψ . Hence, $\mathbf{W}^{(\ell)}$ is the matrix of parameters at GN layer/step ℓ . Similarly, $\mathbf{H}^{(\ell)}$ contains all node representations for each node v within the graph at ℓ , organised in matrix form as follows:

$$\mathbf{H}^{(\ell)} = \begin{bmatrix} \vdots \\ \mathbf{h}_v^{(\ell)} \\ \vdots \end{bmatrix}.$$

Additionally, \mathbf{A} is the adjacency matrix to which we add self-loops through the identity matrix \mathbf{I} , and σ is an activation function. From (2.19), we set $\oplus = \sum$, which enables us to rewrite the equation exploiting matrix products.

Now, it is easy to show the main difference between iterative and feedforward architectures. Precisely, within the iterative paradigm, the parameters $\mathbf{W}^{(\ell)}$ are the same for any step ℓ of (2.20) (i.e., $\mathbf{W}^{(0)} = \mathbf{W}^{(1)} = \dots = \mathbf{W}^{(\ell)} = \dots = \mathbf{W}$). This is why message-passing herein is called “iterative”, since we do not have access to “layers” in the proper term, but rather we perform iterations of the same equation.

Contrastingly, feedforward architectures typically have different parametrisation for different ℓ (i.e., $\mathbf{W}^{(\ell)} \neq \mathbf{W}^{(\ell+1)}$), and we only perform a single “iteration” of (2.20) for a given $\mathbf{W}^{(\ell)}$. In practice, within the feedforward paradigm we choose the number of different parametrisations, or *layers*, in advance. Figure 2.4, indeed, shows a 2-layer GN.

Such differences have two consequences. First, iterative architectures typically require *less* trainable parameters compared to their feedforward counterpart. The second fundamental difference is the **context radius**. The context radius accounts for the largest portion of the graph that influences a node representation \mathbf{h}_v . In fact, k iterations of message-passing entails that each representation \mathbf{h}_v will be influenced by all and only the nodes at most distance k from v , termed k -hop neighbours (see Figure 2.3).

For iterative GNs, this radius is linked to the number of iterative message-passing “calls”, which is typically unbounded. Indeed, we can, in principle, perform an unlimited number of iterations. From a practical standpoint, though, the context radius is limited by vanishing and exploding gradient issues, particularly for long sequence of iterations, as well as by well-known oversmoothing issues (Chen et al., 2020b). To counteract

these issues, one can typically perform a *fixed* number of iterations or iterate until a certain stopping condition is met (Tang et al., 2020). In this respect, *stability* of the node representations has historically played an important role to determine the “right time” to stop iterations. Under this lens, GNs are often seen as dynamical systems on which contractivity constraints are imposed (Scarselli et al., 2009; Gallicchio & Micheli, 2010), in order to ensure “convergence” of the set of node representations. Such convergence is usually ensured under the hypothesis that $\forall u, v \in \mathcal{V}$:

$$\|\mathbf{h}_v^{(\ell+1)} - \mathbf{h}_u^{(\ell+1)}\| \leq c \cdot \|\mathbf{h}_v^{(\ell)} - \mathbf{h}_u^{(\ell)}\|$$

with $0 \leq c < 1$, that is (2.20) is a contractive mapping.

For feedforward architecture, instead, the context radius is usually equal to the depth of the architecture (i.e., number of layers), since we only perform one step for each layer. For instance, in Figure 2.3 every node in the feed-forward architecture is conditioned at most on their 2-hop neighbours.

Such architectural differences make the two approaches suitable for different kinds of tasks. Intuitively, if we aim to learn functions that can be expressed as a composition of different functions, we should tend towards using feedforward architectures, as a different parametrisation at different layers allows for simpler modelling of the composition (e.g., different layers can indeed learn different functions). However, iterative approaches seem to fit more effectively scenarios where the target graph function consist of repeatedly performing the same operation on all nodes within the graph. Indeed, iterative GNs are used in physical simulations (Hamrick et al., 2018; Pfaff et al., 2020) and neural execution of algorithms (Veličković et al., 2019). While we postpone a more thorough discussion of the latter to chapter 3, we conclude this chapter by highlighting and discussing similarities shared by traditional graph algorithms and graph networks, especially considering their iterative versions. In this respect, many traditional algorithms are designed to execute the same exact function across all sections of their input. Consider, for instance, sorting algorithms that continuously swap elements in a list until it is sorted, or shortest path algorithms like Bellman-Ford that consistently apply the same relaxation step (i.e., equation (2.11)) to every node in the graph. As we anticipated, iterative GNs better fits modelling of such functions. The reason is that repeatedly applying the same operation intuitively correspond to having a single parametrised weight map \mathbf{W} that is called iteratively. Indeed, consider a scenario in which Bellman-Ford is the target learning function, even if we had different parametrisations $\mathbf{W}^{(\ell)}$, they would still have to learn the same (2.11) function for each ℓ . Hence, in such cases, a single \mathbf{W} gives us more guarantees that the applied learnt function is consistent across all steps. Another issue to evaluate is that the number of the iterations in algorithms is usually dependent on the size of the input. Precisely, Bellman-Ford performs equation (2.11) $O(|\mathcal{V}|)$ times. This makes the feedforward paradigm, given their limited *context radius*, inapplicable in such scenarios. In fact, given a feedforward architecture with k layers, such network is inherently unable to generalise the Bellman-Ford dynamics for graphs with diameter larger

than k . Contrastingly, with the iterative paradigms we can increase the number of iterations to match that of Bellman-Ford.

We conclude this chapter by stating that whenever we refer to GNs in the remainder of this thesis, we always refer to GNs based on the iterative paradigm, as they represent the most suitable architecture for learning to execute classical algorithms.

3

NEURAL ALGORITHMIC REASONING

Neural Algorithmic Reasoning (NAR) is a burgeoning field at the intersection of computer science, machine learning, and algorithms. It is dedicated to the studying and understanding of the degree to which neural architectures can learn to execute algorithms, thereby connecting traditional algorithmic concepts with modern neural network models. This chapter will serve as an introduction to the foundational concepts of this field of research.

The first section, *Why learn algorithms?*, we discuss potential challenges that arise from the application of classical algorithms to real-world data, underlining the rationale behind transitioning classical algorithms to a neural framework.

Thus, *Principles of Algorithmic Reasoning*, elucidates the crucial aspects of learning to execute algorithms. We define neural architectures arising from *algorithmic alignment* requirements and discuss different training pipelines in comparison to conventional machine learning approaches.

Concluding the chapter, *Learnt algorithms as inductive priors* showcases different modalities through which we may leverage algorithmically-informed neural networks to tackle learning of new tasks.

3.1 WHY LEARN ALGORITHMS?

As explained in [subsection 2.3.2](#), the field of computer science is rooted in algorithms. Algorithms are essentially problem-solving methods that provide us with many guarantees, such as their theoretical correctness, contrarily to deep learning, where we usually can not say much about the generalisation capabilities of the learnt function. This brings up a very obvious debated question: “*Why should we learn algorithms if algorithms are provably correct?*”. The answer lies in the gap between the theoretical guarantees provided by algorithms and the practical realities of applying these algorithms to real-world data.

ALGORITHMS FLAWS. Algorithms are often perceived as flawless executors that invariably produce correct solutions to specific problems, mainly because of their theoretical guarantees regarding correctness and invariances throughout their execution. However, the truth is that they can only meet these expectations when the abstract spaces in which they operate align precisely with the real-world contexts where their results are intended to be applied. To clarify this point, consider the following example, also depicted in [Figure 3.1](#).

Consider a scenario where we aim to solve a routing problem within a large road and traffic network. Now, consider an agent navigating this

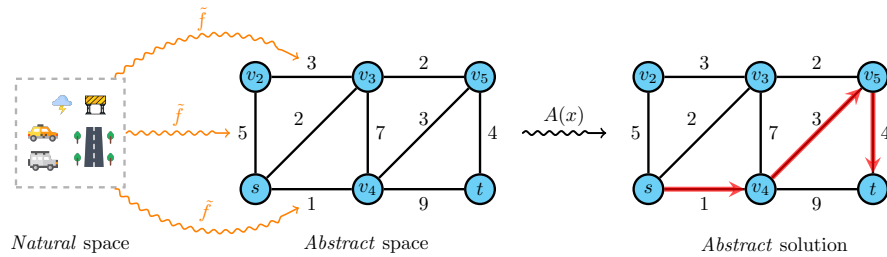


Figure 3.1: Illustration of the algorithmic bottleneck phenomena. Here, we model a shortest path problem in a real-world environment (*Natural space*) as a graph in the *abstract space* of algorithms. However, the encoding of multi-dimensional, noisy natural data (i.e., f) to a single dimension (i.e., scalars of algorithms) is often performed manually and leads to loss of information (Harris & Ross, 1955). Then, we get a provably correct, but likely **suboptimal**, solution in the abstract space through applications of a shortest path algorithm (e.g., Dijkstra).

environment whose goal is to identify the *best* possible path from point A to point B. Theoretically, we can model the large network with a weighted graph $g = \langle \mathcal{V}, \mathcal{E}, \mathcal{W} \rangle$, where edges represent roads and nodes symbolise locations (e.g., intersection points, point of interests, etc.). Each edge (u, v) is assigned a weight $w_{u,v}$ denoting the *cost* of traversing that road. By employing this formalism, we can use our favourite shortest path algorithm to obtain a solution which is provably the optimal one.

However, there are significant challenges in translating this theoretical model into the real-world scenario. In particular, *how can we be certain that the edge weights are estimated correctly?* Most of classical graph algorithms often commit to use a scalar value to represent the cost of traversing an edge. However, quantifying accurately these scalars is extremely difficult in general. Factors such as fluctuating traffic conditions, unpredictable weather, and unforeseen incidents all need to be quantified jointly and compressed into a single dimension to enable the use of graph algorithms. If this estimation is imprecise, our theoretically optimal solution might not be truly optimal in the context of our real-world scenario.

This issue has been known for a long time. Indeed, in 1955, Harris & Ross (1955) analysed and discussed methods for evaluating railways networks capacities, effectively modelling the problem as a max-flow problem. In the very first paragraphs of their investigation, the authors acknowledged that there were no known tested mathematical models for robustly estimate the scalar capacities of the edges in the rail network. This lack of formal methods for estimating such scalars persists even to these days.

In light of these observations, algorithms' outputs, although provably "optimal", can still be considered approximations in case their abstract space can not model our problem of interest exactly. In simpler terms, theoretical correctness does not matter if we execute the algorithm on the *wrong* inputs.

As a last note, we highlight that classical algorithms may also come across other problematics, such as dealing with partially observable data and missing data. In such cases, algorithms quickly become inapplicable as their preconditions are often violated by partially missing specifications.

HOW DOES NEURAL ALGORITHMIC REASONING HELP? One possible approach to address the problems mentioned earlier is to employ neural networks to estimate the edge scalars, effectively replacing the manual feature engineering, and then run an algorithm on the predicted configuration. However, this strategy presents several limitations. First, we would need to backpropagate through the operations of the algorithm. However, algorithms are inherently discrete functions (subsection 2.3.3), and as such, do not provide useful gradients for learning, although research has started exploring ways to overcome such issue (Pogančić et al., 2019). Second, the accuracy of the estimated scalars might be compromised when the available training data is limited. Additionally, attempting to compress the complexities of the real world (e.g., traffic and weather conditions in the previous example) into a single scalar value might lead to a drastic loss of information. Such problem is often referred to as *algorithmic bottleneck* (Veličković & Blundell, 2021). Consequently, once the algorithm commits to these scalars, the result could be suboptimal and, potentially, incorrect.

One alternative solution is to consider performing the algorithm directly in a neural network’s latent space. This is the objective of Neural Algorithmic Reasoning, where we aim at building neural networks that behave as close as possible to a chosen algorithm. Such an approach, assuming that a neural network can indeed behave algorithmically, actually solves both problems. First, the process becomes fully differentiable, making learning far more feasible. Second, neural networks operate in a high-dimensional space, allowing for a more nuanced representation of the real-world complexities that are difficult to capture in a single scalar. By performing the algorithmic computations directly within the neural network’s high-dimensional space, we bypass the limitations associated with the algorithmic bottleneck. Consequently, this allows for a more faithful and adaptable representations of real-world scenarios. On a broad scale, we fundamentally trade off algorithmic guarantees with more accurate representations.

IS THAT ALL? One might argue if the above observations encompass the full objective of neural algorithmic reasoning. The answer, however, is that there remains much more to explore and understand within this domain.

Indeed, from a machine learning perspective, the learning of algorithms is an intriguing and fascinating challenge in its own right. One field which might greatly benefit from NAR is the field of Neural Combinatorial Optimisation (NCO). Precisely, NCO tackles solving combinatorial optimisation problems through the use of neural networks, either in conjunction with established CO methods (Gasse et al., 2019; Gupta et al., 2020) or as end-to-end neural solvers (Bello et al., 2017; Kool et al., 2019). In

this respect, the objective is to solve CO problems to a higher precision by crafting algorithmically-inspired neural networks that incorporate algorithms as prior knowledge, and apply them to a related CO problem. As highlighted in [subsection 2.3.4](#), there exist various approximation algorithms that are reliant on *algorithmic primitives* (e.g., MST, shortest path and sorting algorithms, etc.). This supports the idea that incorporating algorithmic bias into neural networks is useful. In other words, algorithms constitute an important *prior* for solving combinatorial problems. Injecting such priors into neural networks, thus, could lead to a better exploration of the solution space and a better understanding of the underlying structure of these problems. One practical example is, for instance, a neural network targeting the resolution of a TSP. In this scenario, prior knowledge of how to compute a minimum spanning tree is of fundamental importance. Such knowledge can be integrated by learning an algorithm for computing the MST (e.g., Prim or Kruskal ([Cormen et al., 2009](#))).

One of the profound aspirations in applying NAR to combinatorial optimisation, thus, lies in the possibility of neural networks discerning, via algorithmic priors, heuristics for NP-H problems that surpass the advancements made over years in standard approximation algorithms ([Michalewicz & Fogel, 2013](#); [Hromkovič, 2013](#); [Burke et al., 2014](#); [Mart et al., 2018](#)). Notably, the current NAR literature already comprehends examples of how algorithmic biases have proven a useful prior for neural networks ([Davies et al., 2021](#); [Blundell et al., 2022](#); [Beurer-Kellner et al., 2022](#)).

As a last note, NAR’s objectives also aim at building neural networks that extrapolate beyond the support of training data – commonly termed out-of-distribution (OOD) generalisation. Indeed, overfitting is a well-known problem in the machine learning community. Neural models often excel at fitting the training data but struggle to generalise when the test data distribution *shifts* from the training distribution ([Neyshabur et al., 2017](#)). Algorithms, on the other hand, have the inherent ability to generalise on any (acceptable) input, thanks to their strong theoretical guarantees. Hence, in order to build neural networks that effectively behave like algorithms, much effort is put into preserving this property inside neural approaches. In the following sections, we discuss how this objective is pursued in practice.

3.2 PRINCIPLES OF ALGORITHMIC REASONING

In this section, we present and clarify how the task of performing algorithmic reasoning through neural networks is structured. We explore how algorithms are learnt in an end-to-end fashion by analysing each one of the three fundamental principles of neural algorithmic reasoning: *algorithmic alignment*, the *encode-process-decode* architecture and *step-wise* supervision.

3.2.1 Algorithmic alignment

In the context of NAR, the term algorithmic alignment (Xu et al., 2020) refers to the capacity of specific neural architectures to learn and extrapolate on reasoning tasks, such as executing classical algorithm. Here, *alignment* implies that some neural architectures inherently lean towards learning certain families of functions more easily than others. To better understand this concept, consider two popular neural network architectures: MLPs and GNs. Notably, the latter includes the former in its equations (see (2.19)), building upon MLPs and sharing similar approximation capabilities (Scarselli et al., 2008). However, even though both MLPs and GNs have theoretically similar expressive power, the different architectural bias may make the finding of a good approximation to f more or less “difficult”. Now, consider a graph algorithm A and a neural network \hat{f} , a more formal definition of algorithmic alignment is given as follows:

Definition 23. Let $\hat{f}_1, \dots, \hat{f}_n$ be the modules of \hat{f} and let A_1, \dots, A_n be the modules of the algorithm. Thus, \hat{f} and A are said to be M -algorithmically aligned if: (i) if we replace \hat{f}_i with A_i for each i , then the network \hat{f} emulates A ; (ii) the learning problem $\hat{f}_i \approx A_i$ exhibits sample complexity $\mathcal{C}(\hat{f}_i, A_i)$ such that $\sum_{i=1}^n \mathcal{C}(\hat{f}_i, A_i) \leq M$.

Informally, the sample complexity $\mathcal{C}(\hat{f}_i, A_i)$ (Hanneke, 2016) can be phrased as the minimum number of training samples required to get a “good” approximation of A_i via \hat{f}_i . Hence, the concept of algorithmic alignment fundamentally states that a good alignment implies that each of the algorithm’s submodules are “easy” to learn for the neural architecture (i.e., “small” M). That is the reason why considering the architectural bias is crucial when dealing with learning of classical algorithms. Actually, a first hint at the suitability of graph networks to learn graph algorithms was given in subsection 2.4.2, where we discussed how GNs process information equivalently to the 1-WL test algorithm. Since, the 1-WL test algorithm can be phrased under the message-passing framework, one may argue that GNs are a good fit for any message-passing algorithms. Indeed, in this direction, Dudzik & Veličković (2022) show that GNs actually aligns with dynamic programming algorithms. These intuitions suggest that graph networks are the preferable choice over other kinds of architectures (e.g., MLPs) when the target function is an algorithm. To show this precisely, consider the learning task of executing the Bellman-Ford algorithm. Interestingly, Bellman-Ford relaxation steps, outlined in (2.11), can be framed in terms of message-passing through node and edge features. In fact, (2.11) is essentially a special case of (2.19) where \oplus and ϕ are replaced with minimum (or maximum¹) operations. This seamlessly aligns the GN with Bellman-Ford, as detailed by the following equations:

$$\text{(MP)} \quad \min(\mathbf{h}_v, \min(\{\psi(\mathbf{h}_v, \mathbf{h}_u, \mathbf{h}_{uv}) \mid u \in \mathcal{N}(v)\})) \quad (3.1)$$

$$\text{(BF)} \quad \min(d_v, \min(\{d_u + e_{uv} \mid u \in \mathcal{N}(v)\})). \quad (3.2)$$

¹ Note that $\min(a, b) = |\max(-a, -b)|$ thus \min and \max can be used interchangeably

From the presented equations, it is clear that the parametrised network ψ only needs to learn a linear function (i.e., $\psi(\mathbf{h}_v, \mathbf{h}_u, \mathbf{h}_{uv}) \approx d_u + e_{uv}$), whereas other aggregations and operations are inherently addressed through architectural bias. Contrastingly, learning such relaxation step through a different neural network architecture, such as an MLP, would require to learn aggregating the representations and recognising neighbourhoods, which is far beyond the task of “simply” learning a linear function. Another interesting point of discussion is the consequences that this “linear” algorithmic alignment have on OOD generalisation. [Xu et al. \(2021\)](#) provide empirical evidence showing that neural networks with ReLU activations typically generalise in a linear fashion along any dimension outside their training distribution. While this might seem a limitation in standard machine learning tasks, it is actually a desirable property when dealing with most of classical algorithms. By analysing [\(3.1\)](#) and [\(3.2\)](#), we deduce that ψ must extrapolate linearly to align with the behaviour of the relaxation step. Consequently, given its inclination towards linear generalisation, ReLU stands out as the ideal activation function for use within ψ .

In the latest years, more alignment properties between GNs and DP algorithms have been demonstrated in the literature, whether empirically or more formally, testifying that this is an important property to achieve. [Fereydounian et al. \(2022\)](#) formally state that when the target function is *permutation-compatible* (i.e., the function is not influenced by re-labeling of the graph), then GNs can *generate* it. This has direct implications on the alignment between GNs and algorithms, since permutation compatibility can be proved to hold for some algorithmic functions (e.g., minimum cut). [Bevilacqua et al. \(2023\)](#) argue that most of classical algorithms exhibit a *causal model* ([Sloman, 2005](#)) underneath, and aligning to it is indeed beneficial for OOD generalisation. Much work have been done also to show that GNs align to *parallel* algorithms ([Engelmayer et al., 2023](#)) and to augment GNs with external memory to align more closely to recursion ([Jayalath et al., 2023](#); [Jain et al., 2023](#)).

As it is evident from the above discussion, algorithmic alignment does not restrict to the architectural bias alone. In fact, [Cappart et al. \(2023\)](#) actually present a list of “prescriptions” that spans architectures, learning setups and loss functions. In the following sections, we discuss the most important principles, namely the encode-process-decode architecture and step-wise supervision, and we refer the interested reader to ([Cappart et al., 2023](#)) for a more comprehensive list.

3.2.2 The Encode-Process-Decode architecture

The Encode-Process-Decode (EPD) architecture ([Hamrick et al., 2018](#)), depicted in [Figure 3.2](#), is a specific neural network architecture used in a variety of machine learning fields, particularly in the field of neural algorithmic reasoning ([Veličković & Blundell, 2021](#); [Cappart et al., 2023](#)). The EPD architecture consists of three learnable components: the encoder f , the processor p , and the decoder g . The whole architecture can be de-

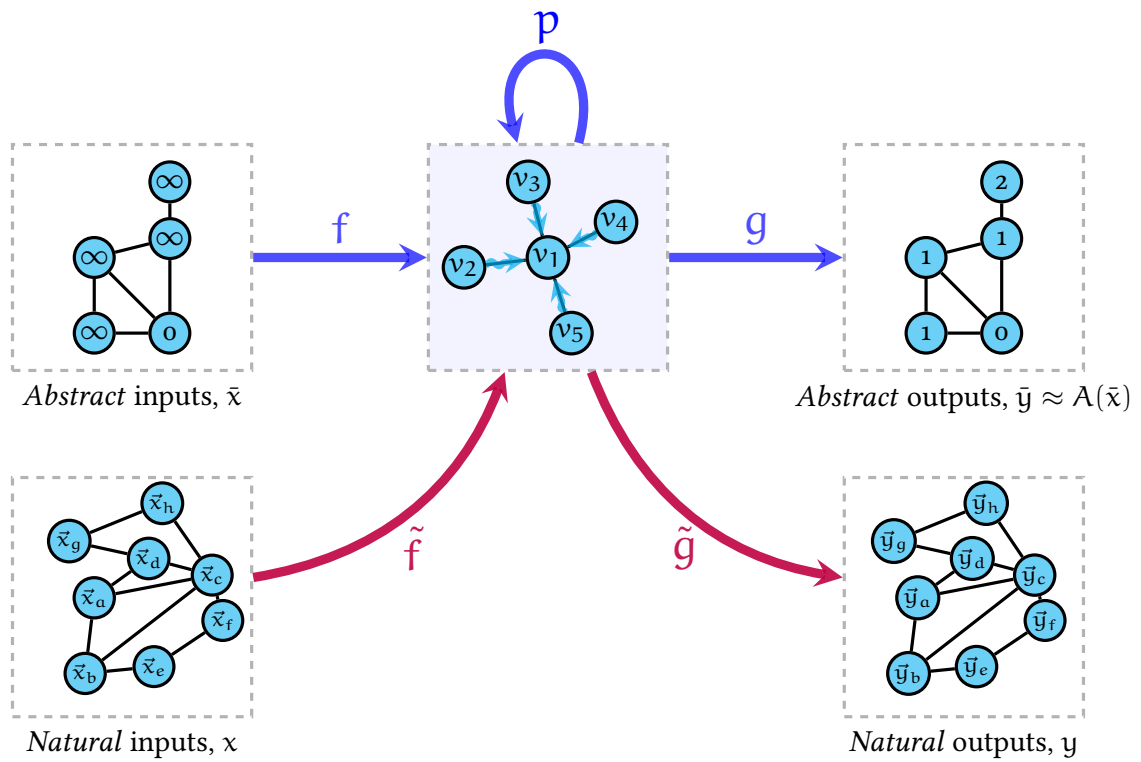


Figure 3.2: The Encode-Process-Decode architecture. The processor is shared across multiple tasks through the application of several encoders/decoders that map from inputs to p 's latent space and to outputs. In this pipeline, the processor p is trained to align to a shortest path algorithm (blue path). Then, we use any of the transfer learning methodologies discussed in section 3.3 to reason on *natural* inputs (red path) while maintaining alignment to shortest path.

scribed as a composition of these three elements $\text{net} = g \circ p \circ f$. Notably, the whole architecture is called iteratively k times (i.e., net^k), symbolising the k steps of an algorithm. This essentially formalises the need to using an *iterative* neural network architecture to obey the constraints of OOD generalisation discussed in [subsection 2.4.3](#). We now describe the general forward pass (at each step k) by examining independently each component of the EPD architecture. In the following, we consider the notation introduced in [subsection 2.3.1](#) with \mathbf{x} and \mathbf{y} denoting inputs and outputs.

ENCODER. The encoder $f : \mathcal{X} \rightarrow \mathbb{R}^d$ primary objective is to transform raw input data into a suitable format for the subsequent processing stage. This is the first step to “break” the scalar bottleneck. Typically, in an EPD architecture we would like our processor to be the only component to be “algorithmically-aligned” to a set of chosen algorithms. Thus, encoders (and decoders) are generally chosen among the simplest classes of learning architectures, namely linear models. Hence, suppose $\mathbf{x}_v \in \mathcal{X}_v$ and $\mathbf{x}_{uv} \in \mathcal{X}_e$ are respectively arbitrary node and edge inputs, the encoder outputs their encoded representations:

$$\begin{aligned} \mathbf{z}_v^{(t)} &= f_\theta(\mathbf{x}_v^{(t)}) \\ \mathbf{z}_{uv}^{(t)} &= f_\theta(\mathbf{x}_{uv}^{(t)}), \end{aligned}$$

where θ symbolises the learnable parameters.

PROCESSOR. The processor $p : \mathbb{R}^d \rightarrow \mathbb{R}^d$ is the core component of the EPD pipeline that operates on the encoded representations \mathbf{z} generated by the encoder. This component is usually given an architectural bias towards the computation dynamics of the target algorithms. Since we mostly deal with graph algorithms, the processor is assumed to be a graph network. Thus, the processor network performs iterative step-wise updates of the node representations:

$$\begin{aligned} \mathbf{h}_v^{(t)} &= p_\theta \left(\mathbf{z}_v^{(t)}, \{ \mathbf{z}_{uv}^{(t)} \}_{(u,v) \in \mathcal{E}}, \mathbf{h}_v^{(t-1)}, \right. \\ &\quad \left. \{ \mathbf{h}_u^{(t-1)} \}_{u \in \mathcal{N}(v)}, \{ \mathbf{h}_{uv}^{(t)} \}_{(u,v) \in \mathcal{E}} \right), \end{aligned}$$

as well as edge representations:

$$\mathbf{h}_{uv}^{(t)} = p_\theta \left(\mathbf{z}_v^{(t)}, \mathbf{z}_u^{(t)}, \mathbf{z}_{uv}^{(t)}, \mathbf{h}_{uv}^{(t-1)}, \mathbf{h}_u^{(t-1)}, \mathbf{h}_v^{(t-1)} \right).$$

Here, $\mathbf{h}^{(0)}$ is initialised as the null vector both for node and edge representations.

In practice, the selection of the message-passing function in the processor network is guided by both algorithmic alignment properties and empirical performance. Here, we generally seek simple and general architectures, avoiding overly complicated graph convolution operations that stray from algorithmic behaviour. For instance, notorious message-passing methods based on Chebyshev polynomials ([Defferrard et al., 2016](#)),

Laplacian matrices (Kipf & Welling, 2017) and graph isomorphism (Xu et al., 2019) are not typically used as NAR processors. The rationale behind this is that spectral processing, normalisation techniques and aggregators commonly used in these operations do not conform to the alignment principles discussed in subsection 3.2.1.

In the following, we list some of the most used processor networks:

- **Message-Passing Neural Networks** (Gilmer et al., 2017): MPNNs corresponds exactly to equation (2.19), where typically $\oplus = \max$ to better align with DP algorithms. Furthermore, graphs are always processed as cliques, regardless of their true connectivity. Herein, there exist also variants such as MPNNs based on *triplet reasoning* (Tri-MPNNs) (Ibarz et al., 2022) that consider *edge-based* message passing, in order to align more closely to a broader set of algorithms (e.g., Floyd-Warshall).
- **Pointer Graph Networks** (Veličković et al., 2020): PGNs are special cases of MPNNs, where messages are computed and exchanged within the true neighbourhoods $\mathcal{N}(v)$ in the graph, hence not considering graphs as fully-connected.
- **Graph Attention Networks** (Veličković et al., 2018): GATs use attention (Vaswani et al., 2017) to weigh contributions of neighbouring nodes. These models have empirically shown to be more effective to tackle computational geometry algorithms (Veličković et al., 2022a).

Indeed, the aforementioned networks are the highest-performing baselines in the CLRS algorithmic benchmark (Veličković et al., 2022a).

Finally, one significant aspect to consider is the termination condition of the processor. Many algorithms, referred to as *iterative algorithms*, terminate after a given loop condition is met. To align with these algorithms, it is essential to introduce termination strategies in our processors. Usually, termination requires the use of a *termination network* T that uses a sigmoid activation to determine when to halt iterations. This network often takes the average of the most recent n node or edge representations as its input, as follows:

$$s^{(t)} = \sigma(T(\{\bar{\mathbf{h}}_v \mid v \in \mathcal{V}\})).$$

Here, σ is the logistic function and $\bar{\mathbf{h}}$ denotes the averaged representation of the few iterations of node v . As a result, $s^{(t)} \in [0, 1]$ indicating whether to terminate the processor at step t . Thus, the termination network essentially learns a stopping criterion. This strategy is reminiscent of the IterGNN (Tang et al., 2020) approach.

Additionally, it is also feasible to apply the inherent termination conditions of the target algorithm. For example, Bellman-Ford (similarly to other shortest path algorithm) terminate once the solution “converges” (i.e., no “new” shortest paths are found within two successive iterations). In such cases, we can straightforwardly apply the same stopping criterion to our processor. We conclude by noting that, whenever we have access

to an *upper bound* on the maximum number of iterations (e.g., diameter of the graph), we can include such stopping condition in our processor.

DECODER. Finally, the decoder $g : \mathbb{R}^d \rightarrow \mathcal{Y}$ maps the embeddings produced by the processor to the actual space of solutions of the algorithm:

$$\mathbf{y}_v^{(t)} = g_\theta(\mathbf{z}_v^{(t)}, \mathbf{h}_v^{(t)}, \mathbf{h}_v^{(t-1)})$$

$$\mathbf{y}_{uv}^{(t)} = g_\theta(\mathbf{z}_{uv}^{(t)}, \mathbf{h}_{uv}^{(t)}, \mathbf{h}_{uv}^{(t-1)}).$$

Notably, the decoder is applied to the embeddings produced at every step t , in order to obtain intermediate outputs (i.e., *hints*) that might be fed back to the encoder in the subsequent step. This means that parts of the inputs $\mathbf{x}^{(t)}$ may include step-wise outputs $\mathbf{y}^{(t-1)}$.

3.2.3 Step-wise supervision

In standard machine learning setups, the one objective is learning an approximation to a hidden function $f : \mathbb{R}^n \rightarrow \mathbb{R}^m$. The most typical way in which we pursue this objective is by learning a stack of non-linear transformations (e.g., MLPs), imposing little or no constraints on the intermediate transformations of the hidden layers. This results in an optimisation problem described as:

$$\theta^* = \arg \min_{\theta} \frac{1}{|\mathcal{D}|} \sum_{\mathbf{x} \in |\mathcal{D}|} \mathcal{L}(f(\mathbf{x}), \text{net}(\mathbf{x} | \theta)),$$

where net represents the neural network and \mathcal{D} represents the training data.

Furthermore, the above learning problem has another implication: we assume that we only want to supervise on input-output pairs. Indeed, when we think of machine learning and deep learning we tacitly imply that optimisation is only performed in this manner, and understandably so. In fact, in the most general case we have no indications of *how* the target function generated its output (i.e., we do not have access to *hints* as for algorithms), that is, in fact, the learning objective. This is the primary reason why we often imply that neural networks learn from pairs of input-output data.

However, within the context of *neural execution* of algorithms, supervising a model under such conditions has historically exhibited poor performance. Consider, for instance, the Neural Turing Machines (NTM) (Graves et al., 2014) – an early effort to teach classical algorithms to neural networks. This model is equipped with an auxiliary differentiable memory and are supervised solely on input-output pairs of the target algorithmic functions. The neural network is then tasked to learn the dynamics of *reading* and *writing* to this memory, without explicit guidance on its management as per the target algorithms. This usually leads to high variance in the results, as we have few guarantees that the neural network will learn to use the memory effectively.

A straightforward approach to tackle this problem is to show the network the step-by-step process of how target algorithms interact with data structures and input data. This is the idea behind *step-wise supervision*, illustrated for the first time in (Veličković et al., 2019). In essence, having access to these manipulations enables us to supervise on each of them, effectively including an auxiliary supervision signal for every step of the algorithm’s trajectory. Following the notation of subsection 2.3.1, we refer to these intermediate manipulations as *hints*. A mathematical formulation is provided as follows:

$$\theta^* = \arg \min_{\theta} \frac{1}{|\mathcal{D}|} \sum_{x \in |\mathcal{D}|} \left(\mathcal{L}(A(x), \text{net}(x | \theta)) + \sum_{h \in \text{hints}} \sum_{t=0}^{T-2} \mathcal{L}(A_t(h^{(t)}), \text{net}_t(h^{(t)} | \theta)) \right), \quad (3.3)$$

where A is the target algorithm and $h^{(t)}$ represents a possible hint at step t of the algorithm, with A_t and net_t indicating the t -th step of the algorithm and the algorithmic reasoner. Including these additional terms to the loss function, thus, effectively constrains the network to behave more closely to the target algorithm at each intermediate step t . This also lets the network disambiguate across similar algorithms. In fact, consider the set of sorting algorithms that, given an input list, returns a sorted version of the list according to some metric. If we ignore the intermediate hints, all sorting algorithms become indistinguishable to one another. Hence, including supervision on hints is sometimes crucial to align correctly to the dynamics of a target algorithm.

3.3 LEARNT ALGORITHMS AS INDUCTIVE PRIORS

As introduced in the previous section, an intriguing reason to employ neural algorithmic reasoning is to adapt algorithms for handling real-world, noisy inputs (i.e., *natural* inputs). Broadly speaking, our goal is to learn a mapping from one natural space $\tilde{\mathbb{A}}$ to another $\tilde{\mathbb{B}}$, where this mapping is of algorithmic nature. However, algorithms operate in an abstracted version of these natural spaces (i.e., *abstract* space). This abstract space is what we typically use when teaching algorithms to machines. Now, denote the learning task on natural spaces as the *target* task \mathcal{T} , and the task of learning on abstract spaces as the *base* task \mathcal{B} . In practice, \mathcal{B} may be any algorithmic tasks, such as finding the shortest path from point A to point B or find the maximum flow within a flow network. The target task \mathcal{T} , in contrast, might be the exact same shortest path problem but with natural data, or any problem correlated to algorithms (e.g., NCO), as per our discussion in section 3.1. Thus, the assumption is that \mathcal{T} and \mathcal{B} share mutual information and hence knowledge of \mathcal{B} may be a valuable inductive prior when solving \mathcal{T} .

Now, in order to infuse \mathcal{T} with knowledge of \mathcal{B} we generally employ a two-step learning scheme:

1. Given synthetically generated inputs and ground truths in the abstract space, learn the parameters of an EPD architecture to execute an algorithm (i.e., solve \mathcal{B}) by optimising (3.3), where $\text{net} = g \circ p \circ f$. Here, we put emphasis on the fact that the EPD model effectively *decouples* the processor network p from raw inputs and outputs, with the encoder and decoder networks handling the necessary *pre-* and *post-*processing (i.e., mapping to and from p 's latent space). Furthermore, as detailed in subsection 3.2.2, f and g contribute little to the learning of the algorithmic function, being implemented as simple linear projections. This ensures that, at the end of the optimisation, we end up with all knowledge of \mathcal{B} encoded inside the processor's parameters. This allows for easily extraction of the processor and effective transfer learning during step 2.
2. Discard f and g and apply any suitable transfer learning (Torrey & Shavlik, 2010) method to p to learn the target task \mathcal{T} .

Through this simple learning scheme, we are able to re-use the processor p for solving the new task \mathcal{T} . We now define how we can effectively implement step 2. Consider $\tilde{x}, \tilde{y} \sim \mathcal{T}$ to be input and ground-truth samples from \mathcal{T} , Xhonneux et al. (2021) discuss different transfer learning settings to practically implement step 2, which we report in the following along others:

- **Pre-train and freeze (PF)**: freeze the parameters of p . Thus, instantiate new encoders and decoders \tilde{f}, \tilde{g} to process \tilde{x} and \tilde{y} , and learn their parameters by minimising an appropriate loss function $\mathcal{L}_{\mathcal{T}}$:

$$\arg \min_{\phi} \mathcal{L}_{\mathcal{T}} \left(\tilde{y}, (\tilde{g} \circ p \circ \tilde{f})(x \mid \phi) \right),$$

where ϕ are the learnable parameters of the new encoders and decoders. This settings is used, for instance, in (Deac et al., 2021; Numeroso et al., 2023).

- **Pre-train and fine-tune (PFT)**: unlike the above approach, here we let p 's parameters change during step 2 (i.e., ϕ include parameters of the processor in the above equation).
- **2-processor transfer (2PROC)**: here, the two aforementioned methods are combined. Precisely, we instantiate a new processor \tilde{p} whose parameters are free to change, whereas parameters of the pre-trained processor p are kept frozen. Activations of the two processors are then combined together through any aggregator function prior application of the decoder \tilde{g} . Suppose $\mathbf{h}_v, \tilde{\mathbf{h}}_v$ to be the activations of the frozen processor p and the new processor \tilde{p} , respectively. Inferred values of \tilde{y}_v are then obtained as:

$$\tilde{y}_v = \tilde{g}(\tilde{\oplus}(\mathbf{h}_v, \tilde{\mathbf{h}}_v)),$$

where $\tilde{\oplus}$ can be a learnable MLP or any simple functions such as summation.

- **Multi-task learning (MTL):** here, the two tasks \mathcal{B} and \mathcal{T} are solved together by means of one pair of encoder and decoder networks for the task \mathcal{B} (i.e., $f_{\mathcal{B}}, g_{\mathcal{B}}$) and one for \mathcal{T} (i.e., $f_{\mathcal{T}}, g_{\mathcal{T}}$). These encoders and decoders share the same processor network p , which is trained to execute the two tasks simultaneously. As a result, the transfer is implicit during step 1 of the above learning scheme.

Through the above transfer learning methods, we have everything we need to successfully apply a learnt \mathcal{B} reasoner on a new task \mathcal{T} . In other words, we illustrated how we can reason algorithmically on natural inputs, by carefully pre-train a processor p to imitate an algorithm. Intuitively, freezing (or not) of the processor regulates how strong of an algorithmic bias we want to infuse \mathcal{T} with. Furthermore, \tilde{f} and \tilde{g} effectively replace the manual feature engineering surpassing the algorithmic bottleneck issue discussed in the previous sections, as both \tilde{f} and \tilde{g} learn to map to and from a multi-dimensional space (i.e., the processor p 's latent space) and are forced to re-use the algorithmic knowledge lying inside p . Note that, while we usually require encoders and decoders to be simple linear transformations when learning \mathcal{B} , such constraint is not only not needed when transferring to \mathcal{T} , but can also limit the performance in case a *non-linear* reasoning is required on the algorithmic steps. Indeed, especially when applying *pre-train and freeze* we can usually implement \tilde{f} and \tilde{g} as more powerful MLPs or any suitable neural networks. [Veličković et al. \(2022b\)](#) exemplify this by pre-training an algorithmic reasoner to perform physical simulations on tabular data, and then deploy encoders and decoders as deep convolutional neural networks ([LeCun et al., 1995](#)) when applying these learnt simulators to images.

As a last note, let us put our focus on the *multi-task learning* setting. There, we discussed how we can use the same processor for learning two tasks at the same time. This concept can be generalised to tackle an arbitrary number of tasks. This means that, for instance, we can actually learn multiple algorithms at the same time by having several independent pairs $\langle f_{\mathcal{A}_i}, g_{\mathcal{A}_i} \rangle$ implementing the necessary mapping from the abstract spaces of the different algorithms $\mathcal{A} = \{\mathcal{A}_1, \dots, \mathcal{A}_n\}$. Introduced in ([Xhonneux et al., 2021](#)), this learning modality shows to be beneficial for OOD generalisation as diverse algorithms may share common sub-routines that the neural algorithmic reasoner can successfully identify and exploit during learning. [Ibarz et al. \(2022\)](#) scale this idea to map all 30 algorithms of the CLRS benchmark ([Veličković et al., 2022a](#)) to the same processor's parameter space, with performance comparable to a network trained exclusively on one single algorithm. Within this thesis, we utilise this technique when learning dual algorithms in [section 5.1](#).

Part II

CONTRIBUTION

4

LEARNING DYNAMIC PROGRAMMING

This chapter contains the first core contributions of this thesis. Herein, we target learning of *min*-aggregated dynamic programming (Min-DP) algorithms, from both theoretical and practical standpoints.

In the first section, *Approximating min-DP algorithms*, we draw connections between the field of *tropical algebra*, where DP algorithms are commonly thought to “live” in (Maclagan & Sturmfels, 2009), and classical euclidean spaces (i.e., where neural networks operate). Such connection will provide evidence that GNs can approximate Min-DP algorithms up to a arbitrary precision.

In the second section, *Planning via learnt heuristics*, we show how we can learn a heuristic function to be used in a path planning problem, which can be framed under dynamic programming. Such heuristic will allow for more effective path discovery, especially when deployed in partially observable environments.

4.1 APPROXIMATE MIN-DP ALGORITHMS

By now, it should be clear that GNs and algorithms computation dynamics share similarities. On this line, Dudzik & Veličković (2022) attempt at formalising such similarities through category theory (Awodey, 2010), particularly by employing *integral transforms* – a popular construct in category theory. This integral transform provides a unified description of both dynamic programming algorithms and computation of graph networks, effectively drawing an equivalence between the two at a macro-level.

In this contribution, we take a different route and attempt at drawing connections between DP algorithms and GNs by leveraging *tropical algebra* (see subsection 2.3.5). In essence, tropical algebra is a “degeneration” of Euclidean algebra which is better “aligned” to the dynamic programming paradigm. Precisely, we draw connections between two **semirings** (see subsection 2.3.5), that of *real numbers* (i.e., “Euclidean” semiring) and the tropical **min-plus** semiring. Both the real and min-plus semirings are particular semirings, which can be represented mathematically as $\langle \mathbb{R}, +, \cdot, 0, 1 \rangle$ and $\langle \mathbb{T} = \mathbb{R} \cup \{+\infty\}, \min, +, +\infty, 0 \rangle$. The former semiring encompasses classical addition and multiplication operations on the set of real numbers \mathbb{R} . Neural networks, in general, operate within this structure. In the following, we will always refer to the tropical min-plus semiring as simply the “tropical semiring”. Within this algebraic structure, many dynamic programming algorithms find a precise description (Maclagan & Sturmfels, 2009), as we also showed in subsection 2.3.5.

In order to show that GNs can effectively approximate DP algorithms up to arbitrary precision, we proceed by “reconciling” these two semirings. We provide practical proof examples for reachability and shortest path algorithms, in particular. Precisely, we consider inputs and outputs coming from tropical sets and formulate a suitable EPD architecture with a GN processor that can seamlessly process such data, effectively casting GNs under the framework of tropical algebra. In particular, we implement encoders and decoders as *Maslov* quantisation maps (Litvinov, 2007) and use a *sum*-aggregated graph network (i.e., Graph Isomorphism Network (Xu et al., 2019)) as the processor of such architecture. We will show that, by employing this architecture, GNs can effectively approximate *min*-aggregated DP algorithms up to an arbitrary precision (Landolfi et al., 2023).

4.1.1 Aligment of encoders and decoders

Suppose we receive inputs in the form of “tropical” objects \mathbb{T} . Standard EPD pipelines (with linear encoding and decoding functions) are unable to directly process such inputs, due to the presence of possible infinities in the input (recall that we consider $\mathbb{T} = \mathbb{R} \cup \{+\infty\}$).

To overcome this limitation, the EPD architecture considered in this section comprises specialised encoders and decoders, known as Maslov quantisation and dequantisation maps (Litvinov & Maslov, 1998; Brugalle et al., 2000) $q_h : \mathbb{T} \rightarrow \mathbb{R}_+$ and $d_h : \mathbb{R}_+ \rightarrow \mathbb{T}$, with \mathbb{R}_+ being the set of non-negative real numbers. A precise mathematical formulation is as follows:

$$q_h(x) = \begin{cases} 0 & \text{if } x = \infty \\ e^{-x/h} & \text{otherwise;} \end{cases} \quad (4.1)$$

$$d_h(x) = \begin{cases} \infty & \text{if } x = 0 \\ -h \ln x & \text{otherwise.} \end{cases}, \quad (4.2)$$

where $h > 0$ is a pre-defined constant that regulates the smoothness of the quantisation and dequantisation operators. Now, we have a natural map from tropical objects to real numbers and viceversa. However, such mappings entail a stronger connection between the min-plus semiring and the semiring of real numbers. In fact, q_h and d_h can be actually shown to be semiring *homomorphisms* between \mathbb{T} and \mathbb{R}_+ .

Proposition 1. $q_h : \mathbb{T} \rightarrow \mathbb{R}_+$ is a semiring homomorphism from $\langle \mathbb{T}, \min, +, +\infty, 0 \rangle$ to $\langle \mathbb{R}_+, +, \cdot, 0, 1 \rangle$ for $h \rightarrow 0^+$. As such, q_h satisfies:

1. $q_h(+\infty) = \text{id}_{\langle \mathbb{R}_+, + \rangle}$.
2. $q_h(0) = \text{id}_{\langle \mathbb{R}_+, \cdot \rangle}$.
3. $\forall a, b \in \mathbb{T} : q_h(a \odot_{\mathbb{T}} b) = q_h(a + b) = q_h(a) \cdot q_h(b)$.
4. $\forall a, b \in \mathbb{T} : q_h(a \oplus_{\mathbb{T}} b) = q_h(\min(a, b)) = q_h(a) + q_h(b)$.

Proof. We will prove that q_h satisfies each of the above properties:

1. By definition of q_h , we have that $q_h(+\infty) = 0 = \text{id}_{\langle \mathbb{R}_+, + \rangle}$.
2. By definition of q_h , we have that $q_h(0) = e^{0/-h} = 1 = \text{id}_{\langle \mathbb{R}_+, \cdot \rangle}$.
3. Given $a, b \in \mathbb{T}$, we have that $q_h(a \odot_{\mathbb{T}} b) = e^{-\frac{(a+b)}{h}} = e^{-\frac{a}{h} + \frac{-b}{h}} = e^{-\frac{a}{h}} \cdot e^{-\frac{-b}{h}} = q_h(a) \cdot q_h(b)$
4. Given $a, b \in \mathbb{T}$, consider $\lim_{h \rightarrow 0^+} q_h(a \oplus_{\mathbb{T}} b) = \lim_{h \rightarrow 0^+} q_h(\min(a, b)) = 0 = \lim_{h \rightarrow 0^+} [q_h(a) + q_h(b)]$.

□

Proposition 2. $d_h : \mathbb{R}_+ \rightarrow \mathbb{T}$ is a semiring homomorphism from $\langle \mathbb{R}_+, +, \cdot, 0, 1 \rangle$ to $\langle \mathbb{T}, \min, +, +\infty, 0 \rangle$ for $h \rightarrow 0^+$. As such, d_h satisfies:

1. $d_h(0) = +\infty = \text{id}_{\langle \mathbb{T}, \min \rangle}$.
2. $d_h(1) = 0 = \text{id}_{\langle \mathbb{T}, + \rangle}$.
3. $\forall a, b \in \mathbb{R}_+ : d_h(a \odot_{\mathbb{R}_+} b) = d_h(a \cdot b) = d_h(a) + d_h(b)$.
4. $\forall a, b \in \mathbb{R}_+ : d_h(a \oplus_{\mathbb{R}_+} b) = d_h(a + b) = \min(d_h(a), d_h(b))$.

Proof. The proof for d_h is analogous to the previous one:

1. By definition of d_h : $d_h(0) = +\infty = \text{id}_{\langle \mathbb{T}, \min \rangle}$.
2. $d_h(1) = -h \ln 1 = 0 = \text{id}_{\langle \mathbb{T}, + \rangle}$.
3. Given $a, b \in \mathbb{R}_+$, we have that $d_h(a \cdot b) = -h \ln(ab) = -h \ln a + (-h \ln b) = d_h(a) + d_h(b)$
4. Given $a, b \in \mathbb{R}_+$, consider $\lim_{h \rightarrow 0^+} d_h(a + b) = \lim_{h \rightarrow 0^+} [-h \ln(a + b)] = 0 = \lim_{h \rightarrow 0^+} \min(d_h(a), d_h(b))$.

□

We have established that both q_h and d_h function as homomorphisms between the two semirings for arbitrarily “small” values of h . Furthermore, it can be shown that $d_h = q_h^{-1}$ by observing that $\ln = \exp^{-1}$ and viceversa. Since q_h admits an inverse, q_h and d_h are, in reality, **isomorphisms**. Consequently, any algebraic structure in \mathbb{R}_+ and any algebraic structure in \mathbb{T} are isomorphic. Of course, homomorphisms and isomorphisms are only valid as h approaches 0. For “sufficiently high” values of h , in fact, addition (condition 4 of homomorphism) may not be preserved. Consequently, q_h and d_h effectively map to and from a family of semirings, where the specific semiring to which they map is contingent upon the chosen value of h . The closer h is to 0, the closer q_h maps to the \mathbb{R}_+ semiring, and viceversa. Despite this observation, there is still tight connection between the operations performed in the h -semiring

and its “tropical” counterpart. In fact, consider the following generalised addition and multiplication:

$$\begin{aligned} a \oplus_h b &= d_h(q_h(a) + q_h(b)) \quad \text{and} \\ a \odot_h b &= d_h(q_h(a) \cdot q_h(b)). \end{aligned}$$

From the above formulations, it follows that $\forall a, b \in \mathbb{T}$:

$$\begin{aligned} a \odot_h b &= d_h(q_h(a) \cdot q_h(b)) \\ &= -h \ln(e^{-a/h} e^{-b/h}) \\ &= -h \ln e^{-(a+b)/h} \\ &= a + b = a \odot_{\mathbb{T}} b, \end{aligned} \tag{4.3}$$

and

$$\begin{aligned} a \oplus_h b &= \lim_{h \rightarrow 0^+} d_h(q_h(a) + q_h(b)) \\ &= \lim_{h \rightarrow 0^+} -h \ln(e^{-a/h} + e^{-b/h}) \\ &= \min(a, b) = a \oplus b. \end{aligned} \tag{4.4}$$

Analogously, matrix operations also approximate the generalized dot product in the tropical semi-ring:

$$\lim_{h \rightarrow 0^+} d_h[q_h[\mathbf{W}]^k] = \mathbf{W}^{\odot_{\mathbb{T}} k}$$

where \mathbf{W} is a matrix and \mathbf{W}^k symbolises \mathbf{W} to the power of k in the h -semiring, $\mathbf{W}^{\odot_{\mathbb{T}} k}$ is its tropical counterpart and $f[\mathbf{W}]$ denotes element-wise application of f on the matrix \mathbf{W} . “Tropical” matrix multiplications are the key points of our discussion. In fact, through matrix multiplications in the tropical space we can actually represent entire *algorithms*. Examples of this property are provided in [subsection 2.3.5](#) (i.e., BFS and Bellman-Ford). Furthermore, the above formulations explicitate a very important observation: operations performed in the h -semiring “approximate” those executed in the tropical semiring. Thus, we have forged a substantive connection between the h -semiring and the tropical one. Such connection degenerates into a bijection between the \mathbb{R}_+ semiring and \mathbb{T} whenever h is sufficiently small. This implies that operations executed within the \mathbb{R}_+ (or \mathbb{R}) semiring must align with their counterparts in the “tropical” semiring. Furthermore, considering that tropical operations can represent “algorithmic steps”, operations within \mathbb{R}_+ equivalently correspond to these algorithms.

[Figure 4.1](#) positions all of this within the context of the EPD architecture and elucidates the various transformations between the two semirings. In particular, the figure shows that we have successfully implemented an encoder $f: \mathbb{T} \rightarrow \mathbb{R}_+$ (i.e., q_h) which maps from the \mathbb{T} semiring – where we supposedly receive DP inputs – to the \mathbb{R} semiring, where our processor network p naturally operates, and a decoder $g = d_h$ that maps back to \mathbb{T} for computing DP outputs. Our processor, then, is taught to approximate tropical steps in the h -semiring. Potentially, this enables our processor to

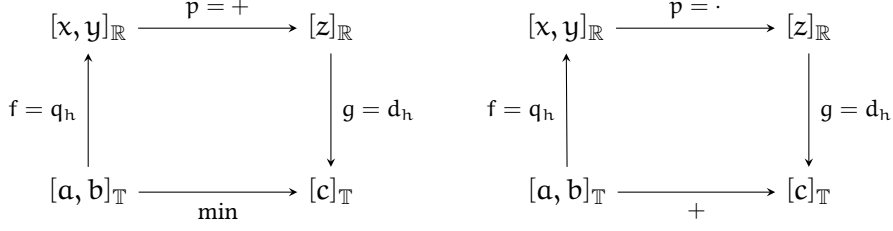


Figure 4.1: Category-theory inspired diagrams showcasing the equivalences $\min_{\mathbb{T}} \equiv +_{\mathbb{R}}$ (left-hand diagram) and $+_{\mathbb{T}} \equiv \cdot_{\mathbb{R}}$ (right-hand diagram). Specifically, in the left-hand diagram, starting from inputs $[a, b]$ in the \mathbb{T} -semiring, we can derive $c = \min(a, b)$ by following two paths. First, apply the \min -morphism to obtain c directly. Second, map $[a, b]$ to \mathbb{R} through Maslov quantisation q_h and perform an update step through the $+$ -morphism to obtain z . Ultimately, c can be decoded by application of d_h to z . The same also holds for the right-hand diagram (i.e., equivalence between tropical addition and real multiplication). The two diagrams together forms the bijection $\langle \mathbb{T}, \min, +, +\infty, 0 \rangle \leftrightarrow \langle \mathbb{R}, +, \cdot, 0, 1 \rangle$. Finally, f, p and g refer to the EPD architecture and elucidate how the different EPD component are instantiated to enable mapping between the two semirings.

approximate steps of algorithms as well. As a consequence, by showing that a processor network p can indeed approximate \mathbb{T} operations up to arbitrary precision, we will successfully show that p can also approximate related algorithmic steps arbitrarily well. Note that in the diagram p should leverage conventional addition and multiplication. Consequently, supposing p is a graph network, we should choose a proper architecture reflecting this property. We explore a suitable choice for our processor in the next section.

4.1.2 Processor alignment and DP approximation

As thoroughly discussed in [subsection 3.2.1](#), in the context of NAR, we typically choose graph network processors with max aggregators. Here, however, we should carefully consider that we are executing message-passing steps in an h -semiring, where inputs have appropriately been parsed through Maslov quantisation and dequantisation maps. As evident from equation (4.4), a \min (or \max) operation corresponds to a sum operation in the h -semiring. Hence, we should consequently choose a GN architecture with a sum aggregator, rather than the typically recommended choice of \max . For such reasons, the Graph Isomorphism Network (GIN) is the natural choice:

$$\mathbf{h}_v^{(\ell+1)} = \text{MLP} \left((1 + \epsilon) \mathbf{h}_v^\ell + \sum_{u \in \mathcal{N}(v)} \mathbf{h}_u^\ell \right), \quad (4.5)$$

or, equivalently in matrix form:

$$\text{GIN}(\mathbf{A}, \mathbf{H}^{(\ell)}) = \mathbf{H}^{(\ell+1)} = \text{MLP} \left((1 + \epsilon) \mathbf{H}^{(\ell)} + \mathbf{A} \mathbf{H}^{(\ell)} \right). \quad (4.6)$$

Here, ϵ is a parameter that regulates the importance of self information in the message passing scheme. Note that we subtly assume that the original \mathbf{A} contains no self loops (self loops will be added directly by the GIN layer). Now, consider a simple EPD architecture with a GIN processor:

$$\mathbf{y}^{(k)} = (g \circ \text{GIN}_\epsilon^k \circ f)(\cdot).$$

The following propositions will show how this simple architecture can model and learn exemplar DP algorithms up to arbitrary precision.

REACHABILITY APPROXIMATION (PROBLEM 1). Consider an unweighted graph $\langle \mathcal{V}, \mathcal{E} \rangle$ and consider its adjacency matrix \mathbf{A} and a vector $\chi_v \in \{0, 1\}^{|\mathcal{V}|}$ such that $\chi_v = 1$ for a given $v \in \mathcal{V}$ and $\chi_{u \neq v} = 0$. Additionally, let the encoder f be the identity function $f(x) = x$ and let $g = \text{MLP} \circ d_1$, with d_1 defined as in (4.1). Consider GIN_0 an instantiation of GIN with $\epsilon = 0$. Thus, GIN_0 can effectively learn to perform BFS starting from node v (that is, identifying the nodes that are reachable in the k -hop neighbourhood of v , $\mathcal{N}^k(v)$).

Proposition 3. Consider \mathbf{A} and χ_v , a positive constant $c > 0$, and $\mathbf{d} = \text{MLP}(d_1[\text{GIN}_0^k(\mathbf{A}, \chi_v)])$, with GIN_0 and MLP having any number of layers with ReLU activations. Thus, there exists a configuration of their parameters such that $|\mathbf{d}_u - \delta_u(\mathcal{N}^k(v))| \leq c$ for any $u \in \mathcal{V}$, where δ_u is the Dirac delta.

Proof. Fix $w_{\theta_1} = 1$ and $b_{\theta_1} = 0$ for every layer of GIN/MLP, if not stated otherwise. Since ReLU acts as an identity function for non-negative elements, we have that $\text{GIN}_0^k(\mathbf{A}, \chi_v) = (\mathbf{A} + \mathbf{I})^k \chi_v$. Let $\mathbf{W} \in \mathbb{T}^{|\mathcal{V}| \times |\mathcal{V}|}$ a matrix defined as in (2.17), with $\mathbf{d}_{u,v} = 0$ for all $(u, v) \in \mathcal{E}$. For any $h > 0$ we have that

$$\begin{aligned} Q_h[\mathbf{W}] &= \mathbf{A} + \mathbf{I} \\ Q_h[\chi_v] &= \chi_v. \end{aligned}$$

If we set $w_{\theta_1} = h$ in the first layer of MLP, we have that

$$\begin{aligned} h \cdot d_1[q_h[\mathbf{W}]^k \cdot q_h[\chi_v]] &= d_h[q_h[\mathbf{W}]^k \cdot q_h[\chi_v]] \\ &\xrightarrow{h \rightarrow 0^+} \mathbf{W}^{\odot k} \odot \chi_v = \mathbf{d}_o, \end{aligned}$$

where $[\mathbf{d}_o]_u = 0$ if $u \in \mathcal{N}^k(v)$ and $[\mathbf{d}_o]_u = \infty$ otherwise. By setting, instead, $w_{\theta_1} = -h$ and $b_{\theta_1} = 1$ in the first layer of MLP, we obtain

$$\begin{aligned} \lim_{h \rightarrow 0} \mathbf{d} &= \lim_{h \rightarrow 0} \sigma[1 - h \cdot D_1[(\mathbf{A} + \mathbf{I})^k \chi_v]] \\ &= \max[0, 1 - \mathbf{d}_o] \\ &= \delta(\mathcal{N}_+^k(v)). \end{aligned}$$

For a $h > 0$ small enough we have that

- for $u \in \mathcal{N}_+^k(v)$, $|\mathbf{d}_u - \delta_u(\mathcal{N}_+^k(v))| < c$ by definition of limit, and
- for $u \notin \mathcal{N}_+^k(v)$, $[\mathbf{d}_o]_u \gg 1$ and hence $\mathbf{d}_u = \delta_u(\mathcal{N}_+^k(v)) = 0$,

thus reaching the conclusion. \square

UNWEIGHTED SHORTEST PATH (PROBLEM 2). Consider the same set of inputs as for the reachability problem in the previous paragraph. The following proposition shows that GIN_ϵ can compute the shortest paths in an unweighted graph (or, equivalently, a equally weighted graph). Note that here we are actually approximating the Bellman-Ford algorithm.

Proposition 4. *Consider \mathbf{A} and χ_v , a positive constant $c > 0$, and $\mathbf{d} = \text{MLP}(\mathbf{d}_1[\text{GIN}_\epsilon^k(\mathbf{A}, \chi_v)])$, with GIN_ϵ and MLP having any number of layers with ReLU activation function, there exist a configuration of their parameters such that $|\mathbf{d}_u - d(u, v)| \leq c$ for any $u \in \mathcal{N}^k(v)$.*

Proof. Fix $w_\theta = 1$ and $b_\theta = 0$ for every layer of GIN/MLP , if not stated otherwise. Let $\mathbf{W} \in \mathbb{T}^{n \times n}$ a matrix defined as in (2.17), with $\mathbf{d}_{uv} = 1$ for all $(u, v) \in \mathcal{E}$. For any $h > 0$ we have that

$$\begin{aligned} Q_h[\mathbf{W}] &= e^{-1/h} \cdot \mathbf{A} + \mathbf{I}, \\ Q_h[\chi_v] &= \chi_v. \end{aligned}$$

By fixing $\epsilon = e^{1/h} - 1$, and $w_{\theta_1} = e^{-1/h}$ in the first layer of GIN , we have that

$$\text{GIN}_\epsilon^k(\mathbf{A}, \chi_v) = e^{-1/h} \cdot ((1 + \epsilon) \cdot \mathbf{I} + \mathbf{A})^k \chi_v = (\mathbf{I} + e^{-1/h} \cdot \mathbf{A})^k \chi_v,$$

and, by setting also $w_{\theta_1} = h$ in the first layer of MLP , we have that

$$\begin{aligned} \mathbf{d} &= h \cdot D_1[Q_h[\mathbf{W}]^k \cdot Q_h[\chi_v]] \\ &= D_h[Q_h[\mathbf{W}]^k \cdot Q_h[\chi_v]] \\ &\xrightarrow{h \rightarrow 0^+} \mathbf{W}^{\odot k} \odot \chi_v = \mathbf{d}_o, \end{aligned}$$

where

$$[\mathbf{d}_o]_u = \begin{cases} d(u, v) & \text{if } u \in \mathcal{N}^k(v) \\ \infty & \text{otherwise.} \end{cases} \quad (4.7)$$

By definition of limit (for a $h > 0$ small enough) we reach the conclusion. \square

WEIGHTED SHORTEST PATH (PROBLEM 2). Contrarily to the previous examples, consider a weighted graph $\langle \mathcal{V}, \mathcal{E}, \mathcal{W} \rangle$ with its tropical distance matrix $\mathbf{W} \in \mathbb{T}^{n \times n}$, defined as in (2.17). Additionally, w.l.o.g., consider its diagonal entries set to $+\infty$. Then $g \circ \text{GIN}_\epsilon \circ f$ can approximate a weighted shortest path assuming that $f = q_1 \circ \text{MLP}$, with q_1 defined as in (4.1), and g is the same as the previous examples.

Proposition 5. *Consider \mathbf{W} and χ_v , a positive constant $c > 0$, and $\mathbf{d} = \text{MLP}_d[\mathbf{d}_1[\text{GIN}_\epsilon^k(q_1[\text{MLP}_E[\mathbf{W}]], \chi_v)]]$, with GIN_ϵ , MLP_E , and MLP_d having any number of layers with ReLU activation function, there exist a configuration of their parameters such that $|\mathbf{d}_u - d(u, v)| \leq c$ for any $u \in \mathcal{N}^k(v)$.*

Proof. Fix $w_\theta = 1$ and $b_\theta = 0$ for every layer of GIN/MLP, apart in the first layer of MLP_E , where we set $w_{\theta_1} = 1/h$, and in the first layer of MLP_D , where we set instead $w_{\theta_1} = h$. As in the proof of (3), we have that $\text{GIN}_0^k(\mathbf{A}, \chi_v) = (\mathbf{A} + \mathbf{I})^k \chi_v$. Noticing that $q_1(x/h) = q_h(x)$ and $h \cdot d_1(x) = d_h(x)$, we obtain that

$$\begin{aligned} \mathbf{d} &= h \cdot d_1[q_1[\frac{1}{h}\mathbf{W}]^k \cdot \chi_v] \\ &= d_h[q_h[\mathbf{W}]^k \cdot Q_h[\chi_v]] \\ &\xrightarrow{h \rightarrow 0^+} \mathbf{W}^{\odot k} \odot \chi_v = \mathbf{d}_\circ, \end{aligned}$$

where \mathbf{d}_\circ is defined as in (4.7). By definition of limit (for a $h > 0$ small enough) we reach the conclusion. \square

To conclude, we have now established a direct link between tropical algebra and graph networks. Particularly, we showed that an EPD architecture with $g = (\text{MLP} \circ d_1)$, $p = \text{GIN}_\epsilon$ and $f = q_1 \circ \text{MLP}$ can approximate reachability and shortest path algorithms on graphs, by learning the h parameter. Furthermore, oftentimes DP can be understood as generalised path-finding algorithms (Dudzik & Veličković, 2022) similar to shortest path. Hence, propositions herein show potential to encompass a wider range of DP problems that can be framed as path-finding (e.g., task scheduling (Shirazi et al., 1990)).

4.1.3 Effects on network design

The propositions presented in the previous section also serve as theoretical ground to support prior NAR findings. An example of this lies in the commonly suggested choice of using max as aggregator in the GN processor. In the literature, this suggestion is often based on empirical evidence (Veličković et al., 2019, 2022a; Ibarz et al., 2022) and the answer to “*why choose a max aggregator?*” is addressed in terms of algorithmic alignment (Xu et al., 2020, 2021; Dudzik & Veličković, 2022). However, here we seek to answer to this question in a more mathematical sense. First, we note that our architectural choices do reflect the use of a component-wise maximum aggregator, even though we plug GIN which uses addition to aggregate node representations. The reason is that, in our regime, GIN operates on an h -semiring where its inputs and outputs are adequately processed by Maslov maps. As shown in Equation 4.4, thus, in this setting the sum operation in the h -semiring is equivalent to a min (or max) operation in the DP “tropical” space. As a result, our sum-aggregated GN aligns with our target *min*-aggregated DP algorithm.

However, in common NAR settings we usually deploy simple linear encoders and decoders (subsection 3.2.2) and we do not directly process data belonging to a tropical semiring. Therefore, assuming we target the same *min*-aggregated class of DP algorithms, *how would a different choice of the aggregator impact the learning problem?* Consider the target function to be Bellman-Ford as in subsection 3.2.1 and let us put our focus on the aggregation step only. Furthermore, assume we choose a

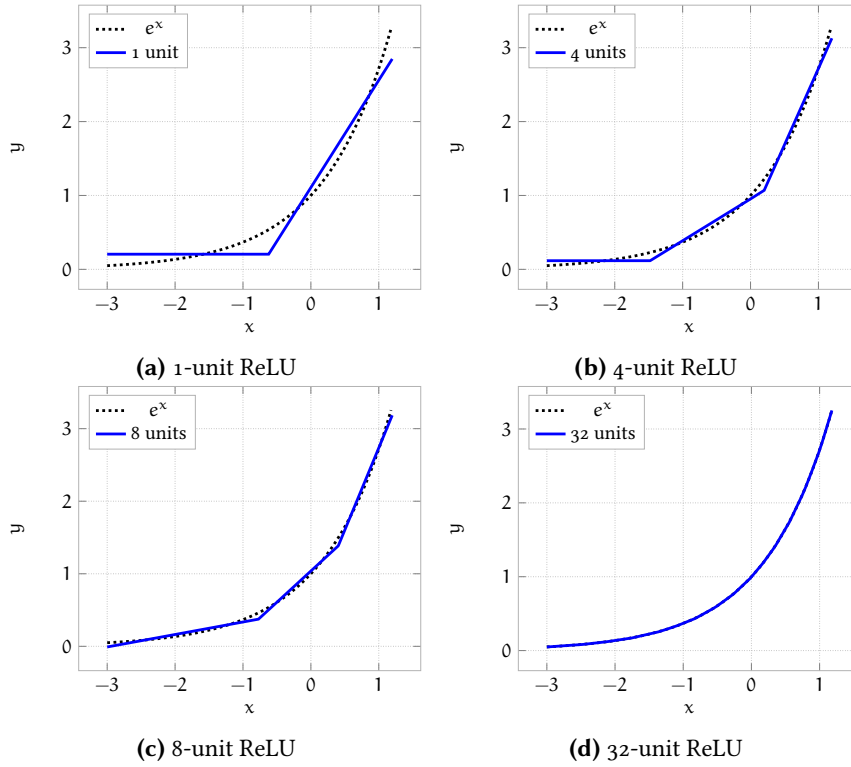


Figure 4.2: Illustration of approximating an exponential function with piecewise linear functions (ReLU). Plots have been obtained by approximating e^x with ReLU-MLPs with 1, 4, 8 and 32 neurons.

sum-aggregated processor similar to GIN. We report both equations in the following:

$$(\Sigma\text{-MP}) \quad \text{sum}(\{\psi(\mathbf{h}_v, \mathbf{h}_u, \mathbf{h}_{uv}) \mid u \in \mathcal{N}(v)\}) \quad (4.8)$$

$$(\text{BF}) \quad \text{min}(\{d_u + e_{uv} \mid u \in \mathcal{N}(v)\}). \quad (4.9)$$

Hence, in order for (4.8) to learn a min operation, there are two possibilities:

1. Encoders and decoders f and g learn exponential and logarithmic maps similar to (4.1).
2. The processor p learns a *softplus* function on neighbourhoods:

$$\max(\{u \in \mathcal{N}(v)\}) \approx h \log\left(\sum_{u \in \mathcal{N}(v)} e^{\frac{\psi(\mathbf{h}_v, \mathbf{h}_u, \mathbf{h}_{uv})}{h}}\right).$$

Here, h represents the *temperature* of the approximation and is the equivalent of the h term in equation (4.1). Note that this is in line with prior findings in linear algorithmic alignment (see, subsection 3.2.1) as the processor here is required to learn a non-linear transformation.

Consequently, we can effectively measure and quantify the drawbacks that a misaligned aggregator would impose on the learning model. In fact,

this either forces usage of non-linear encoders and decoders, as learning exponential and logarithmic functions through linear layers is impractical, or it places an additional learning load on the processor. Indeed, in the latter case the processor would be required to both learn the target DP algorithm *and* learn the aforementioned softplus aggregation with “low” values of temperature h (recall from [subsection 4.1.1](#) that $h \rightarrow 0$). Furthermore, NAR modules are usually deployed with ReLU activations to comply with (linear) algorithmic alignment requirements. Hence, the processor (or non-linear encoders and decoders) are tasked to approximate exponential (and logarithmic) mappings through piece-wise linear functions. [Figure 4.2](#) clearly shows that the “goodness” of such approximation strongly depends on the number of points of discontinuity (i.e., number of neurons in MLPs) we utilise. This means that a sub-optimal aggregator choice directly impacts the latent space complexity of NAR modules, effectively forcing to use a higher number of neurons to get an equally good approximation (compared to a GN with aligned aggregators). Finally, in light of the previously discussed linear extrapolation tendency of ReLU networks ([subsection 3.2.1](#) and (Xu et al., 2021)), we will likely *never* align to the exponential mappings outside the support of the training distribution, unless using exponential activations in the neural network at the cost, however, of possible numerical instabilities.

4.2 PLANNING VIA LEARNT HEURISTICS

In the previous section, we showed the GNs are a good learning model when learning *max*- and/or *min*-aggregated DP functions. This section capitalizes on this property to develop heuristic functions designed to enhance the efficiency of *planning* algorithms (Numeroso et al., 2022), with particular emphasis on the A^* search algorithm (Hart et al., 1968). A^* is a path-planning algorithm that directly improves on the Dijkstra’s algorithm (Dijkstra et al., 1959) and is particularly suited for solving planning tasks. Planning problems, on the other hand, are standard instances of DP problems that involve executing *actions* within an *environment* to achieve a specific *goal*. They can be formally defined as tuples $\langle \mathcal{S}, s_0, \mathcal{A}, \text{goal} \rangle$, where:

- \mathcal{S} is a set of possible *states* representing the possible configurations of the environment.
- s_0 is the *initial state*.
- \mathcal{A} is the set of possible actions. An action $a \in \mathcal{A}$ is a function $a : \mathcal{S} \rightarrow \mathcal{S}$ that describes a transition from one state to another.
- $\text{goal} : \mathcal{S} \rightarrow \{0, 1\}$ is a function that determines whether a given state is a goal state, denoted as s^* .

Consequently, a solution to a planning problem is an action sequence a_0, a_1, \dots, a_n that transitions from the initial state to a goal state. This is akin to the notion of graph paths (see [Definition 8](#)). Indeed, we typically

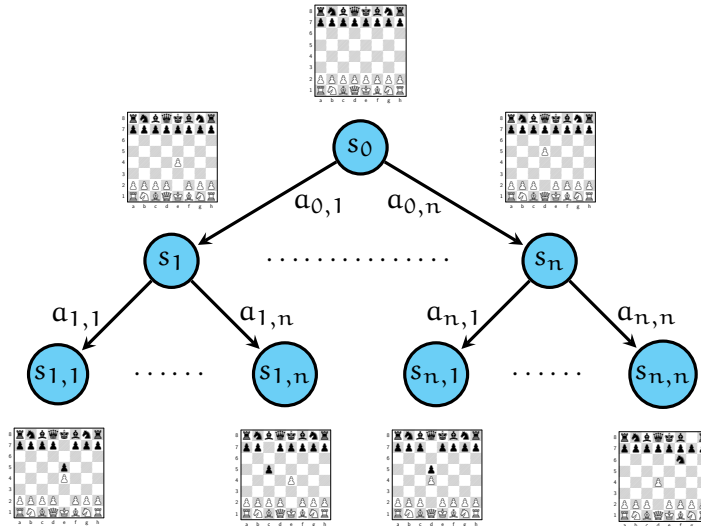


Figure 4.3: An example of a popular state-action graph representing a game of chess. Here, *states* S represent possible board positions, whereas actions \mathcal{A} are moves that change the configuration of the chessboard (represented as edges). Note that actions taken in state s_0 directly affect the range of potential actions available in the subsequent state s_i .

apply algorithms that find a path in the *state-action* graph¹ – which represents the planning problem – from s_0 to s_* . A visual representation of a state-action graph is depicted in Figure 4.3.

Problems of this nature, and their corresponding solution algorithms find applications across numerous fields, including Robotics (Mac et al., 2016), Computer Science (Gebser et al., 2013; Chen et al., 2020a) and Chemistry (Yeh et al., 2012). When seeking for the goal state s^* , the most efficient search algorithms usually exploit heuristic functions to navigate through the state-action graph. Informally, these heuristics are functions $h : \mathcal{S} \rightarrow \mathbb{R}$ that, given a state s , return a real number indicating the quality of that state. In such context, $h(s)$ refers to how “fast” we can reach the goal state through visiting s . Such heuristics, thus, enable faster convergence towards the goal state. In the context of A^* , for instance, the heuristic is used for selecting the next node to evaluate during path planning computation. Precisely, A^* can be seen as a generalisation of the Dijkstra’s algorithm where, the priority key in line 8 of Algorithm 2 is changed from $d[s]$ to $d[s] + h[s]$. Hence, A^* fundamentally prioritises the nodes which are believed to be closer to the goal state. As a result, the effectiveness of the whole algorithm relies on a careful design of such heuristic, which is often specialised for the problem at hand (Khalidi et al., 2020). Such hand-crafted heuristics necessitate domain knowledge and are often subject to extensive trial-and-error phases during their development. To circumvent this manual design process, an appealing alternative is to automate the discovery of such heuristics, by learning them from

¹ a graph where states are nodes \mathcal{V} and actions are connections (or edges \mathcal{E}) among states

data. In the literature, there exist solutions based on supervised learning (ús Virseda et al., 2013; Wilt & Ruml, 2015; Kim & An, 2020) and imitation learning/reinforcement learning (Pándy et al., 2022). In contrast, this work formalises an unsupervised learning problem to learn a proficient heuristic function for graph-based path-planning problems. Such heuristic is then plugged into the A^* algorithm. We delve into technicalities of the approach in the following sections.

4.2.1 Learning consistent heuristics

In this work, we aim to learn an *admissible* and *consistent* heuristic function for A^* on weighted graphs $G = \langle \mathcal{V}, \mathcal{E}, \mathcal{W} \rangle$.

Definition 24 (Admissible Heuristic). *A heuristic $h : \mathcal{V} \rightarrow \mathbb{R}$ is said to be admissible for a graph $g = \langle \mathcal{V}, \mathcal{E}, \mathcal{W} \rangle$ and a target node s^* if, for any node $v \in \mathcal{V}$, it holds that*

$$h(v) \leq h^*(v)$$

where $h^*(v)$ is the true cost of the “shortest path” from node v to the target node s^* .

In other words, $h(v)$ never overestimates the real cost of reaching the target node s^* from v .

Definition 25 (Consistent Heuristic). *A heuristic $h : \mathcal{V} \rightarrow \mathbb{R}$ is said to be consistent (or monotonic) for a graph $g = \langle \mathcal{V}, \mathcal{E}, \mathcal{W} \rangle$ if, for any $(u, v) \in \mathcal{E}$ with cost w_{uv} , it satisfies the following condition:*

$$h(u) \leq w_{uv} + h(v)$$

That is, for every node u and “successor” v , the triangle inequality is satisfied. Note that admissibility directly follows from the definition of consistency, hence any consistent heuristic is also admissible. In the context of A^* , an admissible h will ensure that the algorithm will return the optimal path from s_0 to s^* (or, in planning terms, the best action sequence), where as consistency guarantees that each intermediate node (or state) is evaluated no more than once during optimal path computation (i.e., better efficiency).

LEARNING OBJECTIVE. To learn a consistent heuristic, we frame the learning problem for our neural network as a constrained minimisation problem:

$$\min h(s^*) - h(s_0) \tag{4.10}$$

$$\text{subject to } h(v) - h(u) \leq w_{uv} \quad \forall (u, v) \in \mathcal{E}. \tag{4.11}$$

Note that this formulation guides the learnt heuristic values to low values in the proximity of s^* and progressively higher values to nodes far from the goal. Additionally, the constraints serves to ensure the heuristic consistency property.

Within this study, we also aim to make our learnt heuristic function invariant to graph sizes (i.e., we want the heuristic to be applicable regardless of the number of states in the planning problem). Given that this is one of the key prospects of neural algorithmic reasoning, we exploit it to attain this particular objective. In doing so, we apply the MTL technique presented in [section 3.3](#) to learn jointly the Dijkstra’s algorithm ([Dijkstra et al., 1959](#)) and an optimal assignment to [\(4.10\)](#). This way, we constrain our learnt heuristic function to be computed in an “algorithmic” fashion, effectively biasing it towards size invariance. Parameters of the model are then optimised through a combination of a cross-entropy error signal computed and supervised on the ground truth Dijkstra’s outputs at each step t (i.e., step-wise supervision) and the unsupervised objective described in [\(4.10\)](#). Specifically, we optimise [\(4.10\)](#) by relaxing its constraints and introducing penalties corresponding to the magnitude of each constraint violation. Furthermore, as the main objective $\{h(t) - h(s)\}$ is unbounded, we add an additional penalty term proportional to the squared L^2 -norm of the predicted heuristics (i.e., $\|\mathbf{y}^{(t)}\|_2^2$).

The resulting objective is formulated as follows:

$$\begin{aligned} \mathcal{L}_i(\theta; \lambda) = & \frac{1}{T} \sum_t \mathcal{L}_{\text{CE}}(\mathbf{o}^{(t)}, \mathbf{p}^{(t)}) + \\ & \frac{1}{T} \sum_t \left[(\mathbf{y}_{s_0}^{(t)} - \mathbf{y}_{s^*}^{(t)}) + \right. \\ & \left. \sum_{(u,v) \in E} (\mathbf{y}_v - \mathbf{y}_u) \cdot \mathbf{1}_{[\mathbf{y}_v - \mathbf{y}_u > w_{uv}]} + \lambda \|\mathbf{y}^{(t)}\|_2^2 \right], \end{aligned}$$

where \mathcal{L}_{CE} is the cross-entropy function, $\mathbf{1}_{[\mathbf{y}_v - \mathbf{y}_u > w_{uv}]}$ is an indicator function checking for satisfaction of the specific constraint, and λ is a weighing hyper-parameter.

MODEL CONFIGURATION. The neural algorithmic reasoner architecture is a specification of the encode-process-decode and is depicted in [Figure 4.4](#). The neural forward pass is the same as described in [subsection 3.2.2](#). In the following we provide a specification of the different components.

The encoder layer comprises encoders for Dijkstra’s inputs f_D and for positional features for the computation of heuristic values (i.e., identity of the starting node s_0 and the target node s^*), which are processed through a second encoder f_h . Both f_D and f_h are linear transformations. The processor p is a MPNN ([Gilmer et al., 2017](#)) with max aggregator. Decoder specifications include a linear projector g_h that maps to heuristic values $\hat{h}^{(t)}(v) = \mathbf{y}_v = g_h(\cdot)$ and g_D that predicts Dijkstra’s outputs $\mathbf{o}^{(t)} \approx \mathbf{p}^{(t)}$.

TEST INFERENCE. At test time, we run A^* where the priority key for the queue at line 8 of [Algorithm 2](#) is substituted for:

$$\text{key}(v) = d(v) + \tilde{h}(v),$$

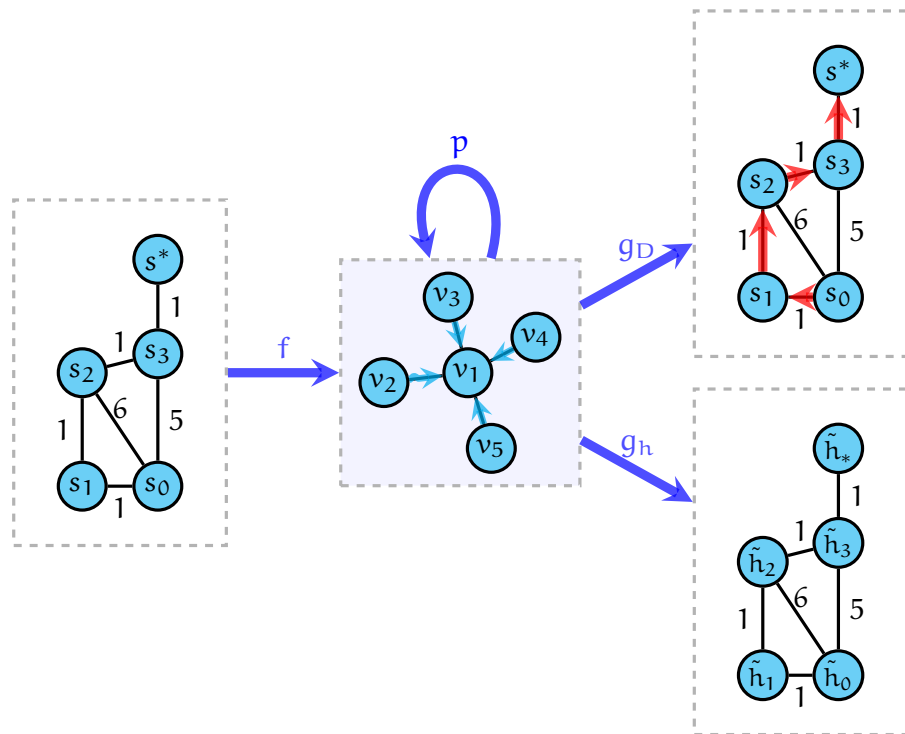


Figure 4.4: Illustration of model architecture used to learn A* heuristics. We employ MTL on the Dijkstra's algorithm and the learning of the heuristic function \tilde{h} (i.e., $\tilde{h}(s_i) = h_i$ in the figure).

Level	Hyperparameter	[a, b]	Distribution
Level 1	Learning rate	$[1 \cdot 10^{-4}, 1 \cdot 10^{-2}]$	log-uniform
	Weight decay	$[1 \cdot 10^{-5}, 1 \cdot 10^{-1}]$	log-uniform
	Hidden dimension	[16, 512]	uniform
	λ	$[1 \cdot 10^{-3}, 1 \cdot 10^{-1}]$	uniform
Level 2	Learning rate	$[9 \cdot 10^{-4}, 4 \cdot 10^{-3}]$	log-uniform
	Weight decay	$[9 \cdot 10^{-4}, 4 \cdot 10^{-3}]$	log-uniform
	Hidden dimension	[80, 100]	uniform
	λ	$[5 \cdot 10^{-2}, 1 \cdot 10^{-2}]$	uniform

Table 4.1: First-level and second-level random search configurations used to optimise learning of \tilde{h} .

where $d(v)$ represents the distance from node v to the source node s_0 and \tilde{h} is our learnt heuristic function. Compared to vanilla Dijkstra, we introduce an additional overhead due to the computation of heuristic values $\tilde{h}(v)$ for each node v within the graph. To keep this overhead limited, we compute $\tilde{h}(v)$ for any v in the graph by only executing one **single pass** of the processor p . This has two implications. First, the introduced overhead can be exactly quantified as $O(|\mathcal{V}|\bar{n})$ where \bar{n} is the average node degree. Second, $\tilde{h}(v)$ is only computed based on its immediate neighbours, and thus a node v might not directly “see” the goal state s^* . This means that we are essentially navigating in a **partially observable environment**, where our heuristic function has to give good indications without actually knowing where the goal state is at early stages of the algorithm. This poses an additional challenge to our learner, as in common A^* settings the heuristic function is assumed to be able to access s^* ’s location.

4.2.2 Experimental evaluation

Here, we detail the experimental setting, including model selection and results.

MODEL SELECTION. To select the best model hyper-parameters, we utilise a bi-level random search strategy, where the best sampled hyper-parameters in the initial stage are further refined through a second, more granular, random search. Details of the two-stage random search are presented in [Table 4.1](#). We sampled $n = 200$ configurations for each level of the random search.

DATA GENERATION. We generate three different graph sets, labelled as VERY DENSE, DENSE, and SPARSE. Each of the three sets includes Erdős-Rényi ([Erdős et al., 1960](#)) graphs with varying edge sampling probabilities $p = 0.5$, $p = 0.35$, and $p = \frac{\log |\mathcal{V}|}{|\mathcal{V}|}$, respectively. To rigorously evaluate

our initial claim of size invariancy of the learnt heuristic function, we produce training and validation sets involving small graphs – 16 nodes – and nine separate test sets, having increasing number of nodes: 16, 32, 64, 96, 128, 160, 192, 224, and 256. We utilise 1000 instances for training and 128 for validation and testing. Notably, our model is solely optimised on the DENSE distribution, whereas the other two distributions are only used for testing purposes.

METRICS. We keep track and report four different metrics:

1. \mathcal{C} : which refers to the percentage of nodes for which the triangle inequality in (4.10) is satisfied. Fundamentally, \mathcal{C} evaluates the consistency of the heuristic function.
2. GAP: which is the optimality gap. This is computed by considering the cost of the path $\pi_{\tilde{h}} = s_0 \dots s^*$ found by executing A^* with the learnt heuristic function, and comparing it to the cost of the optimal path π_* found by executing Dijkstra. The optimality gap is calculated as:

$$\text{GAP} = \frac{c(\pi_{\tilde{h}})}{\pi_*} - 1 \quad \text{where} \quad c(\pi) = \sum_i w_{\pi_i, \pi_{i+1}}.$$

3. \mathcal{J} : which refers to the number of iterations needed to reach the goal state (or target node) s^* . This metric is included to measure the efficiency of the learnt heuristic function.
4. SPEEDUP: which measures the actual speed-up runtime of running A^* equipped with the learnt heuristic compared to running vanilla Dijkstra. The formula to compute the speedup is:

$$\text{SPEEDUP} = \frac{\text{Dijkstra runtime}}{\text{A* runtime}}.$$

RESULTS ANALYSIS. We evaluate our model by executing the A^* algorithm, employing learnt heuristics, across all nine test sets of the three datasets, and average the outcomes over five trials. The results from our experimental analysis are presented in Table 4.2. Additionally, we also include a graphic illustration of results for *dense* graphs in Figure 4.5.

Our learnt heuristic function is compared against a “zero” heuristic function (i.e., $h(v) = 0$ for all v), which is equivalent to the Dijkstra’s algorithm, and a random baseline that samples values uniformly in $[0, 1]$ (i.e., $h(v) \sim \mathcal{U}[0, 1]$). The first conclusion that can be drawn from empirical results of Table 4.2 is that the heuristic function predicted by the model is very close to be fully consistent, as the number of violated triangular inequalities is very low (i.e., $\leq 0.9\%$ on average) on each of the three different test distributions. Furthermore, heuristics seem to be mostly *size invariant*, as performance appear not to degrade as we test it on 2x, 6x, 12x and 16x times larger graphs compared to training data. The optimality gap also reflects a good tendency, particularly for SPARSE data, of the model with respect to finding the optimal paths while evaluating fewer

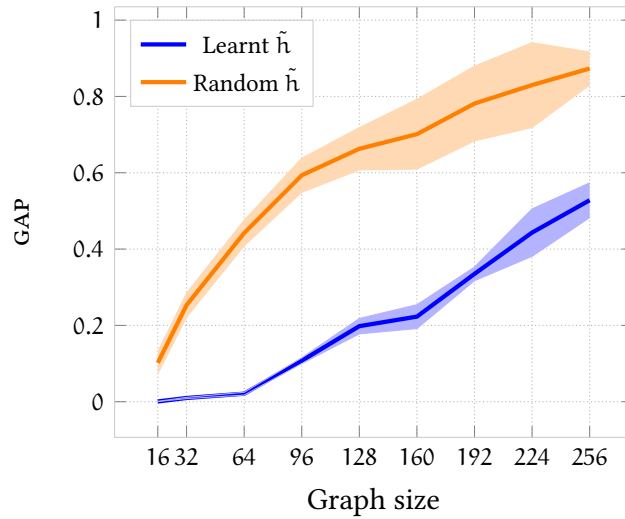
Metrics	32 nodes	96 nodes	192 nodes	256 nodes
SPARSE				
\mathcal{C} (\uparrow)	99.4 \pm 0.06%	99.7 \pm 0.04%	99.8 \pm 0.03%	99.8 \pm 0.03%
GAP (\downarrow)	0.03 \pm 0.01%	0.18 \pm 0.05%	0.19 \pm 0.09%	0.09 \pm 0.01%
\mathcal{J}_{A^*} (\downarrow)	17 \pm 1	43 \pm 1%	74 \pm 2	99 \pm 3
\mathcal{J}_D (\downarrow)	19	53	97	132
SPEEDUP (\uparrow)	0.94	1.08	1.19	1.23
DENSE				
\mathcal{C} (\uparrow)	99.2 \pm 0.08%	99.4 \pm 0.09%	99.5 \pm 0.09%	99.5 \pm 0.09%
GAP (\downarrow)	0.98 \pm 0.16%	10.75 \pm 0.77%	33.5 \pm 1.79%	52.8 \pm 4.55%
\mathcal{J}_{A^*} (\downarrow)	12 \pm 1	22 \pm 2	22 \pm 3	21 \pm 5
\mathcal{J}_D (\downarrow)	17	51	97	132
SPEEDUP (\uparrow)	0.93	2.29	4.30	4.83
VERY DENSE				
\mathcal{C} (\uparrow)	99.1 \pm 0.08%	99.4 \pm 0.11%	99.5 \pm 0.11%	99.5 \pm 0.11%
GAP (\downarrow)	0.7 \pm 0.15%	19.8 \pm 1.53%	59.4 \pm 5.00%	73.5 \pm 6.75%
\mathcal{J}_{A^*} (\downarrow)	11 \pm 1	16 \pm 2%	16 \pm 3	16 \pm 4
\mathcal{J}_D (\downarrow)	17	50	90	130
SPEEDUP (\uparrow)	1.22	2.60	5.06	5.24

Table 4.2: Performance of A^* with learnt heuristic function on 4 out of the 9 test sets, i.e. 32, 96, 192, 256 nodes. \mathcal{C} represents percentage of nodes for which the triangle inequality is satisfied, GAP and SPEEDUP refer to the optimality gap and the runtime speedup, respectively, and \mathcal{J}_{A^*} and \mathcal{J}_D indicate the iterations performed by A^* with learnt heuristic and Dijkstra, respectively. (\uparrow) means “the higher the better”, (\downarrow) means “the lower the better”.

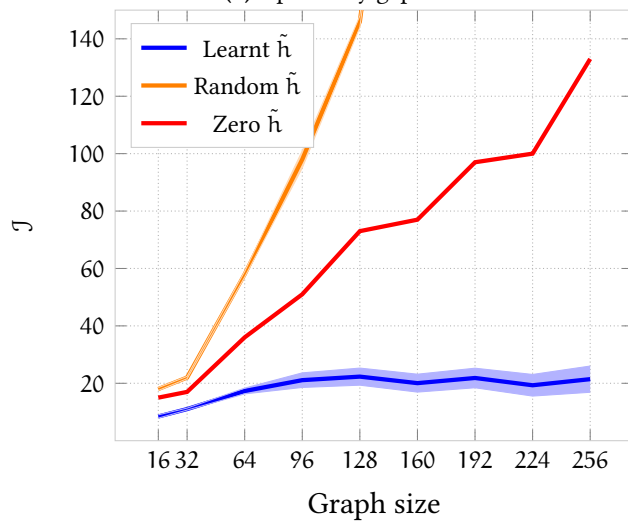
nodes compared to Dijkstra (i.e., \mathcal{J}_{A^*} vs. \mathcal{J}_D). For DENSE and VERY DENSE graphs, however, the optimality gap does degrade for larger graphs, as the number of paths gets combinatorially larger with high connectivity. We recall, however, that heuristics are computed only based on 1-hop neighbours, which might limit the performance in case of high node degree and high number of paths, as it is the case for the two DENSE and VERY DENSE distributions.

Performance-wise, A^* equipped with the learnt heuristic function is more efficient, by far, than Dijkstra (see results on VERY DENSE 256-node graphs in Table 4.2, where $\mathcal{J}_{A^*} \approx 16$ and $\mathcal{J}_D = 130$). This result is confirmed also by the SPEEDUP metric, which measures the exact computational runtime of computing the heuristics plus running the A^* search, indicating that the overall time complexity of the learnt search does not exceed that of running classic Dijkstra. This result can also be visualised in Figure 4.5, for dense graphs.

Finally, the consistent results achieved on each of the three different graph distributions suggest that the model can generalise across different



(a) Optimality gap.



(b) Number of iterations.

Figure 4.5: (a). Comparison of the optimality gap achieved by the learnt heuristic and a random baseline. (b). Number of iterations performed by A* with different heuristic function. Our learnt heuristic performs the best among all, keeping the number of iterations constant across different graph sizes. Note that the zero heuristic corresponds to running the Dijkstra's algorithm.

Erdős–Rényi distributions (recall that the model is only trained on DENSE graphs).

5

LEARNING COMBINATORIAL ALGORITHMS

In this chapter, we delve into the second batch of contributions presented in this PhD thesis, which are mainly about learning algorithms that target combinatorial optimisation problems (see [section 2.2](#)). Herein, we provide empirical evidence of the usefulness of different *algorithmic biases* to target, respectively: algorithmic learning problems; predictive graph learning tasks; and combinatorial optimisation problems.

In this respect, the section “*Leveraging Strong Duality*” shows how we can leverage strong duality (see [Theorem 2](#)) in neural algorithmic reasoning in order to: learn algorithms to a better precision, with particular emphasis on the Ford-Fulkerson algorithm ([Algorithm 5](#)); and utilise duality as a strong inductive prior for solving edge classification tasks.

Finally, in “*Learning approximation via algorithmic primitives*”, we demonstrate the usefulness of algorithmic priors for solving combinatorial optimisation problems through quantitative experiments on NP-hard CO problems. To the best of our knowledge, no prior work in the field of neural combinatorial optimisation ever explored algorithmic-based approaches.

5.1 LEVERAGING STRONG DUALITY

In [section 3.3](#), we learnt about multiple ways of teaching and utilising algorithmic knowledge with neural networks. In particular, we discussed the MTL paradigm, which can be summarised as a technique that enables neural networks to solve multiple tasks at once. As introduced in the aforementioned section, [Xhonneux et al. \(2021\)](#) verify the importance of this methodology for OOD generalisation in the context of neural algorithmic reasoning, by tasking neural networks to learn multiple related algorithms simultaneously. The rationale here is that many classical algorithms share sub-routines, such as Dijkstra and Bellman-Ford, ([Algorithm 2](#) and [Algorithm 1](#)), which help the network learn more effectively and be able to transfer knowledge among the target algorithms. Interestingly, MTL is possible also on sets of diverse (possibly unrelated) algorithms, as shown in ([Ibarz et al., 2022](#)).

PROBLEM STATEMENT. However, learning some specific algorithms might require learning of very specific properties of the input data, for which multi-task learning may not help. In this work, we particularly target one such algorithm, which is the Ford-Fulkerson algorithm, presented in [subsection 2.3.4](#). To elaborate on why Ford-Fulkerson requires stronger reasoning abilities, we have to consider the *algorithmic problem* that we are solving via the execution of Ford-Fulkerson. This problem is max-flow ([Problem 4](#)). As discussed in [subsection 2.1.3](#), in order to solve

max-flow, a learner is required to *identify* and *reason* in terms of a set of *bottleneck* edges. These bottleneck edges are such that a decrease in their capacity causes a proportional decrease in the maximum flow solution in the flow network, and are equivalent to the notion of minimum cut of the flow network (Problem 5).

From an intuitive standpoint, this is inherently more difficult than learning, say, the shortest path update rule of equation (2.11). Furthermore, it is also unclear which other algorithms possess a similar “sub-routine” (i.e., identifying bottleneck edges) that can positively influence the learning of Ford-Fulkerson in the MTL scheme.

Furthermore, unlike simpler algorithms, such as shortest path algorithms, Ford-Fulkerson deals with the optimisation of a *constrained optimisation problem*, described in Equation 2.3, where constraints are non-trivial (see equations (2.1) and (2.2)).

DUALITY AS INDUCTIVE BIAS. Driven by these specific requirements, we explore alternative learning setups to enable better reasoning abilities of our algorithmic reasoners. We find a promising candidate in the *duality* information, introduced and discussed in subsection 2.2.3. The fundamental idea here is that many “algorithmic problems”, such as flow problems and shortest paths, can be naturally reduced to linear programs (subsection 2.2.2), enabling us to effectively utilise duality relationships.

In the context of neural algorithmic reasoning, there are several reasons why considering primal-dual information is sensible:

1. By incorporating *primal-dual* objectives, we allow a neural network to reason on the task from two different (and often complementing) perspectives. This can significantly ease the learning of algorithms, especially those that require recognising and reasoning about properties not directly present in the input data, such as Ford-Fulkerson. Specifically, the *max-flow min-cut theorem* (Ford Jr & Fulkerson, 2015) states that *strong duality* (see Theorem 2) holds for this pair of problems. Consequently, accurately identifying the minimum cut is crucial for deriving an optimal max-flow solution. Hence, duality is naturally present when learning Ford-Fulkerson.
2. Producing a more accurate step-by-step approximation reduces error propagation throughout the neural execution of the algorithm. In the case of Ford-Fulkerson, choosing a *wrong* edge (i.e., an edge which is not in the min-cut) for updating the flow might negatively impact the outcomes of subsequent iterations.
3. Ultimately, we relax the “standard” MTL assumption of having to learn multiple algorithms simultaneously. However, as we will see, we still employ MTL on both primal and dual solutions.

Hence, in this work, we study to what extent neural algorithmic reasoner can utilise dual information to learn max-flow and min-cut. Note that, graph networks are inherently able to learn minimum cut, as the problem itself complies with *permutation-compatible* functions (Fereydounian et al., 2022) (see also subsection 3.2.1). Therefore, resolving the

min-cut can serve as a valuable “milestone” for a network in the process of learning to solve max-flow.

Therefore, we suggest integrating duality information directly into the learning model, both as an additional signal to supervise on and as an input feature, by allowing the network to reuse its dual prediction in subsequent algorithmic steps. We name this approach Dual Algorithmic Reasoning (DAR) (Numeroso et al., 2023).

In the next sections, we delve into specifications of the model architecture utilised for learning Ford-Fulkerson as well as discussion on experimental settings and analysis.

5.1.1 Model architecture

In spirit of algorithmic alignment, we slightly modify the usual EPD architecture to more closely match the dynamics of the Ford-Fulkerson algorithm. A visual representation of the used architecture is provided in Figure 5.1.

Precisely, we still rely on the neural algorithmic reasoning blueprint (Veličković & Blundell, 2021) and the EPD architecture, but we utilise two processors p_{BF} and p_F , instead of one, to align with the two sub-routines composing Ford-Fulkerson (see pseudocode of Algorithm 5). As detailed in subsection 2.3.4, one procedure finds the *augmenting paths*, while the other performs update of the flow within the graph (i.e., $f_{uv} = f_{uv} + df$ and $f_{vu} = f_{vu} - df$).

Consequently, p_{BF} learns to retrieve augmenting paths, while p_F emits simultaneously the minimum cut \mathbf{c} and the flow assignments in the form of a matrix $\mathbf{F} \in \mathbb{R}^{|\mathcal{V}| \times |\mathcal{V}|}$, where:

$$\mathbf{c}_v = \begin{cases} 0 & \text{if } v \text{ is in the same cluster of } s \\ 1 & \text{if } v \text{ is in the same cluster of } t \end{cases},$$

$$\mathbf{F}_{uv} \approx f_{uv} \quad \forall (u, v) \in \mathcal{E}.$$

Specifically, p_{BF} is trained to find augmenting paths through execution of the Bellman-Ford algorithm, similar to (Georgiev & Lió, 2020). The sets of input, hints, and output used to train the architecture is the same as described in subsection 2.3.4.

The model “forward pass”, similarly, is mostly unchanged compared to subsection 3.2.2. Indeed, we still implement encoders and decoders as linear layers, whilst p_F is fed with the output of p_{BF} , as depicted in Figure 5.1. Both processors are instantiated as either MPNNs or PGNs (recall subsection 3.2.2). Precisely, the augmenting paths from s to t $\mathbf{p}_i^{(t)}$ are first decoded through a decoder g_{BF} :

$$\mathbf{p}_v^{(t)} = g_{BF}(\mathbf{z}_v^{(t)}, \mathbf{h}_v^{(t)}) \quad \forall v \in \mathcal{V}, \quad (5.1)$$

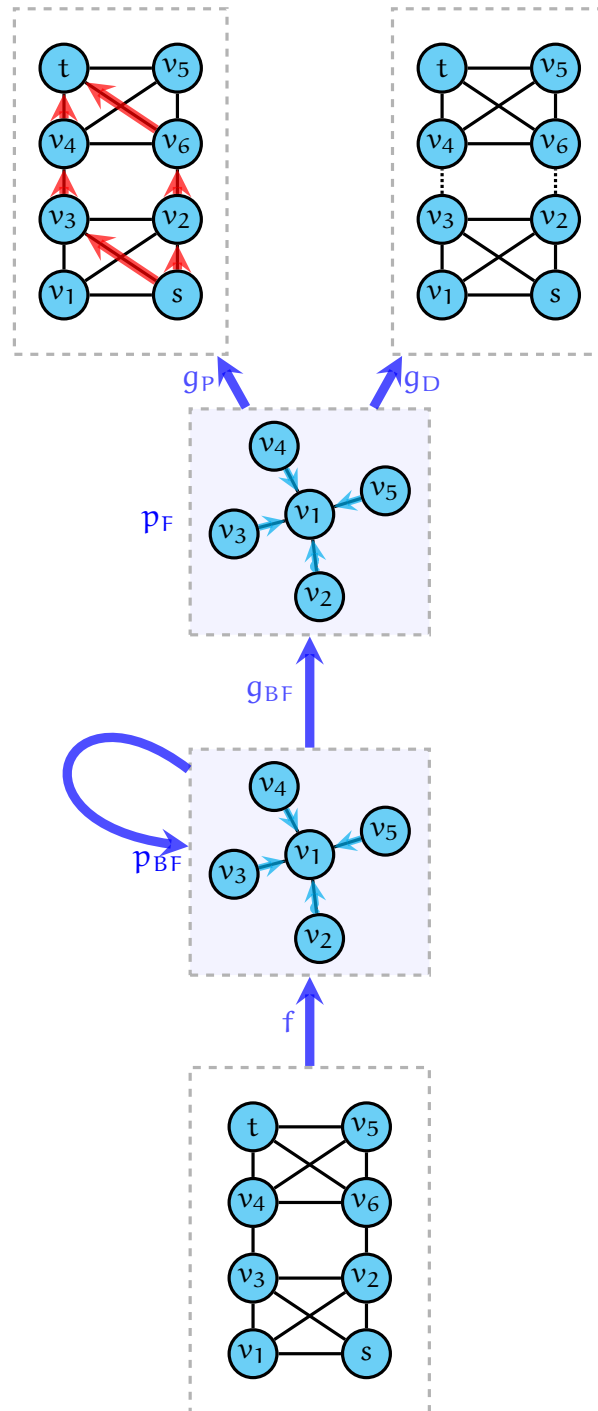


Figure 5.1: High-level architecture of the Dual Algorithmic Reasoner (DAR) used for max-flow and min-cut. Note how p_{BF} is iterated to retrieve augmenting paths, whereas p_F is required to simultaneously solve max-flow (g_P) and min-cut (g_D). The edges have all unitary capacity. Minimum cut is represented as dotted edges.

and then passed to p_F as an input feature to get node representations $\mathbf{h}_v^{(t)}$. Finally, we decode the target quantities of the algorithm as:

$$\begin{aligned}\tilde{\mathbf{F}}_{uv}^{(t)} &= g_P(\mathbf{h}_u^{(t)}, \mathbf{h}_v^{(t)}), \\ \mathbf{c}_v^{(t)} &= g_D(\mathbf{h}_v^{(t)}).\end{aligned}$$

Here, g_P and g_D are respectively the primal and dual encoders.

SATISFYING MAX-FLOW CONSTRAINTS. In order to comply with max-flow constraints discussed in [Problem 4](#), we ought to pay extra care on the $\mathbf{F}^{(t)}$ predictions. Given a graph $g = \langle \mathcal{V}, \mathcal{E}, \mathcal{C} \rangle$, where $c_{uv} \in \mathcal{C}$ is the capacity of the edge (u, v) , we have to ensure that (2.1) and (2.2) are satisfied. Notably, by looking at the problem definition in [Problem 4](#) and (2.2), we derive that the matrix \mathbf{F} must be antisymmetric (i.e., $\mathbf{F} = -\mathbf{F}^\top$). This can be seen trivially by noting that if node u sends a certain amount of flow quantity q to node v , then v must receive q flow from u (i.e., $F_{uv} = -F_{vu}$). Hence, we have a “0-th constraint” to satisfy, which is that of antisymmetry of \mathbf{F} . To comply with this, we apply the following transformation to $\tilde{\mathbf{F}}$:

$$\mathbf{F}_{A\text{-SYM}} = \tilde{\mathbf{F}} - \tilde{\mathbf{F}}^\top,$$

where $\tilde{\mathbf{F}}$ is the raw prediction of the model and $\mathbf{F}_{A\text{-SYM}}$ is inherently ensured to preserve antisymmetry. Moving forward, to ensure (2.1), we employ the *tanh trick*. Precisely, at each step of the algorithm, we scale each entry of $\mathbf{F}^{(t)}$ according to the hyperbolic tangent and the capacity matrix $\mathbf{C} = [c_{uv}] \in \mathbb{R}^{|\mathcal{V}| \times |\mathcal{V}|}$, as follows:

$$\mathbf{F}^{(t)} = \tanh(\mathbf{F}_{A\text{-SYM}}^{(t)}) \odot \mathbf{C}, \quad (5.2)$$

where \tanh and \odot are applied element-wise. Here, applying \tanh rescales the prediction to $[-1, 1]$. Hence, each entry of (u, v) of the resulting matrix can be thought of as a prediction of how much capacity c_{uv} we want to use (positively or negatively).

Finally, ensuring conservation of flows (equation (2.2)) is more challenging. Indeed, there is no clear way of how we can satisfy the constraint in an end-to-end differentiable manner. For this reason, to address this constraint we resort to a hand-crafted corrective procedure that is executed at the end of the neural execution of Ford-Fulkerson, whose pseudocode is reported in [Algorithm 9](#).

As detailed in the pseudo-code, the procedures discriminate between negative nodes \mathcal{V}^- (i.e., nodes v that *keep* some of the in-flow):

$$\mathcal{V}^- = \{v \mid v \in \mathcal{V} \wedge \sum_{(i,v) \in \mathcal{E}} F_{iv} + \sum_{(v,i) \in \mathcal{E}} F_{vi} < 0\},$$

and positive nodes \mathcal{V}^+ (i.e., nodes v that sends out *more* flow that they receive):

$$\mathcal{V}^+ = \{v \mid v \in \mathcal{V} \wedge \sum_{(i,v) \in \mathcal{E}} F_{iv} + \sum_{(v,i) \in \mathcal{E}} F_{vi} > 0\}$$

Thus, flow conservations is enforced through two steps:

Algorithm 9 Flow conservation correction algorithm

```

1: procedure ENSUREFLOWCONSERVATION( $G = \langle \mathcal{V}, \mathcal{E}, \mathcal{C} \rangle, \mathbf{F}, \mathbf{C}, s, t$ )
2:    $\mathcal{V}^- = \{v \mid v \in \mathcal{V} \wedge \sum_{(i,v) \in \mathcal{E}} F_{iv} + \sum_{(v,i) \in \mathcal{E}} F_{vi} < 0\}$ 
3:    $\mathcal{V}^+ = \{v \mid v \in \mathcal{V} \wedge \sum_{(i,v) \in \mathcal{E}} F_{iv} + \sum_{(v,i) \in \mathcal{E}} F_{vi} > 0\}$ 
4:   for each  $v \in \mathcal{V}^-$  do
5:      $\varepsilon = |\sum_{(i,v) \in \mathcal{E}} F_{iv} + \sum_{(v,i) \in \mathcal{E}} F_{vi}|$ 
6:     find a path from  $v$  to  $s$  and send back  $\varepsilon$  amount of flow to  $s$ 
7:   for each  $v \in \mathcal{V}^+$  do
8:      $\varepsilon = |\sum_{(i,v) \in \mathcal{E}} F_{iv} + \sum_{(v,i) \in \mathcal{E}} F_{vi}|$ 
9:     find a path from  $v$  to  $t$  and reduce the out-flow by  $\varepsilon$ 
10:   $\varepsilon_s = |\sum_{(s,i) \in \mathcal{E}} F_{si} - \sum_{(s,i) \in \mathcal{E}} C_{si}|$ 
11:  while  $\varepsilon_s > 0$  do
12:    find a path from  $s$  to  $t$  and reduce the out-flow by enforcing
    capacity constraints
13:    recompute  $\varepsilon_s$ 
14:  return  $\mathbf{F}$ 

```

1. Each $v \in \mathcal{V}^-$ sends back to the source node q flow, where q is equal to the magnitude of the constraint violation. Similarly, all $v \in \mathcal{V}^+$ take back from successors an amount of flow corresponding to the constraint violation. Note that here, we might have re-introduced some edge capacity constraints violation in \mathbf{F} .
2. We enforce back the edge capacity constraint by clamping F_{uv} to c_{uv} , and progressively adjusting the flow sent from s until no violations of (2.1) and (2.2) occur.

5.1.2 Experimental evaluation

We test DAR with two objectives in mind.

First, we aim to assess whether the augmented reasoning capabilities of dual algorithmic reasoners really help in the task of learning to execute Ford-Fulkerson. For this purpose, we train and test the DAR architecture on synthetic graphs. We dive into details of this setting in [subsubsection 5.1.2.1](#).

Second, we deploy DAR to solve a challenging graph learning task, with real world data, in order to prove the usefulness of algorithmic priors discussed in [section 3.1](#) and [section 3.3](#). Precisely, we test DAR against state-of-the-art baselines on a biologically relevant edge classification task on Brain-Vessel Graphs (BVG) ([Paetzold et al., 2021](#)). This benchmark comprehends large-scale graphs and is discussed more thoroughly in [subsubsection 5.1.2.2](#).

5.1.2.1 Executing Ford-Fulkerson

In this section, we provide all the details for reproducing our experiments, as well as a complete discussion on the obtained results.

ABLATION STUDIES. Ablation studies are conducted to rigorously evaluate the impact of the dual information, by training the DAR architecture devoid of the additional *dual decoder* g_D (i.e., outputting min-cut predictions), thereby preventing joint supervision together with the primal max-flow problem. We refer to this architecture as the *primal* architecture, marked as (P) in the following paragraphs. The full model (that of [Figure 5.1](#)), instead, is referred to as the *dual* model (D) . Additionally, we also test a neural architecture with an extra processor designed to learn the minimum cut before employing the Ford-Fulkerson algorithm. This is intended to check whether training jointly on both primal and dual problems is really needed, or having the minimum cut as an input feature would suffice. We refer to such architectures as *pipeline* models, marked as (PL) .

Furthermore, two distinct processor types are used to instantiate both p_{BF} and p_F with:

1. A fully-connected MPNN, executing [\(2.19\)](#) on a full graph regardless of its connectivity. We note that this approach is commonly used in NAR.
2. A PGN, which imposes exchange of node messages on the graph true connectivity and its algorithmically defined neighbourhoods, especially via `hints` (e.g., augmenting paths output by p_{BF} are also used to restrict the exchanged messages).

Furthermore, given the difficulties of linking the max-flow problem to the dynamic programming paradigm, we experiment with other types of GN aggregators other than max as well. Specifically, $\oplus = \{\max, \text{mean}, \text{sum}\}$. All models undergo training for 20,000 epochs using the SGD optimiser, with results averaged over five runs. *Teacher forcing* is employed with a decay factor of 0.999 on the `hints`, offering the network ground-truth `hints` during initial training stages while allowing network predictions during the majority of the training.

MODEL SELECTION. Similarly to experiments performed in [section 4.2](#), a bi-level random search optimisation scheme is employed here as well. Details on the hyperparameter space are reported in [Table 5.1](#). Specifically, we sample $n = 50$ configurations for each level of the bi-level random search. The best hyperparameters are chosen based on the validation error on F predictions, also shown in [Figure 5.2](#). In the figure, (P) , (D) , and (PL) follow the notation introduced in the previous paragraph.

DATA GENERATION. For this set of experiments, we generate two sets of graphs, following two different distributions. First, *2-community* graphs (see [subsection 2.1.2](#)), in which communities are Erdős–Rényi graphs with $p = 0.75$. Thus, nodes in different communities are interconnected with $p = 0.05$. Second, *bipartite* graphs (see also [subsection 2.1.2](#)). To generate algorithmic trajectories, we still employ the CLRS benchmark and training/validation/test setups are in CLRS-style, which is: 1000 training samples in the form of 2-community graphs having 16 nodes; 128

Level	Hyperparameter	[a, b]	Distribution
Level 1	Learning rate	$[1 \cdot 10^{-5}, 1 \cdot 10^{-1}]$	log-uniform
	Weight decay	$[1 \cdot 10^{-5}, 1 \cdot 10^{-1}]$	log-uniform
	Hidden dimension	[16, 512]	uniform
Level 2	Learning rate	$[1 \cdot 10^{-3}, 1 \cdot 10^{-2}]$	log-uniform
	Weight decay	$[1 \cdot 10^{-3}, 4 \cdot 10^{-3}]$	log-uniform
	Hidden dimension	[60, 100]	uniform

Table 5.1: DAR first-level and second-level random search configurations.

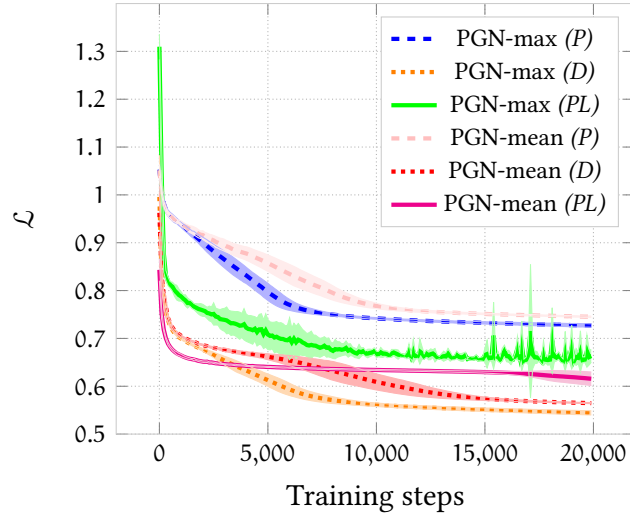


Figure 5.2: Ford-Fulkerson validation loss on synthetic data (PGNs). Note how the family of primal models underperform also in-distribution.

validation samples of 2-community graphs (same size as training one); 256 test samples of size 64 nodes, of which 128 are 2-community graphs and 128 are bipartite graphs. Following this approach, we not only enable testing OOD (on bigger 2-community graphs), but also *out-of-family* (OOF) (on larger bipartite graphs).

Lastly, edge capacities for 2-community graphs are sampled in $[0, 10]$ and then rescaled via a min-max normalisation, whereas bipartite graphs have discrete edge capacities in $\{0, 1\}$.

QUANTITATIVE ANALYSIS. Results regarding the neural approximation of Ford-Fulkerson are documented in [Table 5.2](#), employing Mean Absolute Error (MAE) as a performance metric for evaluating final flow assignment predictions \mathbf{F} . Concurrently, we measure how well the algorithm is approximated across all steps of the algorithm (i.e., $\bar{\mathbf{F}}^{(t)}$ column in [Table 5.2](#)). We also report minimum cut accuracy with respect to ground truths. This metric is only relevant for *dual* and *pipeline* models. We also compare all networks to an algorithm-agnostic graph network (marked as *NA*) in the table which directly produces the matrix \mathbf{F} without approximating Ford-Fulkerson. As clearly shown in the table, such variant demonstrated inferior to its algorithmically-informed counterparts, tes-

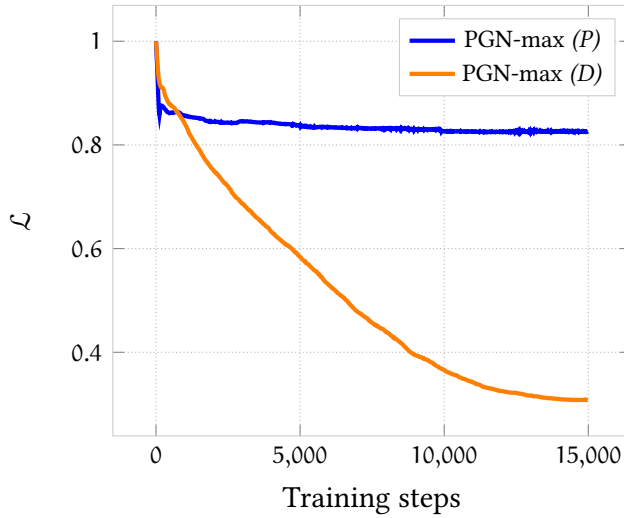


Figure 5.3: Normalised loss curve of reconstructing Ford-Fulkerson with new encoders for l_{ij} , d_{ij} , ρ_{ij} . Contrarily to the primal model, PGN-max (D) seems to be able to generalise the algorithm with the new data.

tifying the need for algorithmic reasoning to output reliable max-flow predictions.

In our testing, the *dual* PGN model utilising a max aggregator emerged as the top-performing model, at least concerning z -community graphs, demonstrating the capability to also flawlessly predict the minimum cuts of all graphs in the test set. More in general, models that integrate dual problem prediction (i.e., *dual* and *pipeline* models) consistently surpass the *primal* models on the two test sets (*OOD* and *OOF*), with respect to both the final prediction F as well as throughout the algorithm executions (i.e., less error on $\bar{F}^{(t)}$). This implies that, indeed, dual min-cut information helps to output more accurate max-flow predictions. To further strengthen this claim, note how performance on max-flow quickly degrades towards that of the primal baseline whenever min-cut predictions are inaccurate (e.g., see {PGN, MPNN}-max (*PL*) on z -community graphs). Notably, note how (*PL*) predictions are less stable on average. This confirms prior findings of (Xhonneux et al., 2021) that deploying MTL when applicable yields, on average, better OOD results.

Testing OOF, however, proves to be still a challenging task even for neural algorithmic reasoners. Even though the performance gap enlarges for bipartite graphs (with both *dual* and *pipeline* proving highly competitive), we achieve on average higher mean error and standard deviations. For the sake of completeness, we have to take into account that capacities here are sampled as either 0 or 1, thus amplifying potential for prediction errors.

Finally, we provide illustrations showcasing how application of Algorithm 9 enforce constraint (2.2). In Figure 5.4, we represent negative nodes v^- as blue and positive nodes v^+ as red. Sources s should always be “positive” nodes (flow is always sent out) while sinks should be “negative” (flow is always received). White nodes represent nodes that are “neutral”

Model	Community (OOD)			Bipartite (OOF)		
	F(\downarrow)	$\bar{F}^{(t)}$ (\downarrow)	c(\uparrow)	F(\downarrow)	$\bar{F}^{(t)}$ (\downarrow)	c(\uparrow)
PGN-max (<i>P</i>)	0.266 \pm 0.001	0.294 \pm 0.002	—	0.56 \pm 0.23	0.82 \pm 0.17	—
PGN-mean (<i>P</i>)	0.274 \pm 0.001	0.311 \pm 0.004	—	1.09 \pm 0.47	1.13 \pm 0.18	—
MPNN-max (<i>P</i>)	0.263 \pm 0.008	0.289 \pm 0.004	—	0.75 \pm 0.47	0.78 \pm 0.11	—
MPNN-mean (<i>P</i>)	0.278 \pm 0.008	0.313 \pm 0.003	—	0.75 \pm 0.47	0.92 \pm 0.22	—
PGN-max (<i>D</i>)	0.234\pm0.002	0.269\pm0.001	100% \pm 0.0	0.49 \pm 0.22	0.78\pm0.29	100% \pm 0.0
PGN-mean (<i>D</i>)	0.240 \pm 0.004	0.285 \pm 0.004	100% \pm 0.0	1.10 \pm 0.30	1.05 \pm 0.12	99% \pm 0.7
MPNN-max (<i>D</i>)	0.236 \pm 0.002	0.288 \pm 0.005	100% \pm 0.0	0.71 \pm 0.32	0.98 \pm 0.22	100% \pm 0.0
MPNN-mean (<i>D</i>)	0.258 \pm 0.008	0.268\pm0.002	100% \pm 0.0	0.81 \pm 0.09	1.06 \pm 0.35	100% \pm 0.0
PGN-max (<i>PL</i>)	0.256 \pm 0.001	0.293 \pm 0.003	61% \pm 0.1	0.45\pm0.18	0.77\pm0.26	95% \pm 0.1
PGN-mean (<i>PL</i>)	0.244 \pm 0.001	0.304 \pm 0.001	100% \pm 0.0	0.98 \pm 0.44	1.03 \pm 0.32	99% \pm 0.8
MPNN-max (<i>PL</i>)	0.261 \pm 0.002	0.312 \pm 0.005	61% \pm 0.3	0.47\pm0.23	0.95 \pm 0.34	90% \pm 1.1
MPNN-mean (<i>PL</i>)	0.255 \pm 0.002	0.292 \pm 0.002	100% \pm 0.0	0.64 \pm 0.35	0.92 \pm 0.20	100% \pm 0.0
Random	0.740 \pm 0.002	—	50% \pm 0.0	1.00 \pm 0.00	—	50% \pm 0.0
PGN-max (<i>NA</i>)	0.314 \pm 0.013	—	—	0.78 \pm 0.02	—	—

Table 5.2: Here, we report different quantitative metrics to assess the performance of all different models. Columns marked with (\downarrow) are evaluated through the Mean Absolute Error (MAE), whereas for columns marked with (\uparrow) accuracy is used. F refers to the final flow assignment, $\bar{F}^{(t)}$ refers to the intermediate flow matrices (error is averaged), and c refers to minimum cut. We report all tested models as rows, where (*P*) corresponds to training on max-flow only, (*D*) corresponds to training with both primal and dual decoders and (*PL*) corresponds to the pipeline model. Finally, (*NA*) corresponds to a model utilising no algorithms, hence learning max-flow directly.

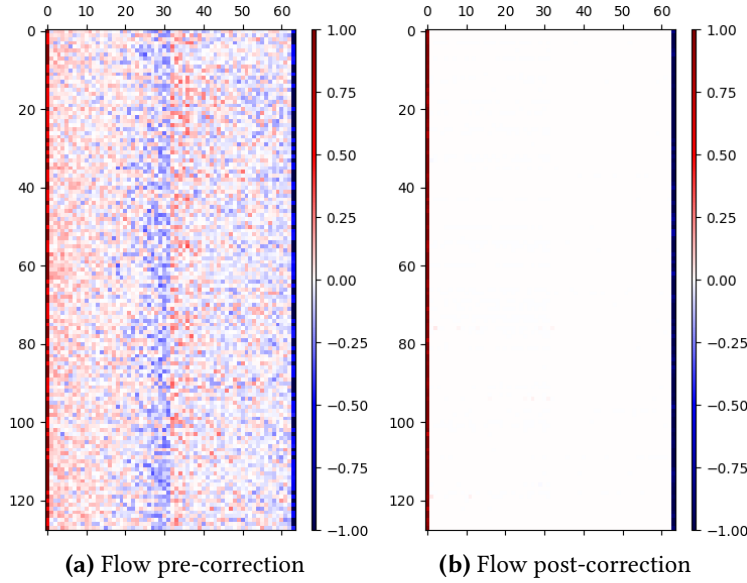


Figure 5.4: This figure shows the (normalised) flow conservation error for all nodes (x axis) of each test graph (y axis). (a) shows the predicted F conservation error prior [Algorithm 9](#). (b) shows the corrected F conservation error. Through [Algorithm 9](#) we are able to correct all the inner error (white represents zero error), with s and t being the only nodes which respectively send and receive flow.

(i.e., algebraic sum of their in-flow and out-flow is 0), hence [\(2.2\)](#) holds. The figure then shows nodes violating [\(2.2\)](#) pre- and post-application of [Algorithm 9](#).

QUALITATIVE ANALYSIS. To further evaluate the performance of DAR, we conducted two qualitative studies. The first one aims to assess to what extent DAR architecture can identify and leverage strong duality properties. Indeed, as we discussed in [section 5.1](#), we know that max-flow and min-cut are *strong duals* and, as such, they share the same optimal value (see [Theorem 2](#)). Hence, given a dual model architecture in [Table 5.2](#) that can correctly predict the minimum cut of a graph, this study aims at answering the following question: *can such an architecture identify the optimum max-flow value more accurately compared to a primal-only model?*

To investigate this property, we have to extract from F the flow quantity that our learnt reasoners “believe” to be the optimum. We consider such quantity as being either the predicted **out-flow** from the source node or **in-flow** of the target node t , by “marginalising” over all s ’s successors and t ’s predecessors, respectively. Thus, we consider the maximum (in absolute value) of the two quantities. We denote this value as f_s and compute it as follows:

$$f_s = \max\left(\sum_{(s,j) \in \mathcal{E}} F_{sj}, \left| \sum_{(j,t) \in \mathcal{E}} F_{jt} \right|\right). \quad (5.3)$$

Note that, in doing so, we are ignoring potential violations of constraint [\(2.2\)](#). However, our objective here is to measure how well the network

Metric	(P)		(D)		(PL)	
	PGN-max	PGN-mean	PGN-max	PGN-mean	PGN-max	PGN-mean
$ f_s - f_s^*(\downarrow) $	$7.86_{\pm 0.47}$	$8.68_{\pm 0.21}$	$0.34_{\pm 0.04}$	$0.41_{\pm 0.01}$	$7.58_{\pm 0.10}$	$0.38_{\pm 0.08}$

Table 5.3: Qualitative analysis. Here, f_s^* is the ground truth maximum flow value. f_s , instead, is the quantity that our learnt reasoners predict to be the amount of flow **exiting** the source node s (i.e., $f_s = \sum_{(s,j) \in \mathcal{E}} F_{sj}$). For simplicity, we only report results of the best-performing models (PGNs).

can guess the optimal value. Hence, we compare f_s to the ground truth optimal max-flow value f_s^* , which is computed exactly as (5.3) but on the ground-truth F^* . Precisely, we measure the discrepancy as MAE and report it in Table 5.3. From the presented results, one can immediately draw a very interesting conclusion: DAR models can effectively leverage the fact that the two learning targets share the same optimum value. This is testified by noting that DAR models, especially the ones trained jointly (i.e., (D)), achieve an error of ≈ 0.34 from the optimum, which is one order of magnitude lower than primal models (i.e., ≈ 7.86). This analysis strengthens our claim that a DAR model can effectively transfer knowledge from the dual to the primal problem, leading to solutions that are both more accurate (see Table 5.2) and of higher quality. This also finds additional support in the observation that both primal architectures and dual architectures, where the minimum cut results are inferior, deviate significantly from the optimal solution. This can be seen by comparing the PGN-max (PL) minimum-cut results in Table 5.2 and the corresponding MAE value in Table 5.3. The second qualitative study, instead, is embeddings-centric. Here, our objective is to assess the degree to which f_s^* can be linearly decodable from the learnt node representations. Ideally, this would provide clear indication of which model representations carry the most information. We setup this study as follows. First, we neurally execute Ford-Fulkerson through all PGN-based models in Table 5.2, and collect learnt node representations \mathbf{h}_v . Thus, we compute a graph representation \mathbf{h}_g as follows:

$$\mathbf{h}_g = \max(\{\mathbf{h}_v \mid v \in \mathcal{V}\}).$$

Finally, we learn linear mappings $\mathbf{h}_g \rightarrow f_s^*$ and compute the R^2 score to evaluate the quality of the predictions. Table 5.4 provide clear indications that *dual* representations are more expressive, since f_s^* can be decoded linearly almost perfectly (i.e., ≈ 0.99 on average on the two graph distributions).

5.1.2.2 Brain Vessel Graph benchmark

In this section, we prove for the first time the real-world utility of neural algorithmic reasoners, in particular of DAR architectures. Here, we target transferring algorithmic knowledge to a task where prior knowledge of max-flow might be helpful, providing a practical instantiation of the discussions details in section 3.1. In the following, we will be providing

Graphs	(P)		(D)		(PL)	
	PGN-max	PGN-mean	PGN-max	PGN-mean	PGN-max	PGN-mean
<i>community</i> (\downarrow)	0.69 \pm 0.12	-0.59 \pm 0.33	1.00\pm0.00	0.93 \pm 0.01	0.80 \pm 0.05	-0.13 \pm 0.29
<i>bipartite</i> (\downarrow)	-0.79 \pm 0.81	-115.6 \pm 64	0.98\pm0.01	-115.2 \pm 64	-0.69 \pm 0.33	0.98\pm0.01

Table 5.4: R^2 score of predicting the maximum flow value from learnt graph representations \mathbf{h}_g . R^2 metric emits score in $(-\infty, 1]$, with 1 being the best possible score.

a thorough description of the real-world benchmark we used as well as experimental details.

BENCHMARK DESCRIPTION. We consider the Brain Vessel Graph (BVG) benchmark (Paetzold et al., 2021). Here, graphs represent mice’s brains, where nodes represent bifurcation points and edges represent vessels. The objective is to perform **edge classification** task. In particular, edges need to be classified in each of the following three categories: *capillaries*, *veins* and *arteries*. Equivalently, we can frame this task as conducting blood-flow simulation¹. Hence, a network that is able to *simulate* blood-flow simulation is likely to be at advantage compared to a simpler model. This represents the ideal test case for our DAR architectures.

Furthermore, for each edge we have access to the following input feature list:

l_{uv} : which is the length of the vessel.

d_{uv} : which is the shortest distance between the two bifurcation points u and v .

ρ_{uv} : which is the curvature of the vessel.

Notably, we do not have access to the capacity of the vessels. This makes direct application of the Ford-Fulkerson algorithm inapplicable to conduct “predictions” on these types of data. This is a scenario where algorithms do exhibit the limitations discussed in [section 3.1](#).

Additionally, the classification task is highly imbalanced (i.e., 95% of samples are capillaries, 4% veins and only 1% arteries), posing an additional learning challenge.

We test our models on three large-scale BVG graphs: CD1-E-1 (the largest, with 5,791,309 edges); CD1-E-2 (2,150,326 edges); and CD1-E-3 (3,130,650 edges). We also exploit a validation synthetic brain vessel graph provided by the BVG benchmark, comprising 3159 nodes and 3234 edges.

TRANSFER ALGORITHMIC KNOWLEDGE TO BVG. We employ the PF transfer learning strategy discussed in [section 3.3](#), with slight modifications, to re-use algorithmic knowledge lying in our processors. Specifically, since we have access to a validation synthetic graph from BVG, we can attempt at re-learning to execute Ford-Fulkerson on such data, even

¹ This can be seen by considering that the more blood can traverse an edge, the more likely the edge is to be an artery rather than a capillary

if the capacity is no longer an input feature. To do that, we perform the following steps:

- Extract and freeze the PGN-max processors p from the models trained on synthetic data of [subsection 5.1.2.1](#).
- Drop the encoders f , but **keep** the decoders g .
- Introduce a new encoder \tilde{f} .
- Learn to approximate Ford-Fulkerson on the validation BVG graph by optimising:

$$\arg \min_{\phi} \mathcal{L} \left(\text{FF}(\mathbf{x}), (g \circ p \circ \tilde{f})(\mathbf{x} | \phi) \right),$$

where FF represent the Ford-Fulkerson algorithm and ϕ are the parameters of the new encoder.

Through the above steps, we effectively *reconstruct* the execution of the Ford-Fulkerson algorithm on the new data. Precisely, the model is tasked to learn to combine the new inputs in a sensible way to estimate the edge flows and, consequently, the capacity of the edges (i.e., our main target in the BVG task). For reconstruction purposes, source and sink nodes s, t are chosen as two random nodes whose shortest distance is equal to the diameter of the graph. We train to reconstruct the algorithm for 15000 epochs, with Adam optimiser (Kingma & Ba, 2015) and learning rate $1e-5$. [Figure 5.3](#) compares the loss curves for the primal and DAR models.

Finally, we perform one Ford-Fulkerson step on the three target graphs, CD1-E-1, CD1-E-2 and CD1-E-3 and extract the learnt node representations. We then obtain edge representations of edges (u, v) as:

$$\mathbf{h}_{uv} = \mathbf{h}_u + \mathbf{h}_v.$$

These representations will constitute an additional input feature for the neural networks trained to solve the BVG task. Note how this approach enables us to easily dump the embeddings, as no further training will occur on such models.

NEURAL ARCHITECTURES. We have selected graph networks from the BVG benchmark paper as our baseline models.

These include Graph Convolutional Networks (GCNs) (Kipf & Welling, 2017), GraphSAGE (Hamilton et al., 2017), and ClusterGCN (Chiang et al., 2019) with GraphSAGE convolution (C-SAGE). We augment such networks with extra input features \mathbf{h}_{uv} obtained as explained in the previous paragraph. Additionally, we also utilise a simple linear classifier (LC) to assess the quality of the \mathbf{h}_{uv} representations. We also train a linear classifier on the set of original input features $l_{ij}, d_{ij}, \rho_{ij}$, to assess whether \mathbf{h}_{uv} add information compared to the basic features.

As an additional sanity check, we also train Node2Vec (Grover & Leskovec, 2016) embeddings on each of the three datasets and use them to augment the GN architectures.

Dataset	GCN	SAGE	C-SAGE	Node2Vec
CD1-E-3	$lr=3 \cdot 10^{-3}$	$lr=3 \cdot 10^{-3}$	$lr=3 \cdot 10^{-3}$	$lr=1 \cdot 10^{-2}$
	no. layers=3	no. layers=4	no. layers=4	walk length=40
	no. hiddens=256	no. hiddens=128	no. hiddens=128	walks per node=10
	dropout=0.4	dropout=0.4	dropout=0.2	no. hiddens=128
	epochs=1500	epochs=1500	epochs=5000	epochs=5
CD1-E-2	as above	as above	$lr=3 \cdot 10^{-3}$ no. layers=4 no. hiddens=128	as above
			dropout=0.2	
			epochs=1500	
CD1-E-1	as above	as above	$lr=3 \cdot 10^{-3}$ no. layers=3 no. hiddens=64	as above
			dropout=0.2	
			epochs=1500	

Table 5.5: Optimal hyperparameters used for the BVG benchmark. Note that C-SAGE needs more epochs for CD1-E-3.

MODEL SELECTION. Here, we consider the optimal BVG hyperparameters reported in (Paetzold et al., 2021). For the CD1-E-1 graph and the C-SAGE model, we performed minimal model selection as the optimal hyperparameters for C-SAGE did not yield good results. Specifically, we optimised *number of layers* and *number of hiddens* by grid-searching over $\{2, 3, 4\}$ and $\{64, 128\}$, respectively. For consistency, all models are trained with early stopping applied after 300 epochs, using the hyperparameters reported in Table 5.5.

QUANTITATIVE ANALYSIS. We perform rigorous and thorough testing of all combinations of the the involved models (i.e., GNs only, GNs with *primal* embeddings, GNs with *dual* embeddings, and GNs with *N2V* embeddings). Given the highly imbalanced nature of the learning problem, we employ the balanced accuracy score, which represents the average recall for each class, and the area under the ROC curve as our metrics to assess performance. Results are showcased in Table 5.6.

First, consider performance related to linear classifiers (LC). It is evident that the representations \mathbf{h}_{uv} generated by the algorithmic reasoners, both the primal and dual versions, carry valuable information. This is demonstrated by an average increase of 16.6% in balanced accuracy and 10.5% in ROC across the three datasets when compared to using simple features $[l_{uv}, d_{uv}, \rho_{uv}]$ alone. Notably, dual representations still outperform their primal counterparts, as a possible consequence of a better algorithm reconstruction (depicted in Figure 5.3). Lastly, LC’s performance also serves as a clear indicator of the successful knowledge transferring from the synthetic world to *natural* real-world data.

Model	CD1-E-3 (\uparrow)		CD1-E-2 (\uparrow)		CD1-E-1 (\uparrow)	
	Bal. Acc.	ROC	Bal. Acc.	ROC	Bal. Acc.	ROC
LC	39.3% \pm 0.2	52.3% \pm 0.6	36.9% \pm 0.5	55.9% \pm 0.1	45.5% \pm 0.1	61.7% \pm 0.0
LC (N_2V)	43.9% \pm 0.2	55.5% \pm 0.1	71.9% \pm 0.1	62.6% \pm 0.0	46.1% \pm 0.1	60.0% \pm 0.0
LC (P)	48.6% \pm 0.4	59.4% \pm 0.4	58.7% \pm 0.1	63.8% \pm 0.2	45.3% \pm 0.1	59.9% \pm 0.1
LC (D)	53.8% \pm 0.3	66.2% \pm 0.2	67.3% \pm 0.1	71.8% \pm 0.0	48.1% \pm 0.5	62.1% \pm 0.3
GCN	58.1% \pm 0.5	67.9% \pm 0.2	74.6% \pm 1.7	78.7% \pm 0.1	59.0% \pm 0.2	67.9% \pm 0.2
SAGE	63.5% \pm 0.2	70.9% \pm 0.3	73.9% \pm 0.6	82.5% \pm 0.2	64.7% \pm 0.7	74.2% \pm 0.2
SAGE (N_2V)	65.0% \pm 0.1	71.9% \pm 0.1	84.1% \pm 1.9	82.5% \pm 0.4	65.9% \pm 0.1	74.8% \pm 0.1
SAGE (P)	64.5% \pm 0.2	72.0% \pm 0.2	83.8% \pm 0.4	83.7% \pm 0.4	66.2% \pm 0.5	74.8% \pm 0.3
SAGE (D)	66.7% \pm 0.4	75.0% \pm 0.2	85.2% \pm 0.1	85.5% \pm 0.2	66.4% \pm 0.3	74.8% \pm 0.1
C-SAGE	68.6% \pm 0.8	74.2% \pm 0.5	81.8% \pm 0.5	85.6% \pm 0.2	59.3% \pm 0.9	68.3% \pm 0.5
C-SAGE (N_2V)	68.6% \pm 0.2	74.1% \pm 0.1	84.8% \pm 0.2	84.8% \pm 0.5	67.4% \pm 0.6	75.9%\pm0.2
C-SAGE (P)	67.3% \pm 0.2	73.6% \pm 1.9	82.5% \pm 1.9	84.0% \pm 1.5	67.7% \pm 0.1	75.8%\pm0.2
C-SAGE (D)	70.2%\pm0.2	76.3%\pm0.1	85.6%\pm0.2	86.7%\pm0.3	68.1%\pm0.2	75.8%\pm0.1

Table 5.6: BVG results. LC refers to a linear classifier, whereas (\cdot) brackets indicate that the models takes in additional features from either Node2Vec (N_2V), primal PGN-max (P) and dual PGN-max (D).

Moving forward, augmented GN architectures significantly improves on their vanilla (i.e., non-algorithmically informed) versions. Among these, C-SAGE with dual embeddings (i.e., C-SAGE (D)) consistently achieves the highest performance across all three datasets, displaying a consistent performance advantage, especially for CD1-E-3 and CD1-E-2. More interestingly, the computed dual \mathbf{h}_{uv} demonstrated to be more informative than N_2V embeddings in this task. Remarkably, N_2V representations are directly trained on CD1-E- X data, whereas DAR is trained to reconstruct the algorithm on validation (and much smaller) BVG data. Note that N_2V computes statistics unsupervisedly through random walks, in order to capture global information of the graph. Hence, although N_2V embeddings are still valuable (as testified by the improvements w.r.t vanilla GNs), DAR embeddings possess more principled flow information, which better suits the BVG task. We also run an additional experiment concatenating N_2V and DAR embeddings, as an attempt to verify whether the two representations encode information of “different natures” – *structural* (N_2V) and *flow-based* information (DAR). We record higher results for these combined embeddings compared to using N_2V and DAR separately (especially for CD1-E-2), thus empirically confirming our conjecture. These results are reported in [Table 5.7](#).

Finally, a last note on DAR/NAR generalisation capabilities. Recall that these networks were only initially trained on graphs with 16 nodes and are able to produce meaningful representations for graphs with millions of nodes, being able to provide a clear performance advantage over previously SOTA baselines.

Model	CD1-E-3 (↑)		CD1-E-2 (↑)		CD1-E-1 (↑)	
	Bal. Acc.	ROC	Bal. Acc.	ROC	Bal. Acc.	ROC
LC (D, N_2V)	53.9% \pm 0.1	66.3% \pm 0.1	77.8% \pm 0.1	74.3% \pm 0.1	48.2% \pm 0.2	62.1% \pm 0.1
SAGE (D, N_2V)	70.1% \pm 0.3	76.5% \pm 0.1	89.2%\pm0.2	86.3%\pm0.2	67.5%\pm0.2	76.0%\pm0.1
C-SAGE (D, N_2V)	70.4%\pm0.1	76.7%\pm0.1	88.3% \pm 0.3	85.0% \pm 0.3	67.0% \pm 0.2	75.8% \pm 0.3

Table 5.7: BVG results following concatenation of N_2V and embeddings.

5.2 LEARNING CO-APPROXIMATION VIA ALGORITHMIC PRIMITIVES

As explained in [section 2.2](#), solving combinatorial optimisation problems is an extremely important long-standing challenge, studied by theoretical computer science either by *exact* solving methods ([Balas & Toth, 1983](#)) or approximated solution ([Karlin et al., 2022](#)). As explained in [section 3.1](#), the ML community has also interest in targeting combinatorial problems ([Vinyals et al., 2015](#); [Bello et al., 2017](#); [Kool et al., 2019](#); [Joshi et al., 2022](#)), mainly under the lens of learning approximation algorithms (i.e., heuristics) for getting “good” solutions in an acceptable amount of time – the Neural Combinatorial Optimisation (NCO) field.

The ultimate NCO goal is to learn heuristics that can surpass the performance of manually-designed CO algorithms, typically involved in theoretical computer science. Notably, previous research addresses NCO by primarily focusing on either supervised learning ([Vinyals et al., 2015](#); [Bello et al., 2017](#); [Joshi et al., 2022](#)) or reinforcement learning ([Kool et al., 2019](#)). However, despite the existence of inherent “algorithmic” solutions for numerous combinatorial problems (see also [subsection 2.3.4](#)), no studies have yet explored the integration of algorithmic knowledge in this context. Precisely, in [subsection 2.3.4](#) we discussed how the Christofides’ algorithm is heavily based on algorithmic primitives, such as matching and MST procedures. Such observation supports NAR’s view that algorithms are useful knowledge in the context of NCO.

In this section, therefore, we target another important ML and NAR application, which is attempting at leveraging algorithmic primitives for learning combinatorial optimisation problems (see [section 3.1](#)). Specifically, we target transfer learning from algorithms that solve problems in P to NP-hard problems (refer to [subsection 2.2.1](#)), focusing especially on the TSP ([Problem 6](#)) and the VKC problem ([Problem 8](#)).

5.2.1 Selecting relevant primitives

By now, it is clear that we intend to pre-train neural solvers on a set of algorithms first, in order to leverage such algorithmic knowledge to better perform when targeting CO. However, we have not yet discussed *which* algorithms we aim to use in the pre-training phase.

Here, we **prioritise** algorithms that show degrees of *relevance* for the target combinatorial problem of interest (i.e., in this section, either TSP or VKC), where relevance is defined, informally, as follows.

Definition 26 (Algorithm relevance). *Consider a combinatorial problem \mathcal{P} , an approximation algorithm \tilde{A} for \mathcal{P} and decomposition of \tilde{A} in its sub-routines (i.e., $\tilde{A} = \tilde{A}_1 \circ \dots \circ \tilde{A}_n$). Now, consider any algorithm A . Thus, A is said to be “relevant” for \mathcal{P} if A is one of \tilde{A} ’s sub-routines (i.e., $A = \tilde{A}_i$ for any i).*

Hence, we have a natural way of discerning which algorithms are relevant for TSP and VKC, by investigating two well-known heuristics: the Christofides algorithm for TSP (see [Algorithm 6](#)), and the Gon algorithm (see [Algorithm 7](#)) for VKC.

However, despite its importancy, relevancy is not the only property that should be taken into account. Indeed, as we will see in the experimental section, selecting algorithms for which our “base” reasoner struggles to learn is highly detrimental for the subsequent CO learning. Furthermore, [Ibarz et al. \(2022\)](#) clearly show the benefits of learning also un-related algorithms together. For such reasons, while prioritising relevant algorithms we investigate usage of other algorithms as well. We detail the final choice of algorithms in the two following paragraphs, dedicated to TSP and VKC, respectively.

TSP. Here, we take into account that the TSP is often framed in a euclidean geometrical space setting (i.e., often \mathbb{R}^2), from which we derive a fully-connected undirected graph. Hence, the set of algorithms we choose for pre-training have to perform well on fully-connected graphs. As the TSP is in fact a geometric graph, computational geometry algorithms in the CLRS-30 benchmark ([Veličković et al., 2022a](#)) are also considered. We also plan to learn a heuristic for TSP that runs in linear time (i.e., $O(|V|)$), hence we monitor performance of the candidate algorithms w.r.t the number of iterations they perform (on average) and discard those with *long* rollouts (e.g., Dijkstra).

In light of the above considerations, we identify a set of 3 algorithms – Bellman-Ford ([Algorithm 1](#)), Prim’s algorithm ([Algorithm 4](#)) and Graham’s scan ([Cormen et al., 2009](#)) for convex hull. Regrettably, upon initial testing, the inclusion of Graham’s scan resulted in poor performance, leading us to exclude it from our finalised choice. This might be linked to the lack of geometrical invariances in NAR architectures ([Bronstein et al., 2021](#)).

VERTEX K-CENTER PROBLEM. Similar discussion regarding algorithm performance still holds for selectin VKC-related algorithms. Notably, upon investigation of the Gon algorithm’s sub-routines we derive that our final model needs knowledge of shortest paths between nodes (i.e., to effectively select the “farthest” node from the centers), and greedy algorithms. The final choice for VKC is then: Bellman-Ford, Minimum finding, greedy activity selection ([Gavril, 1972](#)) and greedy task scheduling algorithms ([Lawler, 2001](#)).

5.2.2 Model architecture.

Similarly to previously presented work, the used architecture here is still an encode-process-decode (subsection 3.2.2), with linear encoders and decoders and a MPNN-max architecture. However, here we add a gating mechanism as in (Ibarz et al., 2022) to let the processor update only the node representations that it deems important. Hence, we introduce a gating network f_{GAT} which modifies representations \mathbf{h}_v as follows:

$$\begin{aligned} \mathbf{g}_v^{(t)} &= f_{\text{GAT}}(\mathbf{z}_v^{(t)}, \mathbf{h}_v^{(t)}), \\ \mathbf{h}_v^{(t)} &= \sigma(\mathbf{g}_v^{(t)}) \odot \mathbf{h}_v^{(t)} + (1 - \sigma(\mathbf{g}_v^{(t)})) \odot \mathbf{h}_v^{(t)}, \end{aligned}$$

where $\mathbf{z}_v^{(t)}$ are encoded inputs as in subsection 3.2.2 and σ is the logistic function. We also tested a variant that computes and keeps track of the evolution of the edge representations $\mathbf{h}_{uv}^{(t)}$.

DECODING CO SOLUTIONS. Finally, since we are targeting combinatorial problems it is important to ensure the correctness of the solutions. For instance, a solution to a TSP problem has to be a permutation of nodes (see Definition 12 and Problem 6), whereas for VKC we should choose exactly k nodes. However, neural networks might generate outputs that do not comply with such constraint (similarly to the max-flow scenario discussed in section 5.1).

Hence, for the TSP we let our reasoner generate a *matrix of pointers* $\mathbf{P} \in \mathbb{R}^{|\mathcal{V}| \times |\mathcal{V}|}$, where each row \mathbf{p}_v corresponds to the vector of predecessors used to represent outputs of shortest path algorithms (see subsection 2.3.4). In particular, \mathbf{p}_v defines a probability distribution over neighbours, where p_{vu} defines the likelihood of u being the predecessor of v . Therefore, we use a beam search decoding scheme (Freitag & Al-Onaizan, 2017; Joshi et al., 2022) to identify the most likely set of pointers that constitute a valid TSP solution.

For VKC, instead, we simply sort the neural network’s predictions in order to select the top k nodes that constitute the set C .

5.2.3 Experimental evaluation

In this section, we provide all information for replicating our experiments.

MODEL SELECTION. Here, we select the best hyperparameters for our reasoners, provided by the CLRS benchmark in (Veličković et al., 2022a). Hence, we use hidden dimension of 128, learning rate of 0.0003 with no weight decay. We optimise the networks using Adam (Kingma & Ba, 2015) with a batch size of 64.

In the pre-training phase, we let algorithmic reasoners be optimised for 100 epochs. In the transfer learning settings, we experimented with every modality discussed in section 3.3 (i.e., PF, PFT, MST, 2PROC). Hence, we fine-tune our models (or encoders/decoders) for 20 epochs on TSP and 40 epochs for the Vertex K Center. We report all transfer learning results averaged across 5 different seeds.

DATA GENERATION. The data generation pipeline for algorithms is similar to the previously presented contributions. However, as we are dealing with full graphs and Erdős–Rényi graphs at a later stage (i.e., TSP and VKC, respectively), we choose to learn algorithmic reasoners on a training distribution that matches that of the downstream task. We sample TSP graphs by randomly selecting points in a 2D space, restricted to $[0, 1]$, and assigning edge weights based on the euclidean distance between the nodes. On the other hand, VKC-related graphs are generated following the Erdős–Rényi distribution, setting $p = 0.5$. Following prior works (Ibarz et al., 2022; Mahdavi et al., 2023), we enhance the training data by sampling varying graph sizes, choosing uniformly in $[8, 16]$. Validation data are 16-node graphs (fixed size), whereas test graphs comprehend 64-node graphs (always of fixed size).

For the target TSP task, we consider larger datasets of graphs of varying size. Notably, learning to generalise in NCO tasks typically requires large amount of data. Specifically, we sample 100,000 training graphs of each of the sizes $[10, 13, 16, 19, 20]$ (500000 total). It is important to point out that our training set size, with respect to both number of samples and graph sizes, is considerably smaller of previous works. Indeed, prior work (Khalil et al., 2017; Kool et al., 2019; Joshi et al., 2022) used training graphs that may have even more than 100 nodes. Additionally, Kool et al. (2019) and Joshi et al. (2022) are less data-efficient, using training sets from several order of magnitude bigger than ours (the former), to twice as much as our data (the latter).

To perform validation, we create a set of 100 graphs, each of size 20. Additionally, we generate several test sets with the intentions of assessing our models OOD. Thus, test sets exhibit the following sizes: $[40, 60, 80, 100, 200, 1000]$, comprising $[1000, 32, 32, 32, 32, 4]$ graphs for each size, respectively. To compute the optimal ground-truth tours, we utilize the Concorde solver, as detailed in Applegate et al. (2006).

For the target VKC task, instead, training, validation and test sets have the same configurations as those generated for TSP. To generate ground-truth solutions, however, here we rely on the Gurobi (Gurobi Optimization, LLC, 2023) solver. Specifically, we generate solutions involving $k = 5$ centers.

ABLATION STUDIES. To thoroughly evaluate the benefits gained by the algorithmic knowledge, we conducted several ablation studies as well as comparisons against various baselines (both classical algorithms and other neural models). In detail, we test the performance of the learnt reasoner with and without the pre-training phase, using the same set of hyperparameters.

For both TSP and VKC, we compare against various algorithmic approaches. TSP baselines comprehend: the Christofides heuristic (Algorithm 6), a beam search approach with beam width of 1280 and a greedy algorithm that, given a node v , selects the node u which is the closest to v to expand the current solution. VKC baselines, instead, include: the Gon algorithm and the critical dominating set (CDS) heuristic (Garcia-Diaz et al., 2017).

For TSP, we also test the performance against a reinforcement learning (Sutton & Barto, 2018) based neural model (Joshi et al., 2022).

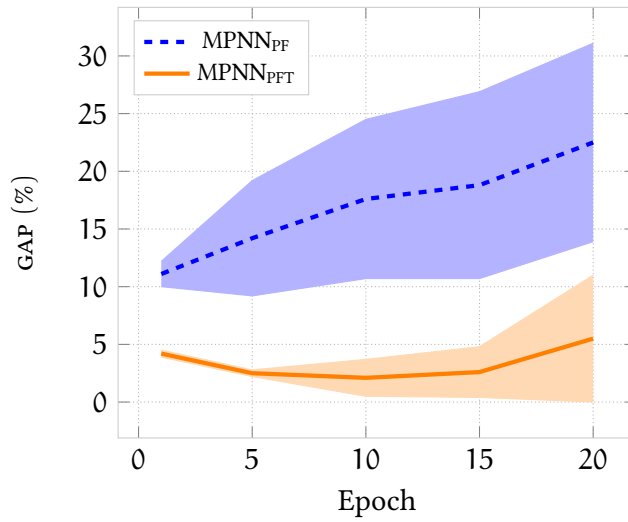
Finally, we monitor and report the optimality GAP metric (also used in section 4.2) as our performance metric.

RESULTS ANALYSIS. Our main results are presented in Table 5.8, for TSP, and in Table 5.9, for VKC. In the TSP Table 5.8, subscripts refer to transfer learning methods presented in section 3.3, with the addition of the subscript “ueh” which indicates that the model learns and updates edge hidden representations. Models with no subscripts are directly trained to solve the TSP/VKC, without algorithmic pre-training. Finally, we report results related to the PF strategy only visually in Figure 5.5, and do not include them in the tables as employing such strategy failed to produce solutions that generalise.

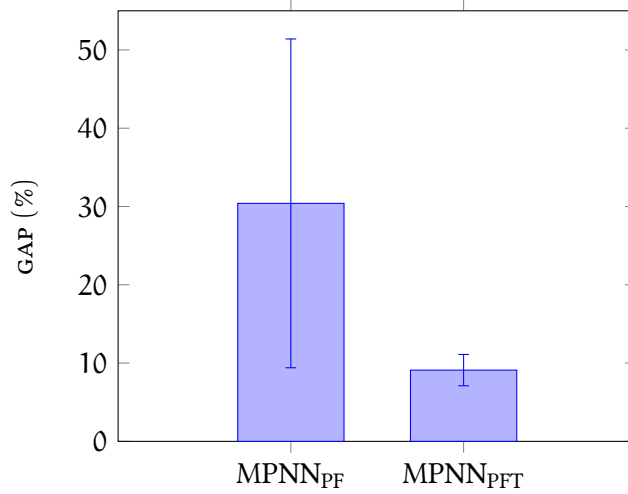
Commencing our analysis of TSP results, we observe that, in nearly all instances, pretraining our model to execute algorithms yields improved performance, with the transfer PFT (i.e., pre-train and fine-tune) setting that exhibits the best performance. This is a surprising result and goes in contrast to common choices of using PF (Veličković & Blundell, 2021; Deac et al., 2021; Numeroso et al., 2023; Cappart et al., 2023), 2PROC or MST strategies (Xhonneux et al., 2021; Ibarz et al., 2022). However, we recall that our task requires transferring knowledge from algorithms and problems that are in P to NP-hard. Hence, in our settings the target task \mathcal{T} is inherently more difficult than the base task \mathcal{B} of learning P algorithms. Hence, our results suggest that in order to implement such transfer successfully, a reasoner might need to use \mathcal{B} -representations only as a starting point. Indeed, pre-trained reasoners learn representations from which we can “easily” decode steps of, for instance, Prim and Bellman-Ford. However, turning this information into a “good heuristic” for the TSP requires extra non-linear learning steps (i.e., PFT) as linearly transforming such information is clearly not enough (i.e., PF) – see also Figure 5.5.

Our learnt reasoners also demonstrate superior performance compared to the architecture proposed in (Joshi et al., 2022) showing a substantial OOD performance advantage, with the exception of the smallest test instances. This is due to well-known reinforcement learning tendencies of fitting well the training environment (Whiteson et al., 2011; Zhang et al., 2018; Song et al., 2019).

An interesting observation is that the performance gap of learnt reasoners seems to diminish compared to the algorithm-agnostic baseline, especially for sizes of ≥ 200 nodes. Figure 5.6 seeks to explain this behaviour. In particular, this trend seems to be influenced by the progressive deterioration of algorithmic reasoning performance as test graph size increases. In fact, note how algorithmic reasoners are not able to generalise Prim for sizes above 200, as testified by the drop of performance in the figure (i.e., $\sim 30\%$). As computing the MST is an important property for the TSP solution, MPNN_{PFT} can simply not rely on this inductive bias for sizes ≥ 200 . Consequently, the model “converges” to an algorithm-agnostic MPNN. This underscores the significance of developing neural



(a) Validation GAP



(b) Test GAP

Figure 5.5: The standard PF transfer learning approach is not applicable for our purposes: the resulting models are unable to generalise both in- and out-of-distribution, as shown in (a) and (b) respectively.

algorithmic reasoning models capable of robust generalisation even for significantly larger graphs, to effectively address CO problems using our approach.

Additionally, Figure 5.7 shows that integrate algorithms leads to faster convergence and delayed overfitting, compared to standard MPNNs.

In conclusion, it is worth highlighting that we consistently achieve superior performance compared to the majority of non-parametric baselines across various test sizes, including both greedy and beam search. Notably, for test instances of size 40 and 60, we even outperform or perform on par with Christofides, although our performance lags behind for larger graphs.

Model	Optimality GAP (\downarrow)					
	40 nodes	60 nodes	80 nodes	100nodes	200 nodes	1000 nodes
Beam search with width w=128						
MPNN	17.7 \pm 5%	23.9 \pm 3%	25.7 \pm 8%	31.9 \pm 6%	38.9 \pm 7%	39.7 \pm 7%
MPNN _{PFT}	9.1 \pm 0.1%	15.5 \pm 4%	23.1 \pm 3%	28.9 \pm 2%	35.4 \pm 2%	44.5 \pm 9%
MPNN _{PFT+ueh}	15.4 \pm 5%	23.5 \pm 8%	29.4 \pm 7%	35.7 \pm 6%	37.9 \pm 3%	48.8 \pm 14%
MPNN _{2PROC}	12.2 \pm 5%	22.1 \pm 4%	28.4 \pm 6%	34.0 \pm 5%	36.6 \pm 6%	38.8 \pm 3%
MPNN _{MTL}	18.1 \pm 6%	26.2 \pm 4%	31.2 \pm 5%	34.8 \pm 4%	37.1 \pm 3%	38.5 \pm 3%
Joshi et al. (AR)	6.2 \pm 4%	37.1 \pm 12%	74.8 \pm 13%	102 \pm 10%	195 \pm 20%	419 \pm 20%
Joshi et al. (nAR) ²	20.6 \pm 10%	62.5 \pm 11%	110 \pm 17%	156 \pm 24%	273 \pm 24%	497 \pm 7%
Beam search with width w=1280						
MPNN	14.4 \pm 4%	21.8 \pm 5%	22.4 \pm 4%	31.1 \pm 6%	33.6 \pm 3%	41.2 \pm 8%
MPNN _{PFT}	7.5 \pm 1%	13.3 \pm 3%	20.1 \pm 5%	26.9 \pm 3%	33.8 \pm 2%	40.5 \pm 7%
MPNN _{PFT+ueh}	12.9 \pm 5%	20.6 \pm 6%	26.0 \pm 3%	32.0 \pm 5%	37.2 \pm 3%	44.3 \pm 9%
MPNN _{2PROC}	9.5 \pm 6%	18.0 \pm 5%	24.1 \pm 6%	28.8 \pm 5%	36.6 \pm 6%	38.5 \pm 3%
MPNN _{MTL}	15.5 \pm 5%	26.5 \pm 6%	30.2 \pm 6%	33.4 \pm 4%	36.8 \pm 5%	42.3 \pm 5%
Joshi et al. (AR)	3.5 \pm 3%	33.0 \pm 11%	63.8 \pm 12%	97.6 \pm 12%	193.3 \pm 17%	417 \pm 4%
Joshi et al. (nAR) ²	14.2 \pm 8%	54.7 \pm 15%	100.0 \pm 15%	141.9 \pm 25%	265.5 \pm 27%	500.7 \pm 23%
Models not using beam search						
Joshi et al. (AR+greedy)	22.1 \pm 10%	57.7 \pm 13%	94.0 \pm 14%	124.0 \pm 12%	219.6 \pm 22%	469 \pm 17%
Joshi et al. (AR+sampling)	9.5 \pm 5%	46.7 \pm 9%	93.1 \pm 10%	137.0 \pm 14%	313.2 \pm 15%	1102 \pm 1%
Deterministic baselines						
<i>Greedy</i>	31.9 \pm 12%	32.8 \pm 10%	33.3 \pm 9%	30.0 \pm 6%	32.1 \pm 6%	28.8 \pm 3%
<i>Beam search</i> (w=1280)	19.7 \pm 8%	23.1 \pm 7%	29.4 \pm 7%	29.7 \pm 5%	33.2 \pm 4%	38.9 \pm 2%
<i>Christofides</i>	10.1 \pm 3%	11.0 \pm 2%	11.3 \pm 2%	12.1 \pm 2%	12.2 \pm 1%	12.2 \pm 0.1%

Table 5.8: Optimality GAP across different TSP sizes. Subscripts refer to the according transfer learning settings or if the model updates edge hiddens.

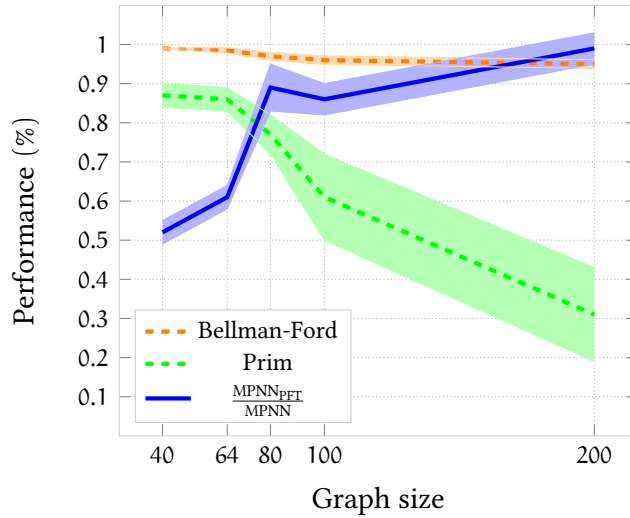


Figure 5.6: Relative performance between MPNN and MPNN_{PFT}. This figure illustrates that the initial superior performance of MPNN_{PFT} is most likely due to the fact that the network can predict the MST with high accuracy (see Prim’s curve). As MPNN_{PFT} struggles to generalise on MST for larger graphs, the performance gain w.r.t MPNN also decreases ($\frac{\text{MPNN}_{\text{PFT}}}{\text{MPNN}}$ approaches 1).

Moving forward, similar arguments to what we made for TSP results still hold when analysing VKC (Table 5.9). Here, we test only the PF transfer strategy, as it gave best results on the TSP task.

In these experiments, we also tried integrating two more relevant algorithms such as Floyd-Warshall and Insertion Sort (Cormen et al., 2009). However, our learnt reasoners did not achieve satisfactory approximations in the pre-training phase (Floyd-Warshall, mean accuracy of $\approx 23\%$; Insertion Sort, $\approx 43\%$) and this negatively cascade on the VKC learning task. This testifies that is important to appropriately choosing the test of algorithms to pre-train on, and exclude those that learnt reasoners struggle with. Replacing these algorithms by an additional greedy algorithm (i.e., Activity Selection) does yield increased performance, outperforming the baseline neural model on sizes 40 and 60.

When compared to the deterministic baseline methods, all neural models exhibit superior performance to the basic Gon heuristic. Regrettably, even the top-performing models do not reach the level of performance achieved by the CDS heuristic. We posit that this disparity can be attributed to the complexity of the CDS heuristic, which comprises multiple intertwined subroutines such as binary search and graph pruning. It is possible that a more modular NAR approach in the future could match such performance.

QUALITATIVE STUDY. Finally, we perform a qualitative study to evaluate the impact of the chosen algorithms to pre-train our neural CO solvers on. We pick a neural network for solving TSP, utilising the PFT strategy, and pre-train it on three random algorithms that were excluded by our initial selections: *Breadth-First Search*, *Topological Sorting*, and *Longest*

Model	Optimality GAP (\downarrow)				
	40 nodes	60 nodes	80 nodes	100 nodes	200 nodes
MPNN	15.88 \pm 1.11%	20.85 \pm 2.64%	24.78 \pm 7.17%	26.48 \pm 6.65%	24.63 \pm 6.50%
MPNN _{FMITB}	14.73 \pm 1.21%	21.97 \pm 4.87%	23.91 \pm 4.52%	28.50 \pm 5.06%	27.04 \pm 4.22%
MPNN _{MTAB}	13.58 \pm 0.60%	16.20 \pm 3.02%	23.10 \pm 3.99%	26.40 \pm 6.62%	26.43 \pm 3.84%
Deterministic baselines					
Farthest First	41.04 \pm 14.21%	43.89 \pm 10.70%	38.31 \pm 9.22%	36.32 \pm 7.28%	37.91 \pm 7.91%
CDS	7.15 \pm 5.42%	7.82 \pm 4.78%	6.49 \pm 3.65%	6.55 \pm 3.29%	5.98 \pm 2.00%

Table 5.9: VKC optimality gap. Each letter in the MPNNs subscripts denotes an algorithm pretrained on: **F**loyd-Warshall, **M**inimum, **I**nsertion sort, **T**ask scheduling, **B**ellman-Ford, **A**ctivity selection

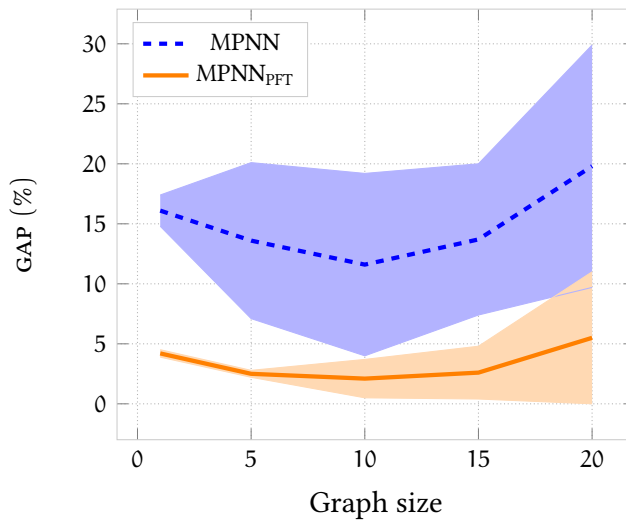


Figure 5.7: NAR modules converge faster on TSP learning. Both models use the same architecture and hyperparameters.

Model	Optimality GAP (\downarrow)				
	40 nodes	60 nodes	80 nodes	100 nodes	200 nodes
Beam search with width $w=128$					
MPNN	17.7 \pm 5%	23.9 \pm 3%	25.7 \pm 8%	31.9 \pm 6%	38.9 \pm 7%
Unrelated	12.3 \pm 2.2%	17.5 \pm 3.1%	22.3\pm3.1%	26.4\pm2.6%	199.0 \pm 373.3%
Related	9.1\pm0.1%	15.5\pm4%	23.1 \pm 3%	28.9 \pm 2%	35.4\pm2%

Table 5.10: TSP optimality GAP comparison between no-transfer, transferring unrelated algorithms and transferring related algorithms. When transferring, the experimental setup matches MPNN_{PFT}, only algorithms differ.

Common Subsequence length (a string algorithm). [Table 5.10](#) shows that choosing sub-optimal algorithms, while still comparable or slightly better for sizes 80 and 100 nodes, makes the model diverge for larger sizes (≥ 200 nodes).

Part III

CONCLUSION

6

CLOSING REMARKS

This dissertation has inspected the impact of incorporating algorithmic inductive bias in machine learning models, primarily looking at the intersection of deep learning for graphs, graph algorithms and neural combinatorial optimisation.

Throughout its chapters, two interlaced questions were pursued:

Q.1 *Can neural networks learn to execute classical algorithms?*

Q.2 *Is this of any use?*

While it is undoubtedly difficult – and likely quite a few years away – that neural networks will reach the level of *algorithmic guarantees* inherent of classical algorithms in *any* scenarios, this thesis provides theoretical and empirical evidence that it is indeed possible to learn *reasoners* that approximate algorithmic properties (e.g., size-invariance). This thesis also sought to answer concerns regarding the practical value of such approaches, by discussing limitations of classical algorithms, such as the *algorithmic bottleneck dilemma*, and showcasing tasks of practical relevance where neural algorithmic reasoning proves useful.

In details, [chapter 4](#) attempted at giving an answer to [Q.1](#) through the lens of tropical algebra, succeeding in providing practical examples for reachability and shortest path problems. There, an investigation of algorithmic alignment properties is conducted through the use of bijections between semirings, demonstrating how NAR architectures can be derived from the algebraic properties of said semirings. Interestingly, our setting enabled us to *re-discover* some of the most common empirical findings in NAR, such as the use of max aggregators in GNs, and put them under a theoretical framework where their impact on the reasoning performance can be *quantified*. To elucidate this point, recall the study performed in [subsection 4.1.3](#), where a sum-aggregated GN implicitly constrained its representations to learn exponential mappings and consequently requiring a higher number of neurons. Overall, this contribution seeks to foster more research in the theoretical aspect of neural algorithmic reasoning, especially considering the wide range of possible tropical semirings from which we can draw connections and/or derive aligned architectures. Indeed, a direct extension to this contribution would be performing similar explorations on different tropical semirings as in ([Litvinov & Maslov, 1998](#)) in order to build NAR modules that align with algorithms therein and proving approximation capabilities similarly to what we have shown in our contribution.

To further expand possible future extensions, establishing connections between tropical semirings and graph networks unlocked possibilities to potentially demonstrate that *any* min-aggregated DP algorithm can

be arbitrarily well approximated by an EPD architecture. To pursue this objective, a further investigation is necessary. Namely, in our tropical setting, we should consider the use of an external memory to be used by the processor (Jayalath et al., 2023). The rationale behind this is that GNs alone, with their fixed-size node and edge representations, can not model recursion typical of certain DP algorithms, such as Depth First Search (Cormen et al., 2009), up to arbitrary depth. Consequently, there is an inherent limitation due to GN architectures to prove approximations for the full spectrum of DP algorithms. However, our tropical framework did not consider possible external memory usage, and therefore needs to be revised and extended to account for storing and recalling of previous processor states.

Moving forward, Dual Algorithmic Reasoning (section 5.1) testified that not only DP algorithms can be targeted by NAR modules, effectively seeking to answer Q.1 for a broader class of algorithms. Indeed, we successfully learnt a good approximation for the Ford-Fulkerson algorithm, which does not fit in the DP paradigm. Furthermore, such approximation was obtained by leveraging strong duality as an inductive bias, hence borrowing a fundamental concept from the combinatorial optimisation world. Interestingly, strong duality was proven to be effectively modelled and leveraged in DAR predictions – a behaviour which was deeply discussed and analysed in subsection 5.1.2.1). Furthermore, this behaviour emerged from simply training the architecture on both primal and dual solutions, without imposing any constraint nor adding any regularisation term to the objective. As such, DAR formulation is general and can seamlessly be integrated with prior NAR modules with slight, non-disruptive architectural adjustments. While we argue that max-flow and min-cut are *representative* for a broad class of problem pairs and algorithms (i.e., those for which strong duality holds), it remains uncertain whether such advantages would extend to cases involving weak duality. In such scenarios, duality still provides valuable information in the form of upper and lower bounds on the primal solutions. However, whether DAR can harness this property is an unexplored area and a potentially exciting direction for future research.

On a more general note, DAR represents also one of the most compelling examples supporting a positive answer to Q.2. Indeed, DAR demonstrated that algorithms are useful prior knowledge for solving related learning problems. For the first time, we recorded a performance improvement in standard graph learning tasks with real-world utility through incorporation of algorithms in a learnable classifier. In this scenario, dual representations also exhibited outstanding generalisation, being able to being able to output informative representations for graphs of size 100,000 times larger than its training data. This achievement also positions DAR as the most scaled-up NAR architecture, yet.

Further attempts at demonstrating that integrating algorithms in neural networks is useful are carried out in section 4.2 and section 5.2, where we target learning of heuristic functions for two different purposes. In the former, we leveraged DP approximation capabilities of GNs to learn heuristic functions for planning problems, particularly in the context of

the A^* path-finding algorithm. There, NAR was used to improve OOD generalisation of the computed heuristics, and was proven of effective use to enhance the performance of A^* . In the latter, instead, we dived into the exploration of transferring algorithmic knowledge from $P \rightarrow NP$, by training algorithmic reasoners on P algorithms and trying to leverage this knowledge to learn heuristics (or approximate algorithms) for NP-hard problems. This investigation exploits the observation that many approximate algorithms, such as Christofides and the Gon algorithm, build on simpler algorithmic “primitives”. Similarly to this manual crafting of algorithms, our learnt approach seeks to leverage algorithms as starting points (i.e., by pre-training NAR modules to execute them) to perform optimisation steps on when learning CO tasks (i.e., by fine-tuning the representations). Through quantitative and qualitative analysis we provided sufficient indications that algorithmically-informed neural networks perform best on combinatorial tasks. There are still, however, plenty of research opportunities to deepen the analysis of whether algorithms, neural networks and their application to NP-hard problems is effective. One possible, and highly fascinating, direction is that such approach has potential to unlock *automatic discovery* of new highly-performing algorithms for NP-hard problems, possibly looking at interactions with the Reinforcement Learning (RL) paradigm (Sutton & Barto, 2018). In particular, deep reinforcement learning has been successfully applied to discover novel algorithms for matrix multiplication (Fawzi et al., 2022) and sorting of short sequences (Mankowitz et al., 2023). One major difference to our approach is that deep reinforcement learning is inherently more *interpretable*. Specifically, it is possible to *write down* the learnt algorithm by trivial investigation of the sequence of actions employed by the learnt agent. In our approach, instead, hidden representations are not interpretable and it is unclear how we can devise algorithms from them. However, aforementioned RL methodologies do not have knowledge of algorithms and are then required to undergo a heavy trial-and-error phase (typical in RL settings). Hence, there is evident room for application of algorithmic reasoning in this scenario. Here, NAR has the potential to navigate the combinatorial space of algorithmic solutions much more efficiently, given its knowledge of algorithms.

There remains, however, much to explore within Neural Algorithmic Reasoning, both from a theoretical standpoint as well as concerning practical applications. Beside all the future prospects discussed above (e.g., theoretical analysis through different tropical semirings, algorithm discovery, ...), other two valuable directions are worth to be mentioned: *fixed point* iterations and modularity. The former represents one of the most prominent algorithmic invariances that spans many algorithms and applications (Karamardian, 2014). Informally, a fixed point of an algorithm is an input x for which the application of an algorithm A results in no change (i.e., $A(x) = x$). To incorporate this invariance into graph networks, it is necessary to ensure that the iterative message-passing scheme also “converges” to a fixed-point. It is worth noting that when training algorithmic reasoners on algorithms that naturally fit the fixed-point iteration framework, such as Bellman-Ford, this behaviour already

emerges empirically, as investigated in (Mirjanić et al., 2023). A more rigorous research question to explore is whether we can derive theoretical guarantees from this integration, such as termination guarantees.

On the other hand, integrating modularity into algorithmic reasoning would greatly benefit the development of general architectures capable of handling algorithms composed of multiple sub-routines. For instance, in the DAR architecture, modularity in the Ford-Fulkerson algorithm was achieved by manually combining two neural submodules, each approximating its own sub-routine. However, an intriguing research question arises: *can this property be automatically attained by one general architecture?* This is precisely the question that modular deep learning seeks to answer (Pfeiffer et al., 2023) and its integration into algorithmic reasoning is one of certain positive impact.

With these final thoughts, I conclude the dissertation. I hope that all the contributions presented in this thesis will inspire further studies within the world of Neural Algorithmic Reasoning, perhaps starting by investigating one of the future research avenues discussed in this final chapter.

BIBLIOGRAPHY

- David Applegate, Ribert Bixby, Vasek Chvatal, and William Cook. Concorde tsp solver, 2006.
- Steve Awodey. *Category theory*. Oxford university press, 2010.
- Davide Bacciu and Danilo Numeroso. Explaining deep graph networks via input perturbation. *IEEE Transactions on Neural Networks and Learning Systems*, pp. 1–12, 2022. doi: 10.1109/TNNLS.2022.3165618.
- Davide Bacciu, Alessio Micheli, and Alessandro Sperduti. An input–output hidden markov model for tree transductions. *Neurocomputing*, 112:34–46, 7 2013. ISSN 09252312. doi: 10.1016/j.neucom.2012.12.044.
- Davide Bacciu, Federico Errica, and Alessio Micheli. Contextual graph markov model: A deep and generative approach to graph processing. In Jennifer G. Dy and Andreas Krause (eds.), *35th International Conference on Machine Learning, ICML*, Proceedings of Machine Learning Research, 2018.
- Davide Bacciu, Federico Errica, Alessio Micheli, and Marco Podda. A gentle introduction to deep learning for graphs. *Neural Networks*, 129: 203–221, 2020.
- Davide Bacciu, Federico Errica, Alessio Gravina, Lorenzo Madeddu, Marco Podda, and Giovanni Stilo. Deep graph networks for drug repurposing with multi-protein targets. *IEEE Transactions on Emerging Topics in Computing*, pp. 1–14, 2023.
- Egon Balas and Paolo Toth. Branch and bound methods for the traveling salesman problem. 1983.
- Pouya Baniasadi, Mehdi Foumani, Kate Smith-Miles, and Vladimir Ejev. A transformation technique for the clustered generalized traveling salesman problem with applications to logistics. *European Journal of Operational Research*, 285(2):444–457, 2020.
- Richard Bellman. On a routing problem. *Quarterly of applied mathematics*, 16(1):87–90, 1958.
- Richard Bellman. Dynamic programming. *Science*, 153(3731):34–37, 1966.
- Richard E Bellman and Stuart E Dreyfus. *Applied dynamic programming*, volume 2050. Princeton university press, 2015.
- Irwan Bello, Hieu Pham, Quoc V. Le, Mohammad Norouzi, and Samy Bengio. Neural combinatorial optimization with reinforcement learning. In *5th International Conference on Learning Representations, ICLR 2017, Toulon, France, April 24–26, 2017, Workshop Track Proceedings*, 2017.

- Dimitri P Bertsekas and John N Tsitsiklis. Neuro-dynamic programming: an overview. In *Proceedings of 1995 34th IEEE conference on decision and control*, volume 1, pp. 560–564. IEEE, 1995.
- Luca Beurer-Kellner, Martin Vechev, Laurent Vanbever, and Petar Veličković. Learning to configure computer networks with neural algorithmic reasoning. *Advances in Neural Information Processing Systems*, 35:730–742, 2022.
- Beatrice Bevilacqua, Kyriacos Nikiforou, Borja Ibarz, Ioana Bica, Michela Paganini, Charles Blundell, Jovana Mitrovic, and Petar Veličković. Neural algorithmic reasoning with causal regularisation. In Andreas Krause, Emma Brunskill, Kyunghyun Cho, Barbara Engelhardt, Sivan Sabato, and Jonathan Scarlett (eds.), *Proceedings of the 40th International Conference on Machine Learning*, volume 202 of *Proceedings of Machine Learning Research*, pp. 2272–2288. PMLR, 23–29 Jul 2023.
- M. Bianchini, M. Maggini, L. Sarti, and F. Scarselli. Recursive neural networks for object detection. pp. 1911–1915. IEEE. ISBN 0-7803-8359-1. doi: 10.1109/IJCNN.2004.1380903.
- M. Bianchini, M. Gori, and F. Scarselli. Processing directed acyclic graphs with recursive neural networks. *IEEE Transactions on Neural Networks*, 12:1464–1470, 2001. ISSN 10459227. doi: 10.1109/72.963781.
- Charles Blundell, Lars Buesing, Alex Davies, Petar Veličković, and Geordie Williamson. Towards combinatorial invariance for kazhdan-lusztig polynomials. *Representation Theory of the American Mathematical Society*, 26(37):1145–1191, 2022.
- Michael M Bronstein, Joan Bruna, Taco Cohen, and Petar Veličković. Geometric deep learning: Grids, groups, graphs, geodesics, and gauges. *arXiv preprint arXiv:2104.13478*, 2021.
- Erwan Brugalle, Ilia Itenberg, Grigory Mikhalkin, and Kristin Shaw. Brief introduction to tropical geometry. pp. 75, 2000.
- Nadia Burkart and Marco F Huber. A survey on the explainability of supervised machine learning. *Journal of Artificial Intelligence Research*, 70:245–317, 2021.
- Edmund K Burke, Edmund K Burke, Graham Kendall, and Graham Kendall. *Search methodologies: introductory tutorials in optimization and decision support techniques*. Springer, 2014.
- Quentin Cappart, Didier Chételat, Elias B Khalil, Andrea Lodi, Christopher Morris, and Petar Velickovic. Combinatorial optimization and reasoning with graph neural networks. *J. Mach. Learn. Res.*, 24:130–1, 2023.
- Binghong Chen, Chengtao Li, Hanjun Dai, and Le Song. Retro*: Learning retrosynthetic planning with neural guided a* search. In *The 37th International Conference on Machine Learning (ICML 2020)*, 2020a.

- Deli Chen, Yankai Lin, Wei Li, Peng Li, Jie Zhou, and Xu Sun. Measuring and relieving the over-smoothing problem for graph neural networks from the topological view. In *Proceedings of the AAAI conference on artificial intelligence*, volume 34, pp. 3438–3445, 2020b.
- Wei-Lin Chiang, Xuanqing Liu, Si Si, Yang Li, Samy Bengio, and Chojui Hsieh. Cluster-gcn: An efficient algorithm for training deep and large graph convolutional networks. In *Proceedings of the 25th ACM SIGKDD international conference on knowledge discovery & data mining*, pp. 257–266, 2019.
- Nicos Christofides. Worst-case analysis of a new heuristic for the travelling salesman problem. Technical report, Carnegie-Mellon Univ Pittsburgh Pa Management Sciences Research Group, 1976.
- Stephen Cook. The p versus np problem. *Clay Mathematics Institute*, 2, 2000.
- Thomas H Cormen, Charles E Leiserson, Ronald L Rivest, and Clifford Stein. *Introduction to algorithms, 3rd edition*. MIT press, 2009.
- G Dantzig and Delbert Ray Fulkerson. On the max flow min cut theorem of networks. *Linear inequalities and related systems*, 38:225–231, 2003.
- G. B. Dantzig and J. H. Ramser. The truck dispatching problem. *Management Science*, 6:80–91, 10 1959. ISSN 0025-1909. doi: 10.1287/mnsc.6.1.80.
- George B Dantzig. Origins of the simplex method. In *A history of scientific computing*, pp. 141–151. 1990.
- Alex Davies, Petar Veličković, Lars Buesing, Sam Blackwell, Daniel Zheng, Nenad Tomašev, Richard Tanburn, Peter Battaglia, Charles Blundell, András Juhász, et al. Advancing mathematics by guiding human intuition with ai. *Nature*, 600(7887):70–74, 2021.
- Andreea-Ioana Deac, Petar Veličković, Ognjen Milinkovic, Pierre-Luc Bacon, Jian Tang, and Mladen Nikolic. Neural algorithmic reasoners are implicit planners. *Advances in Neural Information Processing Systems*, 34:15529–15542, 2021.
- Michaël Defferrard, Xavier Bresson, and Pierre Vandergheynst. Convolutional neural networks on graphs with fast localized spectral filtering. *Advances in neural information processing systems*, 29, 2016.
- Edsger W Dijkstra et al. A note on two problems in connexion with graphs. *Numerische mathematik*, 1(1):269–271, 1959.
- T Doyuran and B Çatay. A robust enhancement to the clarke–wright savings algorithm. *Journal of the Operational Research Society*, 62: 223–231, 1 2011. ISSN 0160-5682. doi: 10.1057/jors.2009.176.
- Andrew J Dudzik and Petar Veličković. Graph neural networks are dynamic programmers. *Advances in Neural Information Processing Systems*, 35:20635–20647, 2022.

- M.E Dyer and A.M Frieze. A simple heuristic for the p-centre problem. *Operations Research Letters*, 3(6):285–288, 1985. ISSN 0167-6377. doi: [https://doi.org/10.1016/0167-6377\(85\)90002-1](https://doi.org/10.1016/0167-6377(85)90002-1). URL <https://www.sciencedirect.com/science/article/pii/0167637785900021>.
- Valerie Engelmayer, Dobrik Georgiev, and Petar Veličković. Parallel algorithms align with neural execution. *arXiv preprint arXiv:2307.04049*, 2023.
- Paul Erdős, Alfréd Rényi, et al. On the evolution of random graphs. *Publ. Math. Inst. Hung. Acad. Sci*, 5(1):17–60, 1960.
- Alhussein Fawzi, Matej Balog, Aja Huang, Thomas Hubert, Bernardino Romera-Paredes, Mohammadamin Barekatin, Alexander Novikov, Francisco J. R. Ruiz, Julian Schrittwieser, Grzegorz Swirszcz, David Silver, Demis Hassabis, and Pushmeet Kohli. Discovering faster matrix multiplication algorithms with reinforcement learning. *Nature*, 610: 47–53, October 2022. doi: 10.1038/s41586-022-05172-4.
- Mohammad Fereydounian, Hamed Hassani, Javid Dadashkarimi, and Amin Karbasi. The exact class of graph functions generated by graph neural networks. *ArXiv abs/2202.08833*, 2022.
- Lester Randolph Ford and Delbert R Fulkerson. Maximal flow through a network. *Canadian journal of Mathematics*, 8:399–404, 1956.
- Lester Randolph Ford Jr and Delbert Ray Fulkerson. *Flows in networks*. Princeton university press, 2015.
- P. Frasconi, M. Gori, and A. Sperduti. A general framework for adaptive processing of data structures. *IEEE Transactions on Neural Networks*, 9(5):768–786, 1998.
- Markus Freitag and Yaser Al-Onaizan. Beam search strategies for neural machine translation. *arXiv preprint arXiv:1702.01806*, 2017.
- Delbert Ray Fulkerson, George Bernard Dantzig, et al. *Computation of maximal flows in networks*. Rand Corporation, 1955.
- Claudio Gallicchio and Alessio Micheli. Graph echo state networks. pp. 1–8. IEEE, 7 2010. ISBN 978-1-4244-6916-1. doi: 10.1109/IJCNN.2010.5596796.
- Jesus Garcia-Diaz, Jairo Javier Sanchez-Hernandez, Ricardo Menchaca-Mendez, and Rolando Menchaca-Méndez. When a worse approximation factor gives better performance: a 3-approximation algorithm for the vertex k-center problem. *J. Heuristics*, 23(5):349–366, 2017. doi: 10.1007/s10732-017-9345-x. URL <https://doi.org/10.1007/s10732-017-9345-x>.
- Michael R Garey and David S Johnson. *Computers and intractability, A Guide to the Theory of NP-Completeness*. 1979.

- Maxime Gasse, Didier Chetelat, Nicola Ferroni, Laurent Charlin, and Andrea Lodi. Exact combinatorial optimization with graph convolutional neural networks. In H. Wallach, H. Larochelle, A. Beygelzimer, F. d'Alché-Buc, E. Fox, and R. Garnett (eds.), *Advances in Neural Information Processing Systems*, volume 32. Curran Associates, Inc., 2019.
- Fănică Gavril. Algorithms for minimum coloring, maximum clique, minimum covering by cliques, and maximum independent set of a chordal graph. *SIAM Journal on Computing*, 1(2):180–187, 1972. doi: 10.1137/0201013.
- Martin Gebser, Benjamin Kaufmann, Javier Romero, Ramón Otero, Torsten Schaub, and Philipp Wanko. Domain-specific heuristics in answer set programming. In *Twenty-Seventh AAAI Conference on Artificial Intelligence*, 2013.
- Dobrik Georgiev and Pietro Lió. Neural bipartite matching. *arXiv preprint arXiv:2005.11304*, 2020.
- Dobrik Georgiev, Danilo Numeroso, Davide Bacciu, and Pietro Lió. Neural algorithmic reasoning for combinatorial optimisation. *arXiv preprint arXiv:2306.06064*, 2023.
- Robert Giegerich. A systematic approach to dynamic programming in bioinformatics. *Bioinformatics*, 16(8):665–677, 2000.
- Justin Gilmer, Samuel S. Schoenholz, Patrick F. Riley, Oriol Vinyals, and George E. Dahl. Neural message passing for quantum chemistry. In Doina Precup and Yee Whye Teh (eds.), *Proceedings of the 34th International Conference on Machine Learning, ICML 2017, Sydney, NSW, Australia, 6-11 August 2017*, volume 70 of *Proceedings of Machine Learning Research*, pp. 1263–1272. PMLR, 2017. URL <http://proceedings.mlr.press/v70/gilmer17a.html>.
- Teofilo F. Gonzalez. Clustering to minimize the maximum intercluster distance. *Theoretical Computer Science*, 38:293–306, 1985. ISSN 0304-3975. doi: [https://doi.org/10.1016/0304-3975\(85\)90224-5](https://doi.org/10.1016/0304-3975(85)90224-5). URL <https://www.sciencedirect.com/science/article/pii/0304397585902245>.
- Alex Graves, Greg Wayne, and Ivo Danihelka. Neural turing machines. *arXiv preprint arXiv:1410.5401*, 2014.
- Aditya Grover and Jure Leskovec. node2vec: Scalable feature learning for networks. In *KDD*, pp. 855–864. ACM, 2016.
- Prateek Gupta, Maxime Gasse, Elias Khalil, Pawan Mudigonda, Andrea Lodi, and Yoshua Bengio. Hybrid models for learning to branch. In H. Larochelle, M. Ranzato, R. Hadsell, M.F. Balcan, and H. Lin (eds.), *Advances in Neural Information Processing Systems*, volume 33, pp. 18087–18097. Curran Associates, Inc., 2020.
- Gurobi Optimization, LLC. Gurobi Optimizer Reference Manual, 2023. URL <https://www.gurobi.com>.

- S. L. Hakimi. Optimum locations of switching centers and the absolute centers and medians of a graph. *Operations Research*, 12:450–459, 6 1964. ISSN 0030-364X.
- Will Hamilton, Zhitao Ying, and Jure Leskovec. Inductive representation learning on large graphs. *Advances in neural information processing systems*, 30, 2017.
- Jessica B. Hamrick, Kelsey R. Allen, Victor Bapst, Tina Zhu, Kevin R. McKee, Josh Tenenbaum, and Peter W. Battaglia. Relational inductive bias for physical construction in humans and machines. In *CogSci*. cognitivesciencesociety.org, 2018.
- Steve Hanneke. The optimal sample complexity of pac learning. *The Journal of Machine Learning Research*, 17(1):1319–1333, 2016.
- T.E. Harris and F.S. Ross. Fundamentals of a method for evaluating rail net capacities. 1955.
- Peter E. Hart, Nils J. Nilsson, and Bertram Raphael. A formal basis for the heuristic determination of minimum cost paths. *IEEE Transactions on Systems Science and Cybernetics*, 4(2):100–107, 1968. doi: 10.1109/TSSC.1968.300136.
- Mordechai I Henig. The principle of optimality in dynamic programming with returns in partially ordered sets. *Mathematics of operations research*, 10(3):462–470, 1985.
- Kurt Hornik, Maxwell Stinchcombe, and Halbert White. Multilayer feed-forward networks are universal approximators. *Neural Networks*, 2: 359–366, 1 1989. ISSN 08936080. doi: 10.1016/0893-6080(89)90020-8.
- Juraj Hromkovič. *Algorithmics for hard problems: introduction to combinatorial optimization, randomization, approximation, and heuristics*. Springer Science & Business Media, 2013.
- Borja Ibarz, Vitaly Kurin, George Papamakarios, Kyriacos Nikiforou, Mehdi Bennani, Róbert Csordás, Andrew Joseph Dudzik, Matko Bošnjak, Alex Vitvitskyi, Yulia Rubanova, et al. A generalist neural algorithmic learner. In *Learning on Graphs Conference*, pp. 2–1. PMLR, 2022.
- Rishabh Jain, Petar Veličković, and Pietro Liò. Neural priority queues for graph neural networks. *arXiv preprint arXiv:2307.09660*, 2023.
- Dulhan Jayalath, Jonas Jürß, and Petar Veličković. Recursive algorithmic reasoning. *arXiv preprint arXiv:2307.00337*, 2023.
- Olin Johnson and Jing Liu. A traveling salesman approach for predicting protein functions. *Source Code for Biology and Medicine*, 1(1):3, 2006. doi: 10.1186/1751-0473-1-3. URL <https://doi.org/10.1186/1751-0473-1-3>.

- Chaitanya K Joshi, Quentin Cappart, Louis-Martin Rousseau, and Thomas Laurent. Learning the travelling salesperson problem requires rethinking generalization. *Constraints*, 27(1-2):70–98, 2022.
- Stepan Karamardian. *Fixed points: algorithms and applications*. Academic Press, 2014.
- Anna R. Karlin, Nathan Klein, and Shayan Oveis Gharan. A (slightly) improved approximation algorithm for metric tsp, 2022.
- Danish Khalidi, Dhaval Gujarathi, and Indranil Saha. T* : A heuristic search based path planning algorithm for temporal logic specifications. In *2020 IEEE International Conference on Robotics and Automation (ICRA)*, pp. 8476–8482, 2020. doi: 10.1109/ICRA40945.2020.9196928.
- Elias B. Khalil, Hanjun Dai, Yuyu Zhang, Bistra Dilkina, and Le Song. Learning combinatorial optimization algorithms over graphs. In Isabelle Guyon, Ulrike von Luxburg, Samy Bengio, Hanna M. Wallach, Rob Fergus, S. V. N. Vishwanathan, and Roman Garnett (eds.), *Advances in Neural Information Processing Systems 30: Annual Conference on Neural Information Processing Systems 2017, December 4-9, 2017, Long Beach, CA, USA*, pp. 6348–6358, 2017.
- Roni Khardon and Dan Roth. Learning to reason. *Journal of the ACM (JACM)*, 44(5):697–725, 1997.
- Soonkyum Kim and Byungchul An. Learning heuristic a*: efficient graph search using neural network. In *2020 IEEE International Conference on Robotics and Automation (ICRA)*, pp. 9542–9547. IEEE, 2020.
- Diederik P. Kingma and Jimmy Ba. Adam: A method for stochastic optimization. In *ICLR (Poster)*, 2015.
- Thomas N. Kipf and Max Welling. Semi-supervised classification with graph convolutional networks. In *5th International Conference on Learning Representations, ICLR*, 2017.
- Wouter Kool, Herke van Hoof, and Max Welling. Attention, learn to solve routing problems!, 2019.
- Ashwani Kumar, SC Srivastava, and SN Singh. Congestion management in competitive power market: A bibliographical survey. *Electric Power Systems Research*, 76(1-3):153–164, 2005.
- Ravi Kumar, Jasmine Novak, and Andrew Tomkins. Structure and evolution of online social networks. In *Proceedings of the 12th ACM SIGKDD international conference on Knowledge discovery and data mining*, pp. 611–617, 2006.
- Sanjay Kumar, Abhishek Mallik, Anavi Khetarpal, and BS Panda. Influence maximization in social networks using graph embedding and graph neural network. *Information Sciences*, 607:1617–1636, 2022.

- Francesco Landolfi, Davide Bacciu, and Danilo Numeroso. A tropical view of graph neural networks. In *ESANN 2023 proceedings*, pp. 35–40, 2023. ISBN 9782875870889. doi: 10.14428/esann/2023-ES2023-27. URL <https://www.esann.org/sites/default/files/proceedings/2023/ES2023-27.pdf>.
- Eugene L Lawler. *Combinatorial optimization: networks and matroids*. Courier Corporation, 2001.
- Yann LeCun, Yoshua Bengio, et al. Convolutional networks for images, speech, and time series. *The handbook of brain theory and neural networks*, 3361(10):1995, 1995.
- AA Lehman and Boris Weisfeiler. A reduction of a graph to a canonical form and an algebra arising during this reduction. *Nauchno-Tekhnicheskaya Informatsiya*, 2(9):12–16, 1968.
- Frank L. Lewis and Draguna Vrabie. Reinforcement learning and adaptive dynamic programming for feedback control. *IEEE Circuits and Systems Magazine*, 9(3):32–50, 2009. doi: 10.1109/MCAS.2009.933854.
- David Liben-Nowell and Jon Kleinberg. The link prediction problem for social networks. In *Proceedings of the twelfth international conference on Information and knowledge management*, pp. 556–559, 2003.
- Grigori L Litvinov. Maslov dequantization, idempotent and tropical mathematics: A brief introduction. *Journal of Mathematical Sciences*, 140: 426–444, 2007.
- Grigori L. Litvinov and Victor P. Maslov. The correspondence principle for idempotent calculus and some computer applications. In Jeremy Gunawardena (ed.), *Idempotency*, Publications of the Newton Institute, pp. 420–443. Cambridge University Press, Cambridge, 1998. ISBN 978-0-521-55344-5. doi: 10.1017/CBO9780511662508.026.
- Thi Thoa Mac, Cosmin Copot, Duc Trung Tran, and Robin De Keyser. Heuristic approaches in robot path planning: A survey. *Robotics and Autonomous Systems*, 86:13–28, 2016. ISSN 0921-8890. doi: <https://doi.org/10.1016/j.robot.2016.08.001>. URL <https://www.sciencedirect.com/science/article/pii/S0921889015300671>.
- Diane Maclagan and Bernd Sturmfels. Introduction to tropical geometry. *Graduate Studies in Mathematics*, 161:75–91, 2009.
- Sadegh Mahdavi, Kevin Swersky, Thomas Kipf, Milad Hashemi, Christos Thrampoulidis, and Renjie Liao. Towards better out-of-distribution generalization of neural algorithmic reasoning tasks. *Transactions on Machine Learning Research*, 2023. ISSN 2835-8856. URL <https://openreview.net/forum?id=xkrtvHlp3P>.
- Daniel J. Mankowitz, Andrea Michi, Anton Zhernov, Marco Gelmi, Marco Selvi, Cosmin Paduraru, Edouard Leurent, Shariq Iqbal, Jean-Baptiste Lespiau, Alex Ahern, Thomas Köppe, Kevin Millikin, Stephen

- Gaffney, Sophie Elster, Jackson Broshear, Chris Gamble, Kieran Milan, Robert Tung, Minjae Hwang, Taylan Cemgil, Mohammadamin Barekattain, Yujia Li, Amol Mandhane, Thomas Hubert, Julian Schrittwieser, Demis Hassabis, Pushmeet Kohli, Martin Riedmiller, Oriol Vinyals, and David Silver. Faster sorting algorithms discovered using deep reinforcement learning. *Nature*, 618(7964):257–263, June 2023. doi: 10.1038/s41586-023-06004-9.
- Rafael Mart, Panos M Pardalos, and Mauricio GC Resende. *Handbook of heuristics*. Springer Publishing Company, Incorporated, 2018.
- Avantika Mathur, Mingming Cao, Suparna Bhattacharya, Andreas Dilger, Alex Tomas, and Laurent Vivier. The new ext4 filesystem: current status and future plans. In *Proceedings of the Linux symposium*, volume 2, pp. 21–33. Citeseer, 2007.
- Zbigniew Michalewicz and David B Fogel. *How to solve it: modern heuristics*. Springer Science & Business Media, 2013.
- A. Micheli. Neural network for graphs: A contextual constructive approach. *IEEE Transactions on Neural Networks*, 20:498–511, 3 2009. ISSN 1045-9227. doi: 10.1109/TNN.2008.2010350.
- Shengjie Min, Zhan Gao, Jing Peng, Liang Wang, Ke Qin, and Bo Fang. Stgsn—a spatial-temporal graph neural network framework for time-evolving social networks. *Knowledge-Based Systems*, 214:106746, 2021.
- Vladimir V Mirjanić, Razvan Pascanu, and Petar Veličković. Latent space representations of neural algorithmic reasoners. *arXiv preprint arXiv:2307.08874*, 2023.
- Christopher Morris, Martin Ritzert, Matthias Fey, William L Hamilton, Jan Eric Lenssen, Gaurav Rattan, and Martin Grohe. Weisfeiler and leman go neural: Higher-order graph neural networks. In *Proceedings of the AAAI conference on artificial intelligence*, volume 33, pp. 4602–4609, 2019.
- David F. Nettleton. Data mining of social networks represented as graphs. *Computer Science Review*, 7:1–34, 2013. ISSN 1574-0137. doi: <https://doi.org/10.1016/j.cosrev.2012.12.001>. URL <https://www.sciencedirect.com/science/article/pii/S1574013712000445>.
- Behnam Neyshabur, Srinadh Bhojanapalli, David McAllester, and Nati Srebro. Exploring generalization in deep learning. *Advances in neural information processing systems*, 30, 2017.
- Danilo Numeroso and Davide Bacciu. Meg: Generating molecular counterfactual explanations for deep graph networks. In *2021 International Joint Conference on Neural Networks (IJCNN)*, pp. 1–8. IEEE, 2021.
- Danilo Numeroso, Davide Bacciu, and Petar Veličković. Learning heuristics for a*. *GroundedML Workshop, ICLR*, 2022.

- Danilo Numeroso, Davide Bacciu, and Petar Veličković. Dual algorithmic reasoning. In *ICLR*. OpenReview.net, 2023.
- Johannes C. Paetzold, Julian McGinnis, Suprosanna Shit, Ivan Ezhov, Paul Büschl, Chinmay Prabhakar, Anjany Sekuboyina, Mihail I. Todorov, Georgios Kaissis, Ali Ertürk, Stephan Günemann, and Bjoern H. Menze. Whole brain vessel graphs: A dataset and benchmark for graph learning and neuroscience. In *NeurIPS Datasets and Benchmarks*, 2021.
- Michal Pándy, Weikang Qiu, Gabriele Corso, Petar Veličković, Zhitao Ying, Jure Leskovec, and Pietro Liò. Learning graph search heuristics. In *Learning on Graphs Conference*, pp. 10–1. PMLR, 2022.
- Tobias Pfaff, Meire Fortunato, Alvaro Sanchez-Gonzalez, and Peter Battaglia. Learning mesh-based simulation with graph networks. In *International Conference on Learning Representations*, 2020.
- Jonas Pfeiffer, Sebastian Ruder, Ivan Vulić, and Edoardo Maria Ponti. Modular deep learning. *arXiv preprint arXiv:2302.11529*, 2023.
- Marin Vlastelica Pogančić, Anselm Paulus, Vit Musil, Georg Martius, and Michal Rolinek. Differentiation of blackbox combinatorial solvers. In *International Conference on Learning Representations*, 2019.
- Angie K Reyes, Juan C Caicedo, and Jorge E Camargo. Fine-tuning deep convolutional networks for plant recognition. *CLEF (Working Notes)*, 1391:467–475, 2015.
- Edward A Rietman, Robert L Karp, and Jack A Tuszynski. Review and application of group theory to molecular systems biology. *Theoretical Biology and Medical Modelling*, 8(1):1–29, 2011.
- Julia Robinson. *On the Hamiltonian game (a traveling salesman problem)*. Rand Corporation, 1949.
- David Sankoff and Mathieu Blanchette. Multiple genome rearrangement and breakpoint phylogeny. *Journal of computational biology*, 5(3):555–570, 1998.
- F. Scarselli, M. Gori, Ah Chung Tsoi, M. Hagenbuchner, and G. Monfardini. The graph neural network model. *IEEE Transactions on Neural Networks*, 20:61–80, 1 2009. ISSN 1045-9227. doi: 10.1109/TNN.2008.2005605.
- Franco Scarselli, Marco Gori, Ah Chung Tsoi, Markus Hagenbuchner, and Gabriele Monfardini. Computational capabilities of graph neural networks. *IEEE Transactions on Neural Networks*, 20(1):81–102, 2008.
- Behrooz Shirazi, Mingfang Wang, and Girish Pathak. Analysis and evaluation of heuristic methods for static task scheduling. *Journal of Parallel and Distributed Computing*, 10(3):222–232, 1990. ISSN 0743-7315. doi: [https://doi.org/10.1016/0743-7315\(90\)90014-G](https://doi.org/10.1016/0743-7315(90)90014-G). URL <https://www.sciencedirect.com/science/article/pii/074373159090014G>.

- Gilles Simonin, Benoit Darties, Rodolphe Giroudeau, and J-C König. Isomorphic coupled-task scheduling problem with compatibility constraints on a single processor. *Journal of Scheduling*, 14(5):501–509, 2011.
- Steven Sloman. *Causal models: How people think about the world and its alternatives*. Oxford University Press, 2005.
- Kenneth Slonneger and Barry L Kurtz. *Formal syntax and semantics of programming languages*, volume 340. Addison-Wesley Reading, 1995.
- Xingyou Song, Yiding Jiang, Stephen Tu, Yilun Du, and Behnam Neyshabur. Observational overfitting in reinforcement learning. *arXiv preprint arXiv:1912.02975*, 2019.
- A. Sperduti and A. Starita. Supervised neural networks for the classification of structures. *IEEE Transactions on Neural Networks*, 8(3):714–735, 1997.
- Richard S Sutton and Andrew G Barto. *Reinforcement learning: An introduction*. MIT press, 2018.
- Hao Tang, Zhiao Huang, Jiayuan Gu, Bao-Liang Lu, and Hao Su. Towards scale-invariant graph-related problem solving by iterative homogeneous gnns. *Advances in Neural Information Processing Systems*, 33:15811–15822, 2020.
- Lisa Torrey and Jude Shavlik. Transfer learning. In *Handbook of research on machine learning applications and trends: algorithms, methods, and techniques*, pp. 242–264. IGI global, 2010.
- Jes ús Virseda, Daniel Borrajo, and Vidal Alcázar. Learning heuristic functions for cost-based planning. *Planning and Learning*, pp. 6, 2013.
- Ashish Vaswani, Noam Shazeer, Niki Parmar, Jakob Uszkoreit, Llion Jones, Aidan N Gomez, Łukasz Kaiser, and Illia Polosukhin. Attention is all you need. *Advances in neural information processing systems*, 30, 2017.
- Petar Velićković, Guillem Cucurull, Arantxa Casanova, Adriana Romero, Pietro Liò, and Yoshua Bengio. Graph attention networks. In *6th International Conference on Learning Representations, ICLR*, 2018.
- Petar Velićković, Rex Ying, Matilde Padovano, Raia Hadsell, and Charles Blundell. Neural execution of graph algorithms. In *International Conference on Learning Representations*, 2019.
- Petar Velićković, Lars Buesing, Matthew Overlan, Razvan Pascanu, Oriol Vinyals, and Charles Blundell. Pointer graph networks. *Advances in Neural Information Processing Systems*, 33:2232–2244, 2020.
- Petar Velićković, Adrià Puigdomènech Badia, David Budden, Razvan Pascanu, Andrea Banino, Misha Dashevskiy, Raia Hadsell, and Charles Blundell. The clrs algorithmic reasoning benchmark. In *International Conference on Machine Learning*, pp. 22084–22102. PMLR, 2022a.

- Petar Veličković, Matko Bošnjak, Thomas Kipf, Alexander Lerchner, Raia Hadsell, Razvan Pascanu, and Charles Blundell. Reasoning-modulated representations. In *Learning on Graphs Conference*, pp. 50–1. PMLR, 2022b.
- Petar Veličković. Everything is connected: Graph neural networks. *Current Opinion in Structural Biology*, 79:102538, 4 2023. ISSN 0959440X. doi: 10.1016/j.sbi.2023.102538.
- Petar Veličković and Charles Blundell. Neural algorithmic reasoning. *Patterns*, 2(7):100273, 2021. ISSN 2666-3899. doi: <https://doi.org/10.1016/j.patter.2021.100273>.
- Oriol Vinyals, Meire Fortunato, and Navdeep Jaitly. Pointer networks. *Advances in neural information processing systems*, 28, 2015.
- P.J. Werbos. Backpropagation through time: what it does and how to do it. *Proceedings of the IEEE*, 78:1550–1560, 1990. ISSN 00189219. doi: 10.1109/5.58337.
- Shimon Whiteson, Brian Tanner, Matthew E Taylor, and Peter Stone. Protecting against evaluation overfitting in empirical reinforcement learning. In *2011 IEEE symposium on adaptive dynamic programming and reinforcement learning (ADPRL)*, pp. 120–127. IEEE, 2011.
- Christopher Wilt and Wheeler Ruml. Building a heuristic for greedy search. In *International Symposium on Combinatorial Search*, volume 6, 2015.
- Wynand Winterbach, Piet Van Mieghem, Marcel Reinders, Huijuan Wang, and Dick de Ridder. Topology of molecular interaction networks. *BMC systems biology*, 7:1–15, 2013.
- Louis-Pascal Xhonneux, Andreea-Ioana Deac, Petar Veličković, and Jian Tang. How to transfer algorithmic reasoning knowledge to learn new algorithms? *Advances in Neural Information Processing Systems*, 34: 19500–19512, 2021.
- Keyulu Xu, Weihua Hu, Jure Leskovec, and Stefanie Jegelka. How powerful are graph neural networks? In *International Conference on Learning Representations*, 2019.
- Keyulu Xu, Jingling Li, Mozhi Zhang, Simon S Du, Ken-ichi Kawarabayashi, and Stefanie Jegelka. What can neural networks reason about? In *International Conference on Learning Representations*, 2020.
- Keyulu Xu, Mozhi Zhang, Jingling Li, Simon Shaolei Du, Ken-Ichi Kawarabayashi, and Stefanie Jegelka. How neural networks extrapolate: From feedforward to graph neural networks. In *International Conference on Learning Representations*, 2021.
- Yunpeng Xu and Chang Che. A brief review of the intelligent algorithm for traveling salesman problem in uav route planning. In *2019 IEEE*

9th international conference on electronics information and emergency communication (ICEIEC), pp. 1–7. IEEE, 2019.

Cheng-Yu Yeh, Hsiang-Yuan Yeh, Carlos Roberto Arias, and Von-Wun Soo. Pathway detection from protein interaction networks and gene expression data using color-coding methods and a* search algorithms. *The Scientific World Journal*, 2012:315797, Apr 2012. ISSN 2356-6140. doi: 10.1100/2012/315797. URL <https://doi.org/10.1100/2012/315797>.

Chiyuan Zhang, Oriol Vinyals, Remi Munos, and Samy Bengio. A study on overfitting in deep reinforcement learning. *arXiv preprint arXiv:1804.06893*, 2018.

Part IV

APPENDIX

A

LIST OF PUBLICATIONS

- Numeroso Danilo, and Davide Bacciu. Explaining Deep Graph Networks with Molecular Counterfactuals. In *Workshop on Machine Learning for Molecules, Neural Information Processing Systems (NeurIPS)*, 2020.
URL: github.com/danilonumeroso/meg
- Numeroso Danilo, and Davide Bacciu. MEG: Generating Molecular Counterfactual Explanations for Deep Graph Networks. In *IEEE International Joint Conference on Neural Networks (IJCNN)*, 2021.
URL: github.com/danilonumeroso/meg
- Bacciu Davide, and Danilo Numeroso. Explaining Deep Graph Networks via Input Perturbation. In *IEEE Transactions on Neural Networks and Learning Systems (TNNLS) Journal*, 2022.
URL: github.com/danilonumeroso/legit
- Numeroso, Danilo, Davide Bacciu, and Petar Veličković. Learning heuristics for A*. In *Workshop on Anchoring Machine Learning in Classical Algorithmic Theory, International Conference on Learning Representations (ICLR)*, 2022. github.com/danilonumeroso/dar
- Kool Wouter, Laurens Bliek, Danilo Numeroso, Yingqian Zhang, Tom Catshoek, Kevin Tierney, Thibaut Vidal and Joaquim Gromicho. The EURO meets NeurIPS 2022 Vehicle Routing Competition. In *Proceedings of the Neural Information Processing Systems (NeurIPS) Competitions Track, PMLR*, 2022.
URL: github.com/danilonumeroso/dar
- Numeroso, Danilo, Davide Bacciu, and Petar Veličković. Dual Algorithmic Reasoning. In *International Conference on Learning Representations (ICLR)*, 2023.
URL: github.com/ortec/euro-neurips-vrp-2022-quickstart
- Bacciu Davide, Landolfi Francesco, and Danilo Numeroso. A Tropical View of Graph Neural Networks. In *European Symposium on Artificial Neural Networks (ESANN)*, 2023.

B | LIST OF TALKS

- Oral presentation of *Explaining Deep Graph Networks with Molecular Counterfactuals*, Workshop on Machine Learning for Molecules, NeurIPS 2020.
- Oral presentation of *MEG: Generating Molecular Counterfactual Explanations for Deep Graph Networks*, IJCNN 2021.
- Poster presentation of *Learning heuristics for A**, Workshop on Anchoring Machine Learning in Classical Algorithmic Theory, ICLR 2022.
- Invited talk at TU/e, *Neural Algorithmic Reasoning*, Eindhoven, 2023.
- Spotlight presentation of *Dual Algorithmic Reasoning*, ICLR 2023.
- Invited talk at QualcommAI, *Algorithmically-Informed Graph Neural Networks*, 2023.